THE MOLECULAR RECOGNITION OF DNA BY RHODIUM(III) - ZINC FINGER PEPTIDE CHIMERAS

Thesis by

Susanne Chosein Lin

In Partial Fulfillment of the Requirements

for the Degree of

Doctor of Philosopy

California Institute of Technology
Pasadena, California

1997

(Submitted September 9, 1996)

Acknowledgments

The one person to whom I owe the most gratitude and thanks is my advisor, Jackie Barton. She has provided unfailing enthusiasm and support for me and my research over the years. She has also been a very understanding person.

I have had many colloborators on my project. Kaspar Zimmermann and Niranjan Sardesai helped developed the synthetic protocol for the rhodium - peptide chimeras. More recently, Sonya Franklin has been instrumental in developing better reagents to improve our yields of metal-peptide chimeras. I would also like to thank all the people responsible for the synthesis and subsequent analysis of my peptides and metal-peptide chimeras. Suzanna Horvath and her Biopolymer Synthesis and Analysis facility the synthesized the zinc finger peptides. Jane Z. Sanders was very helpful in performing the plasma desorption mass spectrometry of the chimeras. Finally, Nathan Dalleska of the Caltech Division of Chemistry and Chemical Engineering Mass Spectrometry Laboratory performed the electrospray mass spectrometry of the rhodium-zinc finger chimeras.

The quality of this thesis was greatly improved by the excellent proofreading skills of Sabine Coates. In addition, I would not have been able to finish this work without the assistance in may ways of Lee Friedman.

I would like to thank the whole Barton group for their assistance over the years both personally and professionally. I am especially grateful to the other members of 119 Noyes (Tim Johann, Dan Hall and Marilena Fitzsimons) for making lab such a fun place to work. In addition, I would like to thank Christy Chow, Yonchu Jenkins, Ai Ching Lim, Johanna Yao, Sonya Franklin, Eric Stemp and Sabine Coates for being such good friends. I would also like to thank Brian Hudson for his drawings and sculptures and R. Erik Holmlin for being a great

traveling companion. I cannot forget to thank Mo Renta for knowing the answers to all of my questions, for all of her help and being a good friend..

The quality of my life at Caltech was also improved through interactions outside of the lab. I always looked forward to Friday lunches with Sandi Burkett where we worked out our problems. Somehow, I have forgiven her for graduating so early. I would like to thank Jonathan Forman for supporting me my first five years of graduate school. I want to thank Bill and Delores Bing for running such fantastic music program at Caltech. I think that I would have gone crazy had it not been for band every Thursday night. I also thank my many friend from the music program, especially Erik Daniel, Scott Babcock and the saxophone section from the Thursday jazz band

I would also like to thank Lee Friedman for bringing joy and happiness to my life and keeping me from being too serious.

I would finally like to thank my parents for all of their love and support over the years. They have always lend me to believe that I could do anything that I wanted to do. This thesis is dedicated to them.

Abstract

Covalent chimeras of zinc finger peptide domains with phenanthrenequinone diimine (phi) complexes of rhodium (III) have been designed, synthesized and their DNA recognition characteristics examined. The rhodium complex binds in the major groove of DNA by intercalation and allows the attached peptide to interact with DNA in a sequence-specific manner. Chimeras of $[Rh(phi)_2(bpy')]^{3+}$ (bpy' = 4-(4-carboxybutyl), 4'-methyl-2,2'-bipyridine) and $[Rh(phi)_2(phen')]^{3+}$ (phen' = (5-amidoglutaryl)-1,10-phenanthroline) and four different zinc finger peptides (Sp1 finger 2 & 3, ADR1b and ADR1b-Ala) have been successfully synthesized using solid phase coupling methodology. Electronic spectroscopy showed the rhodium complex and peptide to be essentially independent units. A method to successfully fold the peptide portion of the chimera with zinc has been developed, and ^1H NMR spectroscopy has been used to confirm folding. The resultant chimeras bind tightly to DNA, and the rhodium intercalator promotes DNA cleavage with photoactivation. Analysis of the DNA sites targeted by the chimeras on DNA restriction fragments have demonstrated that the peptide can direct new recognition. Variations in the rhodium complexes and peptides resulted in differences in specificity as seen by photocleavage. Studies on smaller oligonucleotides containing the recognition sequences have shown the rhodium - Sp1-2 chimera to bind with affinities of 10^7-10^8 M^{-1} for its target sites. Hence, formation of rhodium(III) - zinc finger chimeras provide a route to establish high affinity DNA binding by a single zinc finger domain. At some sites, the rhodium complex and zinc finger appeared to bind independently to adjacent segments. For the $[Rh(phi)_2(phen')]^{3+}$ - Sp1 - 2 chimeras, a strong high affinity site ($K_a \geq 10^8$ M^{-1}) was observed, where it was postulated that the rhodium complex and zinc finger bind to the opposite strands of the GCG binding site in a

cooperative fashion. These rhodium (III) - zinc finger chimeras represent a new route to examine the specific interactions of a single zinc finger with DNA in chemical detail and provide the basis to build a family of sequence-specific DNA binding molecules.

TABLE OF CONTENTS

LIST OF FIGURES

LIST OF SCHEMES

LIST OF TABLES

Chapter 1. The Interactions of Zinc Finger Proteins and Phi Complexes of Rhodium(III) with DNA

1.1. INTRODUCTION

Understanding the molecular recognition of DNA is one of the fundamental goals of chemistry and biology. A myriad of biological processes utilizes the specific interaction of proteins with DNA or RNA. As chemists, we are trying to understand how proteins interact with DNA on the molecular level. The construction of small well-defined systems based on actual proteins can elucidate the details of protein-DNA recognition. Also, systems of this type can be used as a basis for the rational design of small molecules that recognize a desired DNA sequence.

The transcription factor assembly is a good system for the study of protein-DNA interactions, and it can serve as a basis for the design of small DNA recognition molecules. In eukaryotes, the transcription of protein encoding genes is regulated by sequence-specific DNA binding proteins.[1] The structure of a typical transcription factor consists of two functionally distinct domains: the DNA binding domain which recognizes a specific site on DNA, and the activation (repression) domain which mediates the stimulation of transcription.[2] The DNA binding domains can be classified into groups of related structural motifs: the helix-turn-helix, leucine zipper and zinc finger are examples of such motifs.[3] All three motifs use an α-helix to recognize the major groove of DNA; the zinc finger represents the structurally most compact unit that recognizes DNA in modular fashion and is an ideal system for our purposes.

1.2. THE HISTORY OF THE ZINC FINGER PROTEIN (TRANSCRIPTION FACTOR IIIA)

The first zinc finger protein discovered was transcription factor IIIA (TFIIIA) of the frog *Xenopus laevis*' oocytes.[4] It is one of the factors required to activate the 5S RNA gene. In addition to binding to DNA, TFIIIA also forms a complex with 5S RNA. In 1983, Wu and coworkers determined that each mole of protein contains 7 to 11 moles of zinc which were necessary for DNA binding.[5] An analysis of the TFIIIA cDNA sequence[6] revealed the presence of nine sets of a repeating motif that consisted of 30 amino acids: (Tyr, Phe)-X-Cys-X_{2-4}-Cys-X_3-Phe-X_5-Leu-X_2-His-$X_{3,4}$-His-X_{2-6}.[7,8] This motif contained several conserved hydrophobic residues including two histidine and two cysteine residues which were postulated to be zinc binding ligands. Thus, a total of seven amino acids were conserved. In 1986, an EXAFS study of the zinc finger confirmed that the coordination sphere of the zinc was composed of two cysteine and two histidine ligands.[9] Klug first coined the term 'zinc finger' because a simple model of the structure resembled a finger.[7]

1.3. THE STRUCTURE OF THE ZINC FINGER DOMAIN

In 1988, Berg proposed a structure of a zinc finger that was based on the crystal structures of other proteins with the same amino acid sequence.[10] Berg suggested that the N-terminal region, that contains the cysteine residues, forms an antiparallel β-sheet, while the rest of the sequence, including the conserved histidines, forms an α-helix. Gibson produced a similar model of the structure based on interactive graphics modeling and constrained molecular dynamics.[11]

The first NMR data on a single zinc finger was obtained on a peptide from the yeast transcription factor ADR1.[12] The structure revealed an α-helix and a

conserved hydrophobic core. A second, more complete structure was obtained of the 31st finger from the *Xenopus* protein Xfin.[13] In this structure, the first 13 residues formed an antiparallel β-sheet, and the remaining 12-15 residues formed an α-helix. A schematic of the structure of a single finger is shown in Figure 1.1. It should be noted that the NMR structures were very similar to the predicted structures of Berg and Gibson.

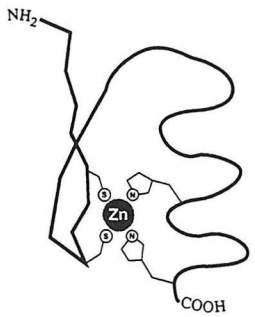

Figure 1.1. *A schematic of the structure of a zinc finger.*

NMR structures of numerous single and multiple fingers from different proteins since then have shown that peptides of the TFIIIA consensus sequence fold into similar stable, compact structures in the presence of zinc.[12-26] The formation of this structure has been detected by numerous spectroscopic techniques. One-dimensional NMR spectroscopy of the peptides showed distinct shifts in residues (esp. histidine, methyl) in the presence of zinc.[23,27,28] Circular dichroism spectroscopy showed an increase in α-helicity when the peptide folded.[29,30] In addition, a distinct UV-visible spectrum is obtained when the zinc finger is folded in the presence of Co^{2+}.[27,29,30]

The stability of the zinc finger structure has been investigated through amino acid mutations. Changes in the conserved hydrophobic residues were found to alter the stability of the zinc finger.[30-34] Interestingly, an aromatic to non-aromatic mutation which destabilizes the structure can be compensated by a non-aromatic to aromatic mutation in another position.[30] In contrast, the mutation of residues implicated in DNA recognition does not disturb the stability of the structure.[35-37]

In fact, all the residues, except for the seven conserved ones, can be mutated without disrupting the zinc finger structure.[38-40] Using a data base of 131 zinc finger sequences, a consensus sequence (CP-1) was designed by

selecting the amino acid that occurred in the largest number at each position.[38] This consensus peptide bound zinc and cobalt, and adopted the expected structure as determined by NMR spectroscopy. Even a 'minimalist' zinc finger, where all the non-conserved residues were replaced with alanines, folded into the expected zinc finger structure in the presence of zinc and cobalt.[39] Therefore, many variations of the non-conserved amino acids of the zinc finger are possible without adversely disrupting its structure.

The metal binding affinities and specificities of the zinc finger have also been investigated. UV-Vis titrations were used to measure the affinity of the zinc finger peptide for cobalt(II) and zinc(II).[41] The second zinc finger of TFIIIA was found to bind Co^{2+} with a dissociation constant of 3.8 ($\pm$0.5) x 10^{-6} M. On the other hand, it coordinated Zn^{2+} with a dissociation constant of 2.8 ($\pm$0.9) x 10^{-9} M. In fact, zinc can displace the bound cobalt. The CP-1 peptide was also found to bind iron(II) and nickel(II) with micromolar dissociation constants.[42] Based on the metal binding studies it was concluded that the zinc finger peptide binds zinc specifically with high affinity.

However, the term zinc finger is often loosely used to refer to any sequence containing cysteine and/or histidine residues that binds zinc. At present, there are at least ten structural distinct families of zinc binding domains that have been identified. They differ in their zinc ligands, conserved residues and binding properties.[43,44] In this thesis, the term zinc finger will be used to describe the TFIIIA consensus type.

Even though zinc fingers almost always occur in groups in proteins, a comparison of the structures of single and double fingers shows only weak interactions between the fingers.[16] A comparison of 1 to 3 zinc fingers of the SWI5 protein reveals that the fingers are structurally independent, but flexibly linked domains.[22] Also, a double zinc finger peptide was found to bind metals in

a non-cooperative fashion.[45] The first three fingers of TFIIIA are known to be in an elongated structure based on anisotropic tumbling measurements.[46] Thus, individual zinc finger motifs appear to act as separate entities.

The 30 amino acid consensus sequence of a zinc finger motif therefore forms a well-defined, compact structure upon zinc coordination that is stable to variations in the non-conserved residues which include the putative DNA recognition amino acids. Studies further indicate that each finger is an independent entity. Thus, the zinc finger appears to recognize DNA as an independent modular unit.

1.4. THE DNA BINDING PROPERTIES OF ZINC FINGER PROTEINS

Based on structural studies, the zinc fingers are expected to interact in an independent and extended fashion with DNA. Experiments on the nine zinc finger protein, TFIIIA, show a DNA binding site of 45 base pairs which is an average of 5 base pairs per finger.[4,47,48] Methylation interference studies on the same system point to TFIIIA binding in the major groove of DNA.[50] Thus, two modes of interaction were proposed. In the first model, the zinc fingers wrap around the major groove of DNA such that each finger is the same relative orientation to the DNA. In the second model, the protein lies on one face of the DNA with the fingers pointing to the front and back of the helix. In this model, every other finger is equivalent.[50]

The first crystal structure of the interaction between a zinc finger protein and DNA confirmed the first model of interaction.[51] Pabo and Pavletich cocrystallized the zinc finger domain of the mouse nerve growth factor Zif268 with its cognate DNA site (Figure 1.2). As shown in the structure, the fingers wrap around the major groove of DNA in an antiparallel sense with the N-terminus at the 3' end of the helix. Each finger recognizes a base pair triplet in

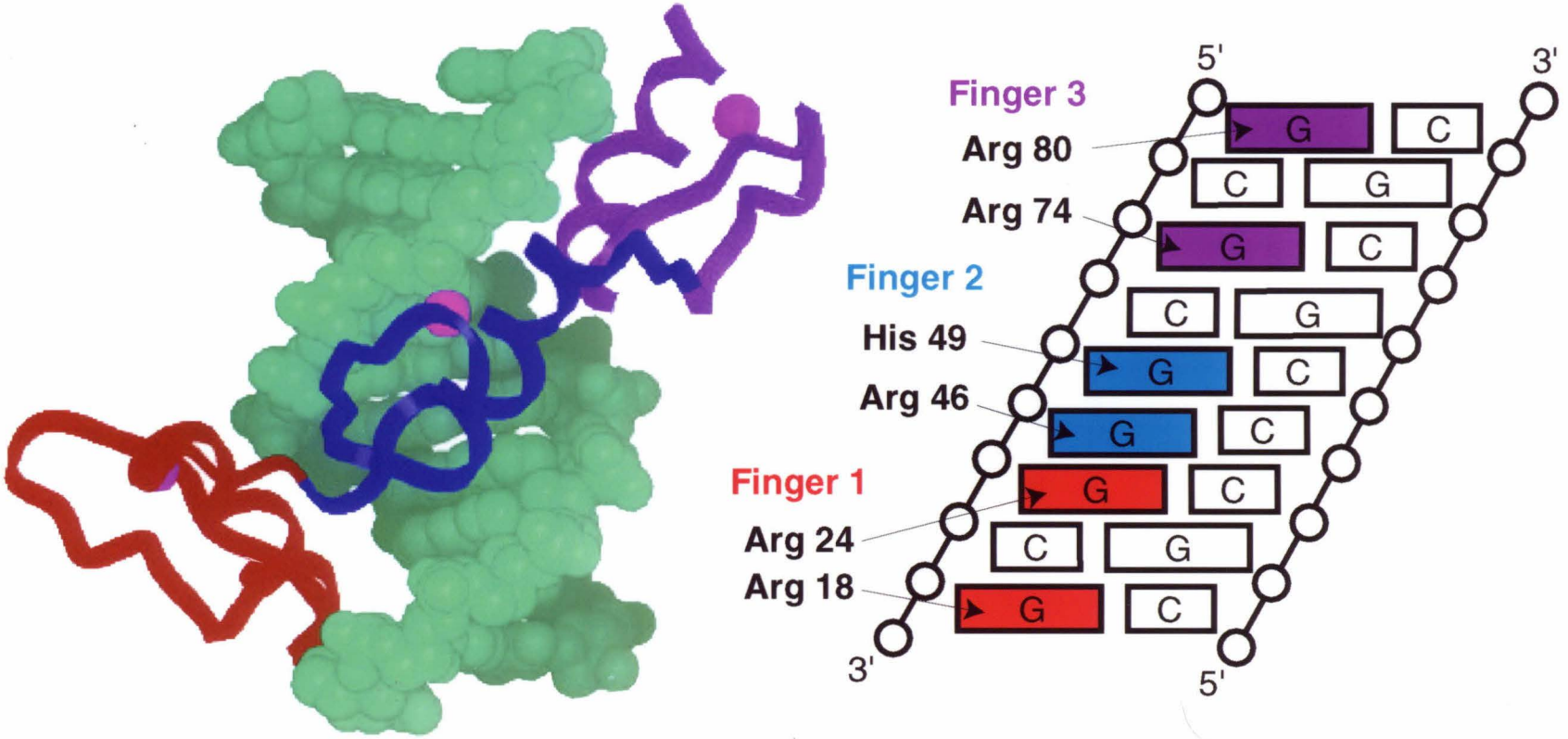

Figure 1.2. *Crystal structure of Zif268 bound to DNA at 2.1Å (left). Finger 1 is in red, finger 2 is in blue, and finger 3 is in purple. The zinc ions are in pink and the DNA is in aqua. A schematic of the contacts between the specific residues of the zinc fingers and the DNA bases is shown on the right.*

the sequence: 5'-GCG GGG GCG-3'. The specific base contacts are only with the guanine residues on the coding strand. The first and third fingers both recognize a 5'-**GCG**-3' triplet using arginines at position -6 and +1 in the α-helix, respectively.[49] The second finger recognizes G**GG** using a histidine at position +3 and an arginine at position -1.[49]

Each finger appears to be independent, and structures of the fingers are almost superimposable. The structure of the second finger correlates well with the NMR structure of Xfin31.[14] All of the fingers of the crystal structure have very similar orientations with respect to the DNA and use residues at the same positions to make specific contacts with the DNA.[49] This evidence supports the idea that each finger is an independent unit.

The crystal structure of a five zinc finger protein (GLI) and its DNA site showed a more complicated recognition pattern (Figure 1.3).[50] Analogous to the Zif structure, fingers 2-5 wrap around the major groove. However, finger 1 does not make any DNA contacts, but instead contacts finger 2. Most of the specific DNA contacts are made by fingers 4 and 5. As a result, not all zinc fingers interact with DNA in the same fashion.

The DNA recognition of GLI is similar to Zif in several respects: the DNA has four bases of the recognition triplet that are consistently contacted by the fingers using four amino acids in certain positions on its helix. However, there are differences in the spacing between the fingers (those of GLI are farther apart), and GLI make specific contacts to both strands while Zif only contacts one strand.

The two zinc fingers of the Tramtrack transcription factor and its DNA site have also been crystallized (Figure 1.4).[51] These fingers wrap around the DNA major groove in the same fashion as Zif and GLI. However, the first finger has an extra β-sheet. The recognition is very similar to the Zif (GLI) case: the notable

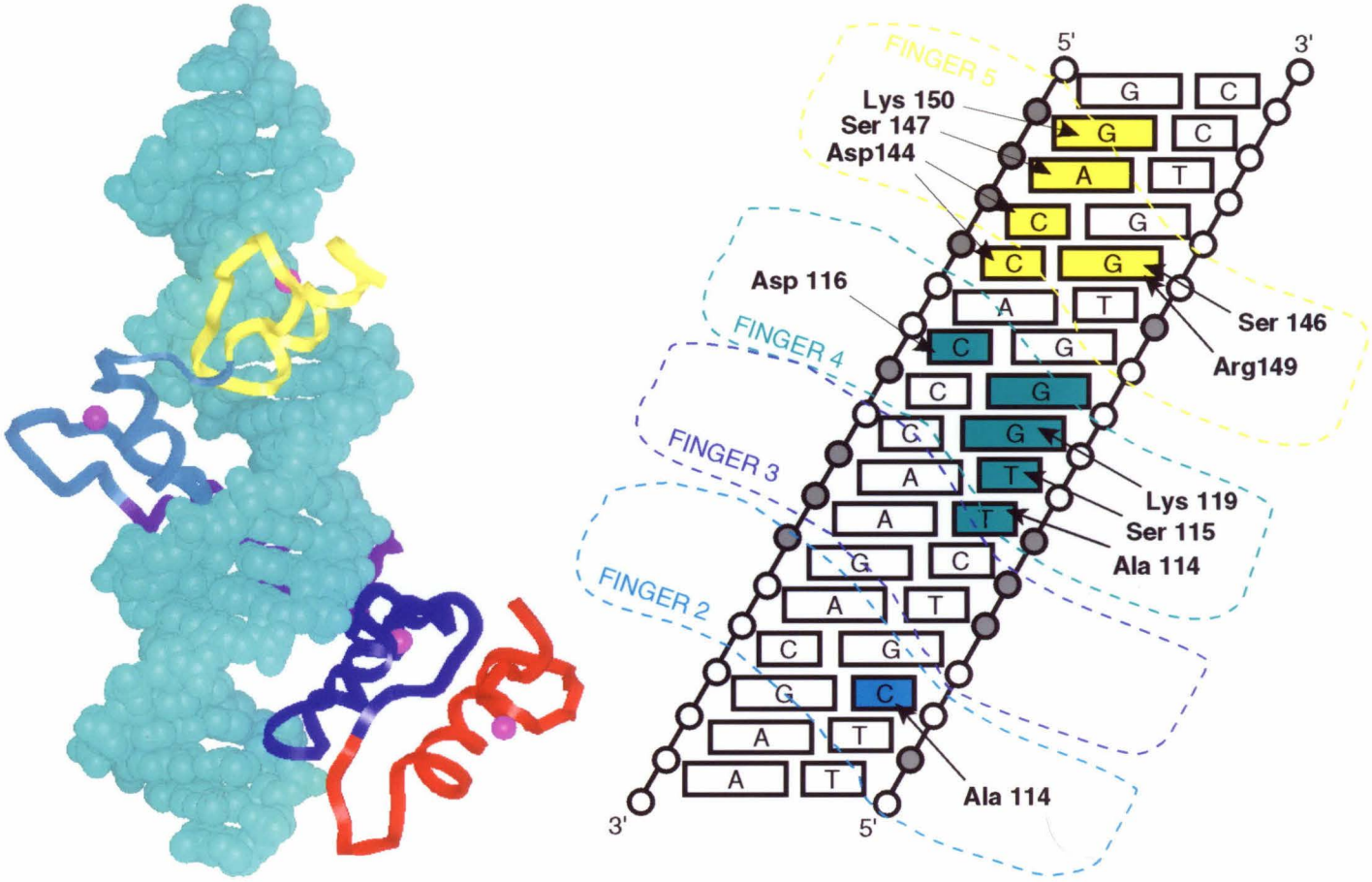

Figure 1.3. *The crystal structure of GLI-DNA at 2.6Å (left). The first finger is in red, the second is in blue, the third (behind the DNA) is in purple, the fourth is in teal, and the fifth is in yellow. All of the zinc ions are in pink, and the DNA is in aqua. Marked areas on the schematic denote the positions of the zinc fingers relative to the DNA (right). In addition, all of the contacts between specific residues and the DNA bases are shown.*

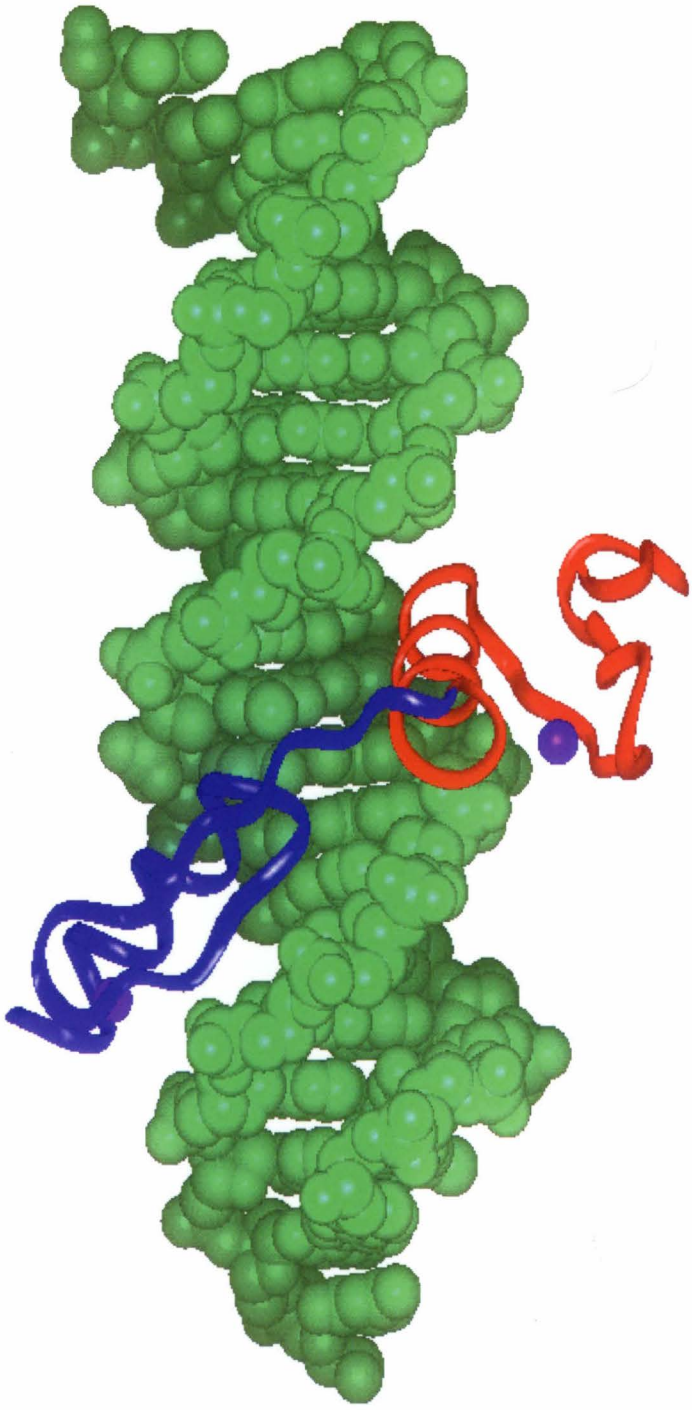

Figure 1.4. *Crystal structure of Tramtrack bound to DNA at a resolution of 2.8Å. The first finger is in red and the second finger is in blue. The zinc is in purple and the DNA is in green.*

exception is that the His at the -1 position of the first finger of Tramtrack makes a phosphate contact while the serine at position 2 makes the DNA contact. Usually, the residue at -1 position makes a contact with the 3' base of the DNA sequence.

Overall, the pattern of DNA recognition by a zinc finger is consistent throughout the crystal structures. There are positions in the zinc finger sequence (-1, +3 and +6) that contact each of the three bases of the DNA recognition triplet (3'-5'). This leads to the possibility of using zinc fingers to design DNA binding proteins that recognize new sequences.

1.5. DESIGNING DNA BINDING ZINC FINGER PROTEINS

Since zinc finger proteins appear to recognize DNA in a modular fashion using specific amino acids to contact specific bases, several researchers have made efforts to change the specificity of the zinc fingers through mutations. In the first study of this kind, the amino acids at the recognition positions for the Krox-20 zinc finger protein were mutated.[52] A His to Thr mutation at position +3, and a Glu to Arg mutation at +6 of finger 2, caused the DNA recognition sequence to change from 5'-GCG GGG GCG-3' to 5'-GCG GCG GCG 3'.

Many studies of this type were done using the Sp1 zinc finger protein. Five amino acids in the α-helical region of Sp1 finger 2 (RDEQR) were changed to the ones present in zinc finger protein Kox 29 (KSAIS).[53] The DNA binding sequence for this Sp1-Kox 29 chimeric protein was determined to be 5'-GGG GGT GGG-3' which is a two base pair mutation from the native Sp1 sequence of 5'-GGG GCG GGG-3'. Another study on the Sp1 protein found that an Arg to Gln mutation at position -1 of finger 2 resulted in a concomitant guanine to adenine change at position 6 of DNA recognition site.[54] In addition, systematic variations on the second finger of Sp1 were done.[55] Based on analysis of a large database of

zinc finger sequences, the -1 and +3 position were varied and specific recognition of all the possible variations of 5'-GGG GNT GGG-3' (N = A, T, G or C) and 5'-GGG GNG GGG-3' were obtained.

DNA specificity studies have been performed on the zinc finger protein ADR1b. Mutations of all three of the DNA recognition positions (-1, +3, +6) in the first finger (ADR1b) led to new specificities of DNA binding at adjacent positions 10, 9 and 8 (3'-GAG-5') in the operator site.[56] Mutations of the +3 position on the second finger (ADR1a) led to expected changes in the recognition of the central base of the triplet.[57,58] Thus, studies on natural zinc finger systems demonstrate that DNA specificity can be altered by simply changing certain amino acids of the zinc finger sequence.

This recognition behavior was extended to de novo, designed zinc finger systems.[59] Three zinc fingers based on a consensus peptide sequence were connected together. Each finger was designed to bind to a different DNA triplet by variations in the DNA contact amino acids.. This zinc finger construct bound to the target DNA site with a nM dissociation constant. Selection of the binding site by this protein from a randomized pool of DNA sites demonstrated that this was the optimal DNA sequence.

A comparison of the binding properties of natural and designed zinc-finger proteins revealed that the Sp1, the consensus peptide, and the minimalist peptide (all alanines), which contain the same DNA contact residues, bind to the same DNA sequence with different affinities.[60] The minimalist peptide was the worst, while the consensus peptide was found to have the best overall DNA-binding affinity, degree of sequence discrimination and resistance to inactivation by chelation agents. Therefore, use of zinc finger proteins for design of DNA binding molecules is not limited to natural sequences.

A powerful method based on phage display was developed to optimize

zinc finger proteins for binding to any desired DNA sequence.[61-65] In this method, a three zinc finger protein, which has been cloned as fusions to the coat proteins of filamentous bacteriophage, has been displayed on the capsid which encloses the viral genome. Thus, libraries have been constructed in which the DNA recognition amino acids on the central zinc finger have been randomized. The target DNA sequence is immobilized on a bead. Rounds of selection and amplification of the phage are used to obtain zinc finger peptides that bind with high affinity to the desired sequences. To discount high-affinity non-specific binding, the selected peptides have been subjected to a 'binding site signature' assay which determined binding affinities for all the variations of the target DNA sequence.[62]

Using phage display techniques, a zinc finger protein was designed to bind to a oncogenic sequence.[66] The new peptide not only bound the DNA sequence *in vitro* and *in vivo,* but also blocked transcription. This was the first example of a designed zinc finger protein that was shown to target its site *in vivo* and subsequently affect function.

All of these studies on designed zinc finger proteins indicate that the zinc finger has a uniquely modular mode of interaction with DNA. This allows for the design of new proteins/peptides to recognize any desired DNA sequence. Thus, it seems possible to develop recognition code for the zinc finger proteins.[67-69]

Approximately 90 amino acid three zinc finger constructs were utilized for these studies since these proteins usually have nanomolar dissociation constants for their nine base pair DNA binding sites.[70] A smaller protein containing only two consecutive zinc fingers also binds to DNA specifically, but with a lower affinity ($K_d = 10^{-7}$).[71,72] Truncation studies on a protein that contained only one zinc finger showed that at least 82 residues were necessary to bind to DNA with

sequence-specificity.[73] In fact, a 30 amino acid single finger does not bind to DNA with any sequence specificity,[29,74,75] Indeed, the second zinc finger from TFIIIA could not be footprinted on its DNA target site and the 31st finger from Xfin was found to bind non-specifically to DNA, only in the presence of zinc, even though NMR studies have shown this finger to fold correctly.[13] Thus, the interaction of an isolated zinc finger with DNA has not been studied.

In conclusion, the zinc finger peptide is a small, structurally stable motif that can interact with DNA in a sequence-specific manner. Various recognition studies have shown that its modular design is ideally suited for use in building new molecules to recognize different elements. Unfortunately, a single zinc finger lacks the affinity to interact specifically with DNA. Therefore, in order to study and use a single zinc finger - DNA recognition, a way to deliver it to the major groove of DNA is needed.

1.6. THE INTERACTION OF PHI COMPLEXES OF RHODIUM(III) WITH DNA

The Barton laboratory has developed a special class of inorganic molecules that interact non-covalently with nucleic acids.[76,77] They are octahedral transition metal complexes of rhodium(III), ruthenium(II), iridium(III) or osmium(II) which are coordinately saturated and substitutionally inert. Recent studies have focused on the design of a range of rhodium(III) complexes which contain the phenanthrenequinone diimine (phi) ligand.[76] These phi complexes of rhodium bind to DNA with high affinity ($K_d \leq 10^{-6}$ M) by intercalation.[78,79] NMR[80-82] and chemical reactivity[78,79] studies are consistent with binding to the double helix from the major groove. For these phi complexes of rhodium, the site-selectivities may be tuned through variations in the ancillary ligands. For example, Δ,α-(R,R)-[Rh(Me_2trien)phi]$^{3+}$ (Figure 1.5) intercalates sequence-specifically into the

GC step of the 5'-TGCA-3' site through an ensemble of methyl-methyl and hydrogen bonding contacts of the ancillary ligands with the major groove base positions.[83] The NMR structure of this metallointercalator bound to a decamer has been determined.[81] In contrast, $[Rh(phi)_2bpy]^{3+}$ (Figure 1.5) binds DNA with sequence-neutrality and serves as a useful photofootprinting reagent.[84] All of the phi complexes of rhodium(III) promote DNA strand scission with photoactivation.[78,79,85,86] Hence, this photochemistry has been used to delineate sites of binding by the metal complex.

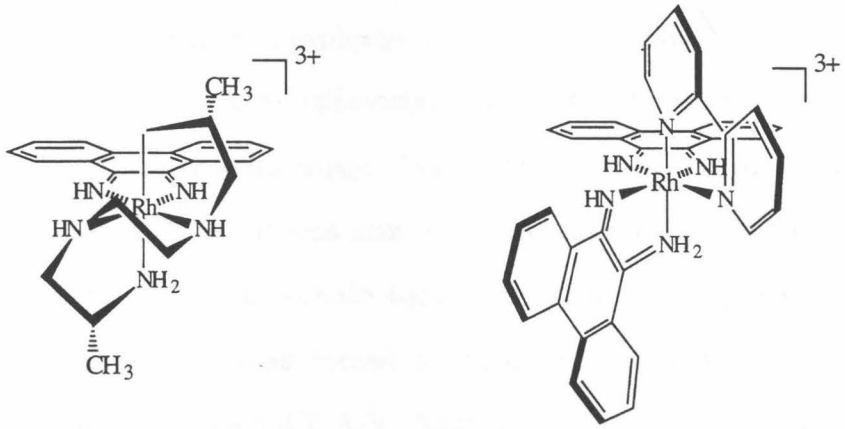

Figure 1.5. *The structures of Δ,α-(R, R)-$[Rh(Me_2trien)phi]^{3+}$ (left)and $[Rh(phi)_2bpy]^{3+}$ (right).*

1.7. THE DESIGN AND USE OF RHODIUM(III) - PEPTIDE CHIMERAS FOR DNA RECOGNITION

The characteristics of phi complexes of rhodium described above lead to their application in the construction of small metal-peptide chimeras which bind DNA sites through specific non-covalent interactions. The rhodium complexes can deliver a small appended peptide to the major groove of DNA. Once there, the peptide makes sequence-specific contacts with the DNA base pairs. Since the rhodium complex is sequence-neutral, the recognition properties of this chimera would be directed solely by the peptide. Thus, the rhodium intercalator serves as a source for non-specific DNA binding in the major groove, and the appended

peptide serves as the recognition element. The DNA cleaving properties of the rhodium intercalator furthermore provide a useful assay to examine recognition by the metal-peptide chimera. Thus, these covalent chimeras provide a new strategy in the assembly of a library of small, sequence-specific DNA-binding molecules. With this strategy, the rational construction of chimeras designed to target almost any desired DNA sequence is possible.

One family of metal-peptide complexes which bind DNA with site-specificity has been constructed based on the P_{22} phage repressor recognition helix.[87] The metal-peptide complexes have been prepared by coupling short peptides (13 residues) to the metallointercalating $[Rh(phi)_2(phen')]^{3+}$ (phen' = (5-amidoglutaryl)-1,10-phenanthroline). The metal-peptide complexes were found to bind to and cleave DNA. It was also determined that the DNA site-specificity depended on the peptide side-chain functional groups. In particular, a single glutamate at position 10 was found to be essential in directing DNA site-recognition to the sequence 5'-CCA-3'. Methylation of the glutamate side chain or direct substitution of glutamine for glutamate abolished the 5'-CCA-3' selectivity. Importantly, the 5'-CCA-3' selectivity is even sensitive to a highly conservative glutamate to aspartate substitution.

Circular dichroism (CD) studies indicated significant α-helical content in these small metal-peptide complexes which depended upon the presence of the glutamate. The glutamate to aspartate mutation caused a significant drop in the helicity of the peptide portion of the chimera (72% to 8%). Thus glutamate is important not only for direct base recognition but also for the maintenance of peptide conformation.

To investigate the importance of the peptide conformation, an attempt was made to "uncouple" the α-helicity and DNA recognition by substituting alanine for the glutamate: AANVAIAAW**A**RAA. CD spectra showed that the

alanine mutant maintained the helicity of the peptide, but the photocleavage gels revealed that the strong preference for 5'-CCA-3' was gone. Therefore, the glutamate must be making some direct contact with the DNA site. In addition, the glutamate may also be holding the helix in a position that disallows the P_{22} recognition residues to contact the base pairs. This dual role of the glutamate (direct DNA contacts and conformation) provides a sensitive "switch" for DNA recognition. The $[Rh(phi)_2(phen')]^{3+}$-P22 chimeras were the first rhodium(III) - peptide conjugates to display sequence-specific DNA recognition that was dependent on the sequence of the peptide.

A second rhodium(III)-α-helix system in which the rhodium intercalator $[Rh(phi)_2(phen')]^{3+}$ was coupled to the recognition helix of 434 repressor was studied.[88] A family of these chimeras containing variations on the 14 residue helix were found to target the operator half-site sequence of 5'-ACAA-3'. Under identical conditions, no specific cleavage by the metallointercalator lacking the appended peptide was observed. However, cleavage was seen both to the 5'-side and within this recognition sequence. Since the stability of the α-helix is not as high as in the P_{22} chimera, the peptide was not a rigid, well-defined structure. Whether this was due to the lack of α-helicity or the flexibility of the peptide relative to the metallointercalator is not known. If the peptide α-helix was oriented as in the crystal structure of the full protein oligonucleotide complex, cleavage would be expected to the 5'-side of the DNA site. These results would indicate that different orientations of the peptide relative to the site and to the metal center might be available and which could be account for the cleavage. Thus, in the rhodium(III)-434 helix system, recognition of the expected peptide binding site was achieved.

In contrast to these α-helix systems, the zinc finger is a small well-defined structural domain that is used for DNA recognition.[43] Studies on DNA

recognition indicate that each zinc finger uses specific amino acids to recognize its three base pair binding site. Even though it has the correct structure, a single finger does not bind to DNA with any sequence specificity.[29,74,75] Previous work with metal-helix chimeras has shown that phi complexes of rhodium can deliver a peptide to the major groove of DNA. In the following chapters, rhodium - zinc finger chimeras will be constructed by covalently attaching the complex to the amino terminus of a single zinc finger peptide. This would provide a small system with which to design a library of sequence-specific DNA binding molecules in addition to providing the first opportunity to study the interaction of a single zinc finger with DNA.

1.8. REFERENCES

(1) Zawel, L.; Reinberg, D. *Annu. Rev. Biochem.* **1995**, *64*, 533-561.

(2) Mitchell, P. J.; Tjian, R. *Science* **1989**, *245*, 371-378.

(3) Pabo, C. O.; Sauer, R. T. *Annu. Rev. Biochem.* **1992**, *61*, 1053-95.

(4) Englke, D. R.; Ng, S.-Y.; Shastry, B. S.; Roeder, R. G. *Cell* **1980**, *19*, 717-728.

(5) Hanas, J. S.; Hazuda, D. J.; Bogenhagen, D. F.; Wu, F. Y.-H.; Wu, C.-W. *J. Bio. Chem.* **1983**, *158*, 14120-14125.

(6) Ginsberg, A. M.; King, B. O.; Roeder, R. G. *Cell* **1984**, *39*, 479-489.

(7) Miller, J.; McLachlan, A. D.; Klug, A. *EMBO J.* **1985**, *4*, 1609-1614.

(8) Brown, R. S.; Sander, C.; Argos, P. *FEBS* **1985**, *186*, 271-274.

(9) Diakun, G. P.; Fairall, L.; Klug, A. *Nature* **1986**, *324*, 698-699.

(10) Berg, J. M. *Proc. Natl. Acad. Sci. USA* **1988**, *85*, 99-102.

(11) Gibson, T. J.; Postma, J. P. M.; Brown, R. S.; Argos, P. *Prot. Engin.* **1988**, *2*,

209-210.

(12) Párraga, G.; Horvath, S. J.; Eisen, A.; Taylor, W. E.; Hood, L.; Young, E. T.; Klevit, R. E. *Science* **1988**, *241*, 1489-1492.

(13) Lee, M. S.; Gippert, G. P.; Soman, K. V.; Case, D. A.; Wright, P. E. *Science* **1989**, *245*, 635-637.

(14) Klevit, R. E.; Herriott, J. R.; Horvath, S. J. *Prot. Struct. Funct. Gen.* **1990**, *7*, 215-226.

(15) Omichinski, J. G.; Clore, G. M.; Appella, E.; Sakaguchi, K.; Gronenborn, A. M. *Biochem.* **1990**, *29*, 9324-9334.

(16) Neuhaus, D.; Nakaseko, Y.; Nagai, K.; Klug, A. *FEBS Lett.* **1990**, *262*, 179-184.

(17) Kochoyan, M.; Keutmann, H. T.; Weiss, M. A. *Biochem.* **1991**, *30*, 7063-7072.

(18) Kochoyan, M.; Havel, T. F.; Nguyen, D. T.; Dahl, C. E.; Keutmann, H. T.; Weiss, M. A. *Biochem.* **1991**, *30*, 3371-3386.

(19) Xu, R. X.; Horvath, S. J.; Klevit, R. E. *Biochem.* **1991**, *30*, 3365-3371.

(20) Palmer III, A. G.; Rance, M.; Wright, P. E. *J. Am. Chem. Soc.* **1991**, *113*, 4371-4380.

(21) Omichinski, J. G.; Clore, G. M.; Robien, M.; Sakaguchi, K.; Appella, E.; Gronenborn, A. *Biochem.* **1992**, *31*, 3907-3917.

(22) Nakaseko, Y.; Neuhaus, D.; Klug, A.; Rhodes, D. *J. Mol. Biol.* **1992**, *228*, 619-636.

(23) Lee, M. S.; Palmer III, A. G.; Wright, P. E. *J. Biomol. NMR* **1992**, *2*, 307-322.

(24) Neuhaus, D.; Nakaseko, Y.; Schwabe, J. W. R.; Klug, A. *J. Mol. Biol.* **1992**, *228*, 637-651.

(25) Bernstein, B. E.; Hoffman, R. C.; Horvath, S.; Heriott, J. R.; Klevit, R. E. *Biochem.* **1994**, *33*, 4460-4470.

(26) Dutnall, R. N.; Neuhaus, D.; Rhodes, D. *Structure* **1996**, *4*, 599-611.

(27) Párraga, G.; Horvath, S. J.; Hood, L.; Young, E. T.; Klevit, R. E. *Proc. Natl. Acad. Sci. USA* **1990**, *87*, 137-141.

(28) Lee, M. S.; Mortshire-Smith, R. J.; Wright, P. E. *FEBS Lett.* **1992**, *309*, 29-32.

(29) Frankel, A. D.; Berg, J. M.; Pabo, C. O. *Proc. Natl. Acad. Sci. USA* **1987**, *84*, 4841-4845.

(30) Weiss, M. A.; Keutmann, H. T. *Biochem.* **1990**, *29*, 9808-9813.

(31) Kochoyan, M.; Keutmann, H. T.; Weiss, M. A. *Proc. Natl. Acad. Sci. USA* **1991**, *88*, 8455-8459.

(32) Mortshire-Smith, R. J.; Lee, M. S.; Bolinger, L.; Wright, P. E. *FEBS Lett.* **1992**, *296*, 11-15.

(33) Qian, X.; Weiss, M. A. *Biochem.* **1992**, *31*, 7463-7476.

(34) Jasanoff, A.; Weiss, M. A. *Biochem.* **1993**, *32*, 1423-1432.

(35) Hoffman, R. C.; Horvath, S. J.; Klevit, R. E. *Prot. Science* **1993**, *2*, 951-965.

(36) Thukral, S. K.; Morrison, M. L.; Young, E. T. *Proc. Natl. Acad. Sci., USA* **1991**, *88*, 9188-9192.

(37) Blumberg, H.; Eisen, A.; Sledziewski, A.; Bader, D.; Young, E. T. *Nature* **1987**, *328*, 443-445.

(38) Krizek, B. A.; Amann, B. T.; Kilfoil, V. J.; Merkle, D. L.; Berg, J. M. *J. Am. Chem. Soc.* **1991**, *113*, 4518-4523.

(39) Michael, S. F.; Kilfoil, V. J.; Schmidt, M. H.; Amann, B. T.; Berg, J. M. *Proc. Natl. Acad. Sci. USA* **1992**, *89*, 4796-4800.

(40) Harper, L. V.; Amann, B. T.; Vinson, V. K.; Berg, J. M. *J. Am. Chem. Soc.* **1993**, *115*, 2577-2780.

(41) Berg, J. M.; Merkle, D. L. *J. Am. Chem. Soc.* **1989**, *111*, 3759-3761.

(42) Krizek, B. A.; Berg, J. M. *Inorg. Chem.* **1992**, *31*, 2984-2986.

(43) Berg, J. M. *Acc. Chem. Res.* **1995**, *28*, 14-19.

(44) Schmiedeskamp, M.; Klevit, R. E. *Curr. Opin. Struct. Biol.* **1994**, *4*, 28-35.

(45) Krizek, B. A.; Zawadzke, L. E.; Berg, J. M. *Prot. Sci.* **1993**, *2*, 1313-1319.

(46) Brüschweiler, R.; Liao, X.; Wright, P. E. *Science* **1995**, *268*, 886-889.

(47) Sakonju, S.; Brown, D. D. *Cell* **1982**, *31*, 395-405.

(48) Rhodes, D. *EMBO J.* **1985**, *4*, 3473-3482.

(49) Pavletich, N. P.; Pabo, C. O. *Science* **1991**, *252*, 809-817.

(50) Pavletich, N. P.; Pabo, C. O. *Science* **1993**, *261*, 1701-1707.

(51) Fairall, L.; Schwabe, J. W. R.; Chapman, L.; Finch, J. T.; Rhodes, D. *Nature* **1993**, *366*, 483-487.

(52) Nardelli, J.; Gibson, T. J.; Vesque, C.; Charnay, P. *Nature* **1991**, *349*, 175-178.

(53) Theisen, H.-J.; Bach, C. *FEBS Letters* **1991**, *283*, 23-26.

(54) Desjarlais, J. R.; Berg, J. M. *Prot. Strut. Funct. Gen.* **1992**, *12*, 101-104.

(55) Desjarlais, J. R.; Berg, J. M. *Proc. Natl. Acad. Sci., USA* **1992**, *89*, 7345-7349.

(56) Thukral, S. K.; Morrison, M. L.; Young, E. T. *Mol. Cell. Biol.* **1992**, *12*, 2784-2792.

(57) Taylor, W. E.; Suruki, H. K.; Lin, A. H. T.; Naraghi-Arani, P.; Igarashi, R. Y.; Younessain, M.; Katkus, P.; Vo, N. V. *Biochem.* **1995**, *34*, 3222-3230.

(58) Cheng, C.; Young, E. T. *J. Mol. Biol.* **1995**, *251*, 1-8.

(59) Desjarlais, J. R.; Berg, J. M. *Proc. Natl. Acad. Sci., USA* **1993**, *90*, 2256-2260.

(60) Shi, Y. G.; Berg, J. M. *Chem. Biol.* **1995**, *2*, 83-89.

(61) Rebar, E. J.; Pabo, C. O. *Science* **1994**, *263*, 671-673.

(62) Choo, Y.; Klug, A. *Proc. Natl. Acad. Sci. USA* **1994**, *91*, 11168-11172.

(63) Jamieson, A. C.; Kim, S.-H.; Wells, J. A. *Biochem.* **1994**, *33*, 5689-5695.

(64) Choo, Y.; Klug, A. *Curr. Opin. Str. Biol.* **1995**, *6*, 431-436.

(65) Rebar, E. J.; Greisman, H. A.; Pabo, C. O. *Meth. Enz.* **1996**, *267*, 129-149.

(66) Choo, Y.; Sanchez-Garcia, I.; Klug, A. *Nature* **1994**, *372*, 642-645.

(67) Suzuki, M.; Brenner, S. E.; Gerstein, M.; Yagi, N. *Prot. Eng.* **1995**, 319-328.

(68) Suzuki, M.; Yagi, N. *Proc. Natl. Acad. Sci. USA* **1994**, *91*, 12357-12361.

(69) Suzuki, M.; Gerstein, M.; Yagi, N. *Nucl. Acids Res.* **1994**, *22*, 3397-3405.

(70) Kadonaga, J. T.; Courey, A. J.; Ladika, J.; Tjian, R. *Science* **1988**, *242*, 1566-1570.

(71) Sakaguchi, K.; Appella, E.; Omichinski, J. G.; Clore, G. M.; Gronenborn, A. M. *J. Biol. Chem.* **1991**, *11*, 7306-7311.

(72) Fairall, L.; Harrison, S. D.; Travers, A. A.; Rhodes, D. *J. Mol. Biol.* **1992**, *226*, 349-366.

(73) Pedone, P. V.; Ghirlando, R.; Clore, G. M.; Gronenborn, A. M.; Felsenfeld, G.; Omichinski, J. G. *Proc. Natl. Acad. Sci. USA* **1996**, *93*, 2822-2826.

(74) Lee, M. S.; Gottsfeld, J. M.; Wright, P. E. *FEBS Lett.* **1991**, *279*, 289-294.

(75) Nedved, M.; Moe, G. R. *Nucl. Acids Res.* **1994**, *22*, 4705-4711.

(76) Johann, T. W.; Barton, J. K. *Phil. Trans. Royal Soc. London Ser. A Math. Eng. Sci.* **1996**, *354*, 299-324.

(77) Stemp, E. D. A.; Barton, J. K. In *Metal Ions In Biological Systems*; Marcel Dekker, Inc.: New York, NY, 1996; Vol. 33, pp 325-365.

(78) Pyle, A. M.; Long, E. C.; Barton, J. K. *J. Am. Chem. Soc.* **1989**, *111*, 4520-4522.

(79) Sitlani, A.; Long, E. C.; Pyle, A. M.; Barton, J. K. *J. Am. Chem. Soc.* **1992**, *114*,

2303-2312.

(80) David, S. S.; Barton, J. K. *J. Am. Chem. Soc.* **1993**, *115*, 2984-2985.

(81) Hudson, B. P.; Dupureur, C. M.; Barton, J. K. *J. Am. Chem. Soc.* **1995**, *117*, 9379-9380.

(82) Collins, J. G.; Shields, T. P.; Barton, J. K. *J. Am. Chem. Soc.* **1994**, *116*, 9840-9846.

(83) Krotz, A. H.; Hudson, B. P.; Barton, J. K. *J. Am. Chem. Soc.* **1993**, *115*, 12577-12578.

(84) Uchida, K.; Pyle, A. M.; Morii, T.; Barton, J. K. *Nucl. Acids Res.* **1989**, *17*, 10259-10279.

(85) Pyle, A. M.; Chiang, M. Y.; Barton, J. K. *Inorg. Chem.* **1990**, *29*, 4487-4495.

(86) Krotz, A. H.; Kuo, L. Y.; Barton, J. K. *Inorg. Chem.* **1993**, *32*, 5963-5974.

(87) Sardesai, N. Y.; Zimmermann, K.; Barton, J. K. *J. Am. Chem. Soc.* **1994**, *116*, 7502-7508.

(88) Sardesai, N. Y. Ph.D. Thesis, California Institute of Technology 1995.

Chapter 2. The Synthesis of Covalent Chimeras of Phi Complexes of Rhodium(III) and Zinc Finger Peptides*

2.1. INTRODUCTION

The synthesis of peptides which are covalently bound to transition metal ions or complexes has been the focus of much research.[1-24] The metal ion can provide a unique, well defined coordination geometry which can be used to define the tertiary structure of a peptide,[1-18] or the metal ion can serve a catalytic function.[19-24] Conveniently, transition metal complexes also provide a spectroscopic handle to assay function. Examples of the incorporation of coordination chemistry into peptide design include the application of metal ion coordination to stabilize peptide α-helices,[1-8] β-turns,[9] and the *de novo* design of three and four helix bundle proteins, through crosslinking peptide helices by metal ions,[1-6,10-13] and the construction of donor-acceptor assemblies in studies of photoinduced electron transfer across peptides.[14-17]

A general method for the synthesis and characterization of rhodium complexes tethered to different peptides has been developed in our laboratory.[25] For example, Figure 2.1 illustrates a rhodium(III) - zinc finger peptide chimera. Our strategy involves extending the solid phase peptide synthesis by covalently coupling metal complexes to the peptides. New ligands (L†) of 1,10-

---

*Adapted from Sardesai, N. Y.; Lin, S. C.; Zimmermann, K.; Barton, J. K. *Bioconj. Chem.* **1995**, *6*, 302-312.

†The abbreviations used in this chapter are as follows: Bom: benzyloxymethyl; BOP: benzotriazole *N*-oxytrisdimethylaminophosphonium hexafluorophosphate; Br-Z: 2-bromobenzyloxycarbonyl; Bzl: Benzyl; Cl-Z: 2-chlorobenzyloxycarbonyl; bpy: 2,2'-bipyridyl; bpy': 4-(4-carboxybutyl),4'-methyl-2,2'-bipyridine; DBU: 1,8-diazabicyclo[5.4.0]undec-7-ene; DCC: *N,N*-dicyclohexylcarbodiimide; DIEA: *N,N*-diisopropylethylamine; DMAP: 4-(dimethylamino)-pyridine; DMF: *N,N*-dimethylformamide; DSC: *N,N*-disuccinimidyl carbonate; DTT: dithiothreitol; ESI: electrospray ionization; FAB: fast atom bombardment; FMOC: 9-fluorenylmethoxycarbonyl; HMP: 4-hydroxymethylphenoxy; HOAt: 1-hydroxy-7-azabenzotriazole; HOBt: 1-hydroxybenzotriazole; L: ligand, bpy' or phen'; MALDI: matrix assisted laser desorption/ionization mass spectrometry; MeOBzl: 4-methoxybenzyl; MS: mass spectrometry; Mts: mesitylene-2-sulfonyl;

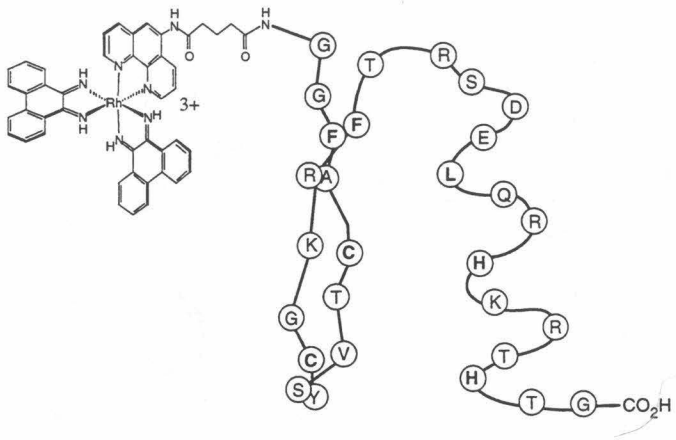

Figure 2.1. *Representative rhodium(III) - zinc finger peptide chimera showing a 29 residue peptide tethered to* $[Rh(phi)_2(phen)]^{3+}$ *via a glutaryl linker on the 1,10-phenanthroline.*

phenanthroline (phen) and 2,2'-bipyridine (bpy) containing carboxylate groups were synthesized and then coordinated to 9,10-phenanthrenequinone diimine (phi) complexes of rhodium(III). This created rhodium complexes containing a reactive moiety which facilitated coupling of the complex to a peptide (Figure 2.2). Peptides that were between 5 and 30 amino acids long have been synthesized using standard solid phase synthesis techniques.[26-28] Two distinct coupling methods have been developed to link the metal complex to the amino terminus of the peptide: the direct coupling method and the coordination method. In the direct coupling method, the carboxylate moiety of the rhodium complex is used to couple the metal complex to the peptide, using standard peptide coupling techniques.[26-28] In contrast, the coordination method first couples the resin-bound peptide to L, followed by coordination of the $[Rh(phi)_2]^{3+}$ unit to L.

NMM: N-methylmorpholine; NMP: 4-methylpyrrolidone; OBzl: benzyl; ODhbt: 3,4-dihydro-4-oxo-1,2,3-benzotriazin-3-yl; OPfp: pentafluorophenyl; PAM: phenylacetamidomethyl; PD: plasma desorption; PEG: polyethylene glycol; phen: 1,10-phenenthroline; phen': (5-amidoglutaryl)-1,10-phenanthroline; phi: 9,10-phenanthrenequinone diimine; PMC: 2,2,5,7,8-pentamethylchroman-6-sulfonyl; tBoc: *tert.*-butyloxycarbonyl; tBu: *tert.*-butyl; TFA: trifluoroacetic acid; TFMSA: trifluoromethanesulfonic acid; t_r: HPLC retention time; TSTU, *O*-(*N*-succinimuidyl)-*N,N,N'*-tetramethyluronium tetrafluoroborate; Trt: triphenylmethyl.

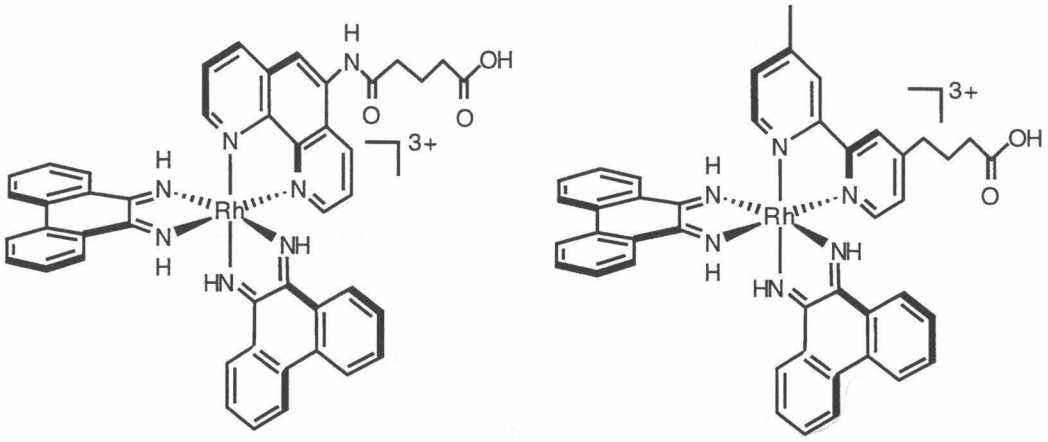

Figure 2.2. *The structures of* $[Rh(phi)_2(phen')]^{3+}$ *(left) and* $[Rh(phi)_2(bpy')]^{3+}$ *(right).*

In this thesis, all the rhodium(III) - zinc finger chimeras that are discussed were synthesized using the direct coupling method. Details of the synthesis of zinc finger peptide chimeras and improvements over the literature protocol will be described in this chapter.

2.2. EXPERIMENTAL

2.2.1. Materials. $RhCl_3 \cdot 6H_2O$ was purchased from Alfa-Aesar Johnson-Matthey and 5-amino-1,10-phenanthroline was purchased from Polysciences Inc. All other chemicals were purchased from Aldrich. Anhydrous solvents were purchased from Fluka. 4-(4-carboxybutyl)-4'-methyl-2,2'-bipyridine (bpy') was prepared by the method of Ciana, Hamachi and Meyer.[29] $[Rh(phi)_2Cl_2]Cl$ was synthesized following published protocols.[30] For manual FMOC synthesis, PEG resin, BOP and the amino acids were purchased from Milligen.

2.2.2. Instrumentation. The ^1H NMR spectra were recorded on a General Electric QE Plus 300 MHz spectrometer. Circular dichroism studies were performed on a Jasco J-500 spectrometer. Fast protein liquid chromatography (FPLC) was performed on a Pharmacia system consisting of a LCC-500 Plus

liquid chromatography controller, two p-500 pumps, a LKB 2141 variable wavelength monitor and a Frac-100 fraction collector using a Pep/RPC 10/10 C-18 reverse phase column. High performance liquid chromatography (HPLC) was carried out on a Waters 600E system equipped with a Waters 484 tunable UV-visible detector. Ultraviolet-visible spectra were recorded on a Hewlett-Packard 8452A diode array or a Cary 219 UV-visible spectrophotometer. The concentrations of metal-peptide complexes were determined by UV-visible spectroscopy using ε_{350} (isobestic)=23,600 $M^{-1}cm^{-1}$. Automated FMOC and tBoc syntheses were done on ABI433 and ABI430 peptide synthesizers, respectively, and the amino acid analysis was done on an ABI420 amino acid analyzer by the Biopolymer Synthesis and Analysis Resource Center at Caltech. The fast atom bombardment mass spectrometry (FAB MS) was performed at the UC Riverside Mass Spectrometry facility. ^{252}Cf plasma desorption mass spectrometry (PD MS) was recorded on a time-of-flight spectrometer (Bio-Ion/ Applied Biosystems 20 K, Uppsala, Sweden). The mass scale was calibrated with the hydrogen and nitrate ions and the experimental error is <1 m/z per 2000 m/z. Electrospray ionization mass spectrometry (ESI MS) was done on a Hewlett-Packard 59987A Electrospray Interface and an HP 5989B MS Engine quadrapole mass spectrometer by the Caltech Division of Chemistry and Chemical Engineering Mass Spectrometry Laboratory which was part of the Bank of America Environmental Analysis Center. Under the low resolution conditions used, the molecular weights determined will fall between the 'monoisotopic mass' and the average molecular weight. The experimental error was ± 0.1 m/z.

2.2.3. Synthesis of Ligands and Metal Complexes. ***5-(amidoglutaryl)-1, 10-phenanthroline (phen').*** 5-amino-1,10-phenanthroline (1.0 g, 5.1 mmol) was placed in a 100 mL round bottom flask and 50 mL anhydrous pyridine was

added. The slurry was heated to 70°C and then glutaric anhydride (1.17 g, 10.2 mmol) was added. Finally, the temperature was increased to 100°C. More glutaric anhydride was added after stirring for 1 hr (585 mg, 5.1 mmol) and after 2 hrs (1.17 g, 10.2 mmol). After 4 hrs, the solution was transferred to larger flask, the solvent volume was reduced to 5 mL and 250 mL of acetonitrile was added. The solution sat at room temperature for 1 hr to precipitate the desired product. The precipitate was collected by filtration and washed with acetonitrile (2 x 20 mL) to yield phen' as an off-white powder (1.02 g, 3.3 mmol, 64%). TLC (thin layer chromatography) [silica gel, without fluorescent indicator; CH_2Cl_2-MeOH (1:1); stained with $(NH_4)_2Fe(SO_4)_2$] : R_f = 0.41. ^1H NMR: (d_6-DMSO) 1.88 (*quint., J* = 7.3, 2H, CH_2-$\underline{CH_2}$-CH_2); 2.33 (*t, J = 7.3*, 2H, CH_2-COO); 2.56 (*t, J = 7.3*, CH_2-CON); 7.70 (*dd, J = 8.1*, 4.3, 1H, H-C(8)); 7.78 (*dd, J = 8.4, 4.3*, 1H, H-C(3)); 8.15 (*s*, 1H , H-C(6)); 8.41 (*dd, J = 8.1, 1.7*, 1H, H-C(7)); 8.60 (*dd, J = 8.4, 1.6*, 1H, H-C(4)); 8.99 (*dd, J = 4.3, 1.7*, 1H, H-C(9)); 9.09 (*dd, J = 4.3, 1.6*, 1H, H-C(2)); 10.11 (*s br*, 1H, NH); 12.12 (*s br*, 1H, OH).

Bis(phenanthrenequinone diimine)bis(dimethylformamide)rhodium(III) tritriflate, [Rh(phi)$_2$(DMF)$_2$](OTf)$_3$. [Rh(phi)$_2$Cl$_2$]Cl (187.6 mg, 301.7 μmol), prepared as described earlier,[30] and silver triflate (AgOTf) (233.2 mg, 907.6 μmol, 1 eq) were placed in a 25 mL round bottom flask and evacuated and purged with argon five times. Then, 10 mL dry DMF was added and the solution was heated to 65°C and stirred overnight in the dark. The solution was filtered through a medium frit and used immediately in coordination reactions.

Bis(phenanthrenequinone diimine)((5-amidoglutaryl)-1,10-phenanthroline)rhodium(III) trichloride, [Rh(phi)$_2$(phen')]Cl$_3$. A solution of [Rh(phi)$_2$(DMF)$_2$](OTf)$_3$ (300 μmol) in DMF was filtered directly into a flask containing phen' (113.0 mg, 365.3 μmol) and heated under argon for 18 hrs at 65°C. The reaction mixture was diluted with 50 mL 1:1 H_2O/CH_3CN and loaded

onto a Sephadex SP C-50, 40-120μ (H^+-form) cation exchange column. The column was then washed with 300 mL H_2O/CH_3CN. The product mixture was chromatographed with a HCl-gradient (0.1 N- 0.2 N HCl in H_2O/CH_3CN). The main orange band was eluted at ca. 0.15 N HCl. The solvents were removed in vacuo and the residue was dissolved in 250 mL H_2O. After lyophilization, $[Rh(phi)_2(phen')]Cl_3$ (270.7 mg, 96%) was obtained as an orange fluffy powder. ^{1}H-NMR (d_6-DMSO, 300 MHz): 1.86-1.96 (*m*, 2H, $CH_2C\underline{H_2}CH_2$); 2.36 (*t, J = 7.3*, 2H, CH_2COO); 2.71 (*t, J = 7.3*, 2H, CH_2CON); 7.52 (*t, J = 7.6*, 1H); 7.63 (*t, J = 7.6*, 1H); 7.78 (*t, J = 7.7*, 1H); 7.84 (*t, J = 7.8*, 1H); 8.09 (*dd, J = 8.3, 5.4*, 1H); 8.18 (*dd, J = 8.6, 5.3*, 1H); 8.43-8.54 (*m*, 8H); 8.61-8.64 (*m*, 1H); 8.66 (*s*, 1H); 8.75 (*d, J = 7.8*, 1H); 8.86 (*d(br), J = 7.9*, 1H); 8.90 (*d, J = 5.4*, 1H); 8.984 (*d, J = 7.7*, 1H); 8.985 (*d, J = 8.3*, 1H); 9.03 (*d, J = 5.3*, 1H); 9.28 (*d, J = 8.6*, 1H); 10.94 (*s*, 1H, H-N (amide)); 14.09, 14.12 (*2s*, 1H ea.); 14.26, 14.29 (*2s*, 1H ea.). UV-Vis (H_2O, pH 5) λ_{max} (ε $M^{-1}cm^{-1}$): 251 (69,800); 270 (83,300); 380 (32,900). FAB MS: $Rh(phi)_2(phen')^{3+}$: (obs.) 824, (calc.) 824.7; $[Rh(phi)_2(phen')^{3+}-H^+]^{2+}$: (obs.) 823, (calc.) 823.7; $[Rh(phi)_2(phen')^{3+}-2H^+]^+$: (obs.) 822, (calc.) 822.7; $[Rh(phi)(phen')]^{3+}$: (obs.) 618, (calc.) 618.5; $[Rh(phi)_2]^{3+}$: (obs.) 515, (calc.) 515.4; $[Rh(phen')]^{3+}$: (obs.) 412 , (calc.) 412.2.

Bis(phenanthrenequinone diimine)(4-(4-carboxybutyl), 4'-methyl-2,2'-bipyridine)rhodium(III) trichloride, $[Rh(phi)_2(bpy')]Cl_3$. A solution of $[Rh(phi)_2(DMF)_2](OTf)_3$ (189 μmol) in DMF was filtered directly into a flask containing bpy' (56.5 mg, 220.3 μmol), and the solution was heated at 65°C overnight. The reaction mixture was diluted with 50 mL 1:1 H_2O/CH_3CN and loaded onto a Sephadex SP C-50, 40-120μ (H^+-form) cation exchange column. The column was washed with 300 mL H_2O/CH_3CN and eluted with a gradient of 0 - 0.2 N HCl. The main orange band was collected and lyophilized to yield 118.6 mg (135.1 μmol, 71.5%) of $[Rh(phi)_2(bpy')]Cl_3$ as an orange powder. TLC: (silica gel, without FI; n-BuOH-H_2O-AcOH = 5:3:2; R_f = 0.17 - 0.21 (orange,

double spot). ^{1}H-NMR (D_2O, water suppression 300 MHz): 2.06 (*m (quint.)*, 2H, C^2H_2); 2.46 (*t, J = 7.2*, 2H, C^3H_2); 2.64 (*s*, 3H H_3C-(C(4'))); 2.98 (*t, J = 7.5*, 2H, C^1H_2); 7.54-7.65 (*m (quint. t)*, 6H), 7.80-7.88 (*m (q)*, 4H), 8.25-8.42 (*m*, 10H), 8.52 (*s br*, 2H) signals of aromatic protons of bpy and phi. UV/VIS (H_2O, pH 5) λ_{max} (ε $M^{-1}cm^{-1}$): 270 (66700); 295 (48200); 385 (32300). PD MS: $[Rh(phi)_2(bpy')^{3+}-2H^+]^+$: (obs.) *m/z* 769.8, (calc.) *m/z* 769.7; $[Rh(phi)(bpy')^{3+}-2H^+]^+$: (obs.) *m/z* 564.8, (calc.) *m/z* 563.5; $[Rh(phi)_2^{3+}-2H^+]^+$: (obs.) *m/z* 515.2, (calc.) *m/z* 513.4) $[Rh(bpy')^{3+}-2H^+]^+$: (obs.) *m/z* 357.2, (calc.) *m/z* 357.2; $[Rh(phi)^{3+}-2H^+]^+$: (obs.) *m/z* 309.0, (calc.) *m/z* 307.3) $[bpy']^+$: (obs.) *m/z* 256.1, (calc.) *m/z* 256.3; $[phi]^+$: (obs.) *m/z* 206.1, (calc.) *m/z* 206.3.

Resolution of Enantiomers of [Rh(phi)$_2$(phen')]Cl$_3$. The eluent potassium (+) *tris*[*l*-cysteinesulphinato(2-)-S,N]cobaltate(III), $K_3[Co(l\text{-cysu})_3]$, was synthesized according to literature procedure.[31,32] A 115 x 2.5 cm column was filled with Sephadex-SP C-25 cation exchange resin that had been swelled in water. The resin was washed with 0.1 M KCl and then with copious amounts of water. $[Rh(phi)_2(phen')]Cl_3$ (100 mg) was dissolved in water and loaded on a minimum of resin. A 0.1 M $[Co(l\text{-cysu})_3]^{3-}$ solution was recirculated at a flow rate of approximately 1 mL/min. After 12 h, two distinct orange bands could be seen. Each band was isolated and eluted off the resin using 0.2 M HCl in 1:1 H_2O/CH_3CN. The bands were dried in vacuo, dissolved in water and lyophilized to yield Δ- and Λ- $[Rh(phi)_2(phen')]Cl_3$ (20 mg each). For the Δ-isomer, $\Delta\varepsilon_{280}$= -26 $M^{-1}cm^{-1}$; $\Delta\varepsilon_{450}$= -10 $M^{-1}cm^{-1}$.

The Stability of the Enantiomers of [Rh(phi)$_2$(phen')]Cl$_3$. The Δ-enantiomer of $[Rh(phi)_2(phen')]Cl_3$ (0.5 mg) was treated with 200 µL Reagent K (82.5% TFA, 5% H_2O, 5% phenol, 5% thioanisole and 2.5% ethanedithiol) for 5 hrs. After purification by FPLC, the circular dichroism spectrum showed no change in molar ellipticity.

2.2.4. Synthesis of Peptides. Automated tBoc syntheses were performed on an ABI430 peptide synthesizer by the Caltech Biopolymer Synthesis and Analysis Resource Center. *N*-α-tBoc-L-amino acids were used with the following side chain protecting groups: Arg(Mts),‡ Asp(OBzl), Cys(4-MeOBzl), Glu(OBzl), His(Bom), Lys(Cl-Z), Ser(Bzl), Thr(Bzl), Trp(CHO), Tyr(Br-Z).

Automated FMOC syntheses were done on an ABI433 peptide synthesizer by the Caltech Biopolymer Synthesis and Analysis Resource Center. The following protected side chain amino acids were used: Arg(PMC), Asn(Trt), Asp(OtBu), Cys(Trt), Gln(Trt), Glu(OtBu), His(Trt), Lys(tBoc), Ser(tBu), Thr(tBu), Tyr(tBu). The manual FMOC synthesis was performed according to standard procedures.[28] The *N*-α-FMOC-L-amino acids were OPfp esters, except for serine and threonine which were ODhbt esters, and arginine which was the free acid. The FMOC protecting group was removed using 2% (v/v) DBU in DMF.[33] The amino acid OPfp esters and ODhbt esters (4 eq.) were activated with HOBt (4 eq.). The free acids (4 eq.) were activated with BOP (4 eq.) and NMM (4 eq.). All couplings were monitored by ninhydrin[34] and the cycle was repeated until >99% coupling efficiency was achieved. The resin was capped with 0.3 M acetic anhydride/HOBt in 9:1 DMF/CH_2Cl_2.

The resins were received with the amino terminal protecting group removed. The peptide resins were stored dry at room temperature. A portion of each resin (50 mg) was cleaved and deprotected for characterization by HPLC, amino acid analysis and mass spectrometry.

Deprotection and Cleavage of Peptides. Cleavage and deprotection of the

---

‡ The one letter and three letter abbreviations for the amino acids are as follows: alanine: A, Ala; arginine: R, Arg; asparagine: N, Asn; aspartic acid: D, Asp; cysteine: C, Cys; glutamic acid: E, Glu; glutamine: Q, Gln; glycine: G, Gly; histidine: H, His; isoleucine: I, Ile; leucine: L, Leu; lysine: K, Lys; methionine: M, Met; phenylalanine: F, Phe; proline: P, Pro; serine: S, Ser; threonine: T, Thr: tryptophan: W, Trp, Tyrosine: Y, Tyr; valine: V, Val.

tBoc peptides was accomplished using HF cleavage in the presence of *p*-cresol and *p*-thiocresol for 60 min at 0°C.[26] The cleavage and deprotection of the FMOC peptides was done using 1 mL Reagent K per 50 mg coupled resin for 2 hrs at 25°C.[35] The cleavage solution was filtered into chilled (-20°C) *tert*-butyl methyl ether (50 mL) and centrifuged for 10 minutes at 10,000 rpm. The ether was decanted off and another 50 mL of ether was added. After centrifugation and decantation of the ether, the white precipitate was dissolved in 5% acetic acid and purified by HPLC.

HPLC Purification of Peptides. Peptides were purified on a Vydac semi-preparative C_{18} reverse phase column using a water (0.1% TFA)/acetonitrile (0.1% TFA) gradient (15% acetonitrile for 5 min., then 15%-40% acetonitrile over 20 min) with a flow rate of 4.0 mL/min. The elution profile was monitored at 220 nm. The time of elution (t_r) of the major peak is given. This product was collected and lyophilized.

Mass Spectrometric Characterization. Molecular weight determinations of the peptide were carried out using ^{252}Cf PD MS at an accelerating voltage of 15 kV or MALDI MS. For PD MS, the samples were adsorbed onto nitrocellulose surfaces by applying solutions of the peptides (200 pmol) in 25% acetonitrile (0.1% TFA)/ 75% water and allowed to dry. Excess salt, if present, was removed from the adsorbed samples by rinsing with 1:1 EtOH/water prior to data accumulation. For MALDI analysis, the lyophilized peptides were dissolved in water/0.1% TFA to the concentration of 1 mg/mL.

Test: GGFAE-CO_2H. This peptide was synthesized on the PEG resin using manual FMOC techniques. Amino acid analysis observed (calculated): Glx 2.2 (1), Gly 1.9 (2), Ala 1.2 (1), Phe 1.0 (1).

Sp1-2d: GGFACTVSYCGKRFTRSDELQRHKRTHTGE-CO_2H. This peptide was synthesized on the PAM resin using automated tBoc techniques. PD MS:

$[M]^+$ (obs.) *m/z* 3428.5 (calc.) *m/z* 3428.8.

Sp1-2f: GGFACTVSYCGKRFTRSDELQRHKRTHTG-CO_2H. This peptide without the two amino terminal glycines was synthesized on the HMP resin using automated FMOC techniques. The final two glycines were added using manual techniques. PD MS: $[M]^+$ (obs.) *m/z* 3299.6 (calc.) *m/z* 3299.7. The second synthesis was done completely using automated FMOC techniques. MALDI MS: $[M]^+$ (obs.) *m/z* 3299.8 (calc.) *m/z* 3299.7. HPLC: t_r = 16.4 min.

Sp1-3c: GGFACPECPKRFARSDHLSKHIKTHQN-CO_2H. This peptide without the two amino terminal glycines was synthesized on the HMP resin using automated FMOC techniques. The final two glycines were added using manual techniques. PD MS: $[FMOC-M]^+$ (obs.) *m/z* 3288.6 (calc.) *m/z* 3288.5.

ADR1b: GSFVCEVCTRAFARQEHLKRHYRSHTN-CO_2H. This peptide was synthesized twice on the HMP resin using automated FMOC techniques. PD MS: $[M]^+$ (obs.) *m/z* 3233.7, 3234.8 (calc.) *m/z* 3234.7. HPLC: t_r = 20.0 min.

ADR1b-Ala: GSFVCEVCTRAFARQEHLKRHARSHTN-CO_2H. This peptide was synthesized on the HMP resin using automated FMOC techniques. PD MS: $[M]^+$ (obs.) *m/z* 3141.1 (calc.) *m/z* 3141.6. HPLC: t_r = 19.6 min.

2.2.5. Synthesis of Metal-Peptide Chimeras. The coupling of $[Rh(phi)_2(bpy')]^{3+}$ and $[Rh(phi)_2(phen')]^{3+}$ to the above mentioned peptides has been successfully accomplished. The rhodium complexes are stable to HF and TFA peptide cleavage and deprotection conditions, allowing the complexes to be coupled using solid phase techniques to the peptide prior to cleavage from the resin.

Direct Coupling Strategy. *(a) DSC/DMAP method.*[25] $[Rh(phi)_2(phen')]Cl_3$ (13 mg, 14 μmol), DSC (3.6 mg, 14 μmol), DMAP (3.1 mg, 4.2 μmol) and DMAP (ca. 1 mg, 4 μmol) were placed in a 5 mL round-bottom flask. Anhydrous NMP

(0.5 mL) was added and the solution was stirred at room temperature for 15 min. This activation can also be done using DCC (1 eq.) and HOBt (1 eq.). The rhodium solution was added to peptide-resin (7 μmol) in a 5 mL round-bottom flask. The slurry was stirred under argon, in the dark, for 24 hrs. The resin was then washed with NMP until the filtrate was clear and then washed with CH_2Cl_2, 1:1 CH_2Cl_2/MeOH and absolute EtOH. Finally, the resin was dried in vacuo for several hours and the coupling was repeated. The intensity of the red color of the resin is an indicator of the efficiency of the coupling.

(b) OPfp method: $[Rh(phi)_2(bpy')]Cl_3$ (18 mg, 20 μmol), OPfp (12.5 μL, 20 mg, 110 μmol) and DCC (7.0 mg, 34 μmol) were placed in a 5 mL round-bottom flask. Anhydrous NMP (0.5 mL) was added and argon was bubbled through the solution for 15 minutes. The peptide resin (200 mg, ~25 μmol) was swelled in 0.5 mL anhydrous NMP. The rhodium solution was added to the resin followed by 2 μL DIEA (11 μmol) resulting a dark red color. The slurry was stirred under argon, in the dark, for 3 days. The resin was then washed with NMP until the filtrate was clear and then washed with CH_2Cl_2, 1:1 CH_2Cl_2/MeOH and absolute EtOH. Finally, the resin was dried in vacuo for several hours. The intensity of the red color of the resin is an indicator of the efficiency of the coupling.

(c) Collidine method: $[Rh(phi)_2(phen')]Cl_3$ (20 mg, 21 μmol), HOAt (3.0 mg, 22 μmol), DCC (4.4 mg, 21 μmol) and peptide resin (100 mg, ~13 μmol) were placed in a 5 mL round-bottom flask. Anhydrous NMP (1.0 mL) and 2,4,6-collidine (11.2 μL, 10.3 mg, 85 μmol) were added. The slurry was stirred under argon, in the dark, overnight. The resin then was washed with NMP until the filtrate was clear and then washed with CH_2Cl_2, 1:1 CH_2Cl_2/MeOH and absolute EtOH. Finally, the resin was dried in vacuo for several hours. The intensity of the red color of the resin is an indicator of the efficiency of the coupling.

Rhodium(III) - peptide resins were stored at room temperature.

Generally, a 20 mg portion was cleaved and deprotected for each analysis.

Deprotection and Cleavage of Metal-Peptide Chimeras. Cleavage and deprotection of the metal - tBoc peptide chimeras was done in the same fashion as the free peptides. The cleavage and deprotection of the metal - FMOC peptides chimeras was done using 1 mL Reagent K per 20 mg coupled resin for 8-16 hrs at 25°C.[35] The cleavage solution was filtered into chilled (-20°C) *tert*-butyl methyl ether (50 mL) and centrifuged for 10 minutes at 10,000 rpm. The ether was decanted off and another 50 mL of ether was added. After centrifugation and decantation of the ether, the orange precipitate was dissolved in 2 mL 5% acetic acid and immediately purified by HPLC.

HPLC Purification of Metal-Peptide Complexes. The metal-peptide complexes were purified in the same manner as the free peptide, but in one injection. All of the metal - peptide chimeras have a longer retention time (t_r) than the free peptide. The elution profile was monitored at 360 nm. The major peak was collected and the peptide was immediately folded using zinc(II) as will be described in chapter 3.

Mass Spectrometric Characterization. PD MS and MALDI samples of the chimeras were prepared in the same manner as the free peptides. For electrospray ionization MS, the HPLC samples were lyophilized and dissolved to 10 μM in 19.5% H_2O/79.5% CH_3CN/1% HOAc. The sample (10 μL) was introduced to the spray via loop injection with a sample flow rate of 10 μL/min. Nitrogen gas was passed over the sample at a flow rate of 6 - 13 L/min. at 175°C. Nebulizing gas was supplied at 80 psi. Peak widths were set to 1 m/z at half height.

[Rh(phi)$_2$(phen')]$^{3+}$-GGFAE-CO$_2$H. The rhodium complex was coupled using the DSC/DMAP technique. After cleavage and deprotection of 20 mg of resin for 2 hrs, 220 nmol (3.5%) of chimera was isolated. Amino acid analysis

observed (calculated) ratio: Glx 1.0 (1), Gly 2.0 (2), Ala 1.1 (1), Phe 1.0 (1). PD MS: $[M^{3+}\text{-}2H^{+}]^{+}$ (obs.) *m/z* 1283.3 (calc.) *m/z* 1284.2.

[Rh(phi)$_2$(phen')]$^{3+}$-Sp1-2d: The rhodium complex was coupled using the DSC/DMAP technique. After cleavage and deprotection of 160 mg resin by HF, 480 nmol (2.2%) of chimera was isolated as an orange powder. Amino acid analysis observed (calculated) ratio: Asx 0.9 (1) Glx 2.6 (3), Ser 2.0 (2), Gly 4.1 (4), His 1.7 (2), Arg 4.2 (4), Thr 3.8 (4), Val 1.2 (1), Ala 1.1 (1), Tyr 0.8 (1), Val 1.2 (1), Cys 2.9 (2.0), Ile 1.0 (1), Lys 1.9 (2). PD MS: $[M^{3+}\text{-}2H^{+}]^{+}$ (obs.) *m/z* 4234.2 (calc.) *m/z* 4233.6. HPLC: t_r = 18.3 min. (oxidized).

[Rh(phi)$_2$(bpy')]$^{3+}$-Sp1-2f: The rhodium complex was coupled using the OPfp technique. After cleavage and deprotection of 25 mg of resin with Reagent K for 16 hrs, 140 nmol (4.7%) of chimera was obtained. ESI-MS: $[M^{3+} + 2H^{+}]^{5+}$ (obs.) *m/z* 810.7 (calc.) *m/z* 810.3; $[M^{3+} + 3H^{+}]^{6+}$ (obs.) *m/z* 675.8 (calc.) *m/z* 675.1; $[M^{3+} + 4H^{+}]^{7+}$ (obs.) *m/z* 579.45 (calc.) *m/z* 578.48; $[M^{3+} + 5H^{+}]^{8+}$ (obs.) *m/z* 507.05 (calc.) *m/z* 506.05. HPLC: t_r = 20.2 min (reduced), 19.6 min (oxidized).

[Rh(phi)$_2$(phen')]$^{3+}$-Sp1-2f: The rhodium complex was coupled using the collidine technique. After cleavage and deprotection of 50 mg of resin with Reagent K for 16 hrs, 25 nmol (0.4%) of chimera was obtained. ESI-MS: $[M^{3+}+ H^{+}]^{4+}$ (obs.) *m/z* 1026.7 (calc.) *m/z* 1026.4; $[M^{3+} + 2H^{+}]^{5+}$ (obs.) *m/z* 821.3 (calc.) *m/z* 820.9; $[M^{3+} + 3H^{+}]^{6+}$ (obs.) *m/z* 684.7 (calc.) *m/z* 683.9;$[M^{3+} + 4H^{+}]^{7+}$ (obs.) *m/z* 586.95 (calc.) *m/z* 586.06. HPLC: t_r = 21.8 min (reduced).

[Rh(phi)$_2$(bpy')]$^{3+}$-Sp1-3c: The rhodium complex was coupled using the collidine technique. After cleavage and deprotection of 20 mg of resin with Reagent K for 15 hrs, 30 nmol (1.3%) of chimera was obtained. ESI-MS: $[M^{3+}+ H^{+}]^{4+}$ (obs.) *m/z* 954.7 (calc.) *m/z* 954.6;$[M^{3+} + 2H^{+}]^{5+}$ (obs.) *m/z* 763.9 (calc.) *m/z* 763.4; $[M^{3+} + 3H^{+}]^{6+}$ (obs.) *m/z* 636.8 (calc.) *m/z* 636.0; $[M^{3+} + 4H^{+}]^{7+}$ (obs.) *m/z* 545.95 (calc.) *m/z* 545.0. HPLC: t_r = 18.9 min (reduced).

[Rh(phi)$_2$(phen')]$^{3+}$-Sp1-3c: The rhodium complex was coupled using the collidine technique. After cleavage and deprotection of 20 mg of resin with Reagent K for 16 hrs, the chimera was obtained. ESI-MS: [M^{3+}+ H^+]$^{4+}$ (obs.) *m/z* 968.1 (calc.) *m/z* 967.8; [M^{3+} + $2H^+$]$^{5+}$ (obs.) *m/z* 774.5 (calc.) *m/z* 774.5; [M^{3+} + $3H^+$]$^{6+}$ (obs.) *m/z* 645.55 (calc.) *m/z* 644.9; [M^{3+} + $4H^+$]$^{7+}$ (obs.) *m/z* 553.5 (calc.) *m/z* 552.6. HPLC: t_r = 18.5 min (oxidized), t_r =19.3 min (reduced).

[Rh(phi)$_2$(bpy')]$^{3+}$-ADR1b: The rhodium complex was coupled using the OPfp technique. After cleavage and deprotection of 25 mg of resin with Reagent K for 16 hrs, 120 nmol (4.1%) of chimera was obtained. ESI-MS: [M^{3+}+ H^+]$^{4+}$ (obs.) *m/z* 996.40 (calc.) *m/z* 996.59;[M^{3+} + $2H^+$]$^{5+}$ (obs..) *m/z* 797.40 (calc.) *m/z* 797.07; [M^{3+} + $3H^+$]$^{6+}$ (obs.) *m/z* 664.55 (calc.) *m/z* 664.06; [M^{3+} + $4H^+$]$^{7+}$ (obs.) *m/z* 569.80 (calc.) *m/z* 569.05; [M^{3+} + $5H^+$]$^{8+}$ (obs.) *m/z* 498.70 (calc.) *m/z* 497.79. HPLC: t_r = 21.3 min (oxidized), t_r = 22.2 min (reduced).

[Rh(phi)$_2$(phen')]$^{3+}$-ADR1b: The rhodium complex was coupled using the collidine technique. After cleavage and deprotection of 20 mg of resin with Reagent K for 16 hrs, 15 nmol (0.6%) of the chimera was obtained. ESI-MS: [M^{3+} + $2H^+$]$^{5+}$ (obs.) *m/z* 808.2 (calc.) *m/z* 807.7; [M^{3+} + $3H^+$]$^{6+}$ (obs.) *m/z* 673.6 (calc.) *m/z* 672.9; [M^{3+} + $4H^+$]$^{7+}$ (obs.) *m/z* 577.55 (calc.) *m/z* 576.6. HPLC: t_r = 21.8 min (oxidized), t_r = 23.0 min (reduced).

[Rh(phi)$_2$(bpy')]$^{3+}$-ADR1b-Ala: The rhodium complex was coupled using the collidine technique. After cleavage and deprotection of 20 mg of resin with Reagent K for 16 hrs, 90 nmol (3.8%) of the chimera was obtained. ESI-MS: [M^{3+}+ H^+]$^{4+}$ (obs.) *m/z* 973.8 (calc.) *m/z* 973.6;[M^{3+} + $2H^+$]$^{5+}$ (obs..) *m/z* 779.1 (calc.) *m/z* 778.7; [M^{3+} + $3H^+$]$^{6+}$ (obs.) *m/z* 649.5 (calc.) *m/z* 648.7; [M^{3+} + $4H^+$]$^{7+}$ (obs.) *m/z* 556.85 (calc.) *m/z* 555.9. HPLC: t_r = 20.5 min (reduced).

[Rh(phi)$_2$(phen')]$^{3+}$-ADR1b-Ala: The rhodium complex was coupled using the collidine technique. After cleavage and deprotection of 20 mg of resin

with Reagent K for 16 hrs, the chimera was obtained. ESI-MS: $[M^{3+}+ H^{+}]^{4+}$ (obs.) *m/z* 986.9 (calc.) *m/z* 986.8; $[M^{3+} + 2H^{+}]^{5+}$ (obs.) *m/z* 789.7 (calc.) *m/z* 789.3; $[M^{3+} + 3H^{+}]^{6+}$ (obs.) *m/z* 658.3 (calc.) *m/z* 657.5; $[M^{3+} + 4H^{+}]^{7+}$ (obs.) *m/z* 564.4 (calc.) *m/z* 563.5. HPLC: t_r = 21.7 min (reduced).

Synthesis of Diasteriomerically Pure Chimeras. Λ and Δ-$[Rh(phi)_2(phen')]^{3+}$ were coupled to ADR1b using the DCC/HOBt method. The chimeras were cleaved and deprotected using Reagent K for 6 hours. The circular dichroism spectra of isolated chimeras showed no loss of diasteriomeric purity.

2.3. RESULTS

2.3.1. Synthesis of Functionalized Ligands and Rhodium Complexes.

Both bpy' and phen' may be readily prepared. Bpy' is synthesized as described by others in 30% yield (Figure 2.3).[29] Phen' is achieved in one step by reaction of 5-amino-1,10-phenanthroline with glutaric anhydride in dry pyridine in 50% yield (Scheme 2.1).

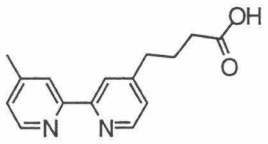

Figure 2.3. *The structure of bpy'.*

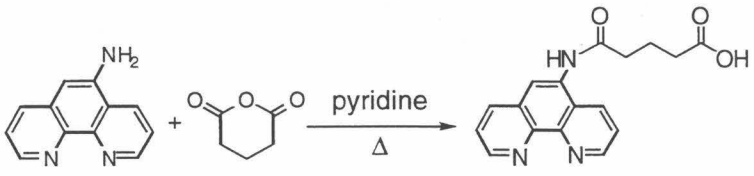

Scheme 2.1. *The synthesis of phen'.*

Scheme 2.2 illustrates the assembly of $[Rh(phi)_2(phen')]^{3+}$, which contains a pendant carboxylate for attachment to a peptide. To produce

$[Rh(phi)_2(phen')]Cl_3$, $[Rh(phi)_2Cl_2]Cl$ is first reacted with silver triflate to exchange the chloride ligands. The substitutionally facile $[Rh(phi)_2(DMF)_2](OTf)_3$ complex is heated with phen' to coordinate of the third chelating ligand. $[Rh(phi)_2(bpy')]Cl_3$ is synthesized in an analogous fashion.

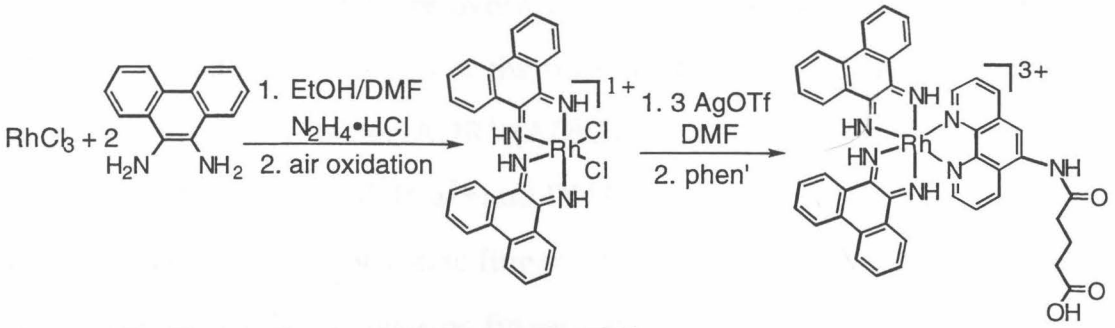

Scheme 2.2. *The synthesis of $[Rh(phi)_2(phen')]Cl_3$.*

The enantiomers of $[Rh(phi)_2(phen')]^{3+}$ can be resolved on a cation exchange column using the chiral eluent, (+) *tris*[*l*-cysteinesulphinato(2-)-S,N]cobaltate(III).[31,32] The isomers separate into two bands which show the characteristic CD spectra of enantiomers (Figure 2.4). The assignment of isomers is made based upon comparison to spectra of $[Rh(phen)_2(phi)]^{3+}$ and $[Rh(en)_2(phi)]^{3+}$ (en = ethylenediamine).[36,37]

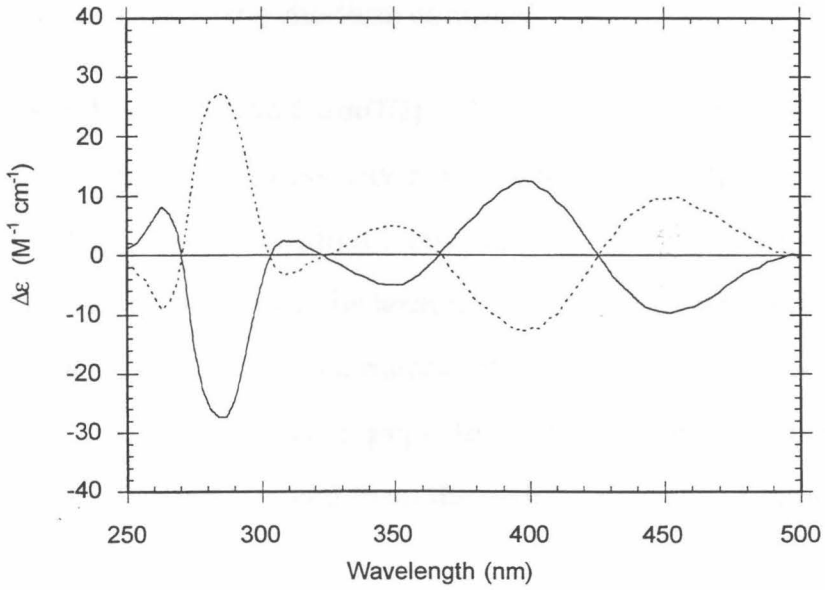

Figure 2.4. *Circular dichroism of the Δ- (——) and Λ- (·····) enantiomers of $[Rh(phi)_2(phen')]Cl_3$ in 10 mM Tris•HCl, pH 7.0.*

2.3.2. Synthesis of Peptides. One five amino acid peptide (test) and four zinc finger peptides have been synthesized using tBoc and FMOC chemistry. A small portion of each resin was cleaved and the free peptide analyzed by HPLC and mass spectrometry to check the integrity and efficiency of the synthesis. The zinc finger peptides that were synthesized correspond to the second finger (Sp1-2) and third finger (Sp1-3) of the transcription factor Sp1, and the second finger of transcription factor ADR1 (ADR1b). The ADR1b finger was chosen because the NMR structural data[38] and DNA specificity mutational studies have been published.[39,40] The Sp1 zinc finger protein was chosen because it derives from the same family of the zinc fingers as the Zif268 protein whose crystal structure bound to DNA has been published[41-43] and, unlike Zif268, has a wealth of biochemical studies done.[44-48] The two Sp1 zinc fingers and the ADR1b zinc finger also recognize different DNA sequences.[40,49] A zinc finger peptide (ADR1b-Ala) which has the native tyrosine of ADR1b replaced with an alanine was also made. For all the zinc finger peptides, two glycines or a glycine-serine dipeptide were placed before the first conserved phenylalanine to give flexibility and length to the linkage to the rhodium complex.

2.3.3. Synthesis of Rhodium(III) - Peptide Chimeras. All of the zinc finger peptides have been successfully coupled to both $[Rh(phi)_2(bpy')]^{3+}$ and $[Rh(phi)_2(phen')]^{3+}$ using the direct coupling method (Scheme 2.3). The functionalized metal complex and the terminal amine of the peptide bound to the resin are condensed in one step, in a manner that is analogous to the addition of another residue onto the growing peptide chain. Then, the metal-peptide complex is deprotected and cleaved from the resin in the same manner as for the free peptide.

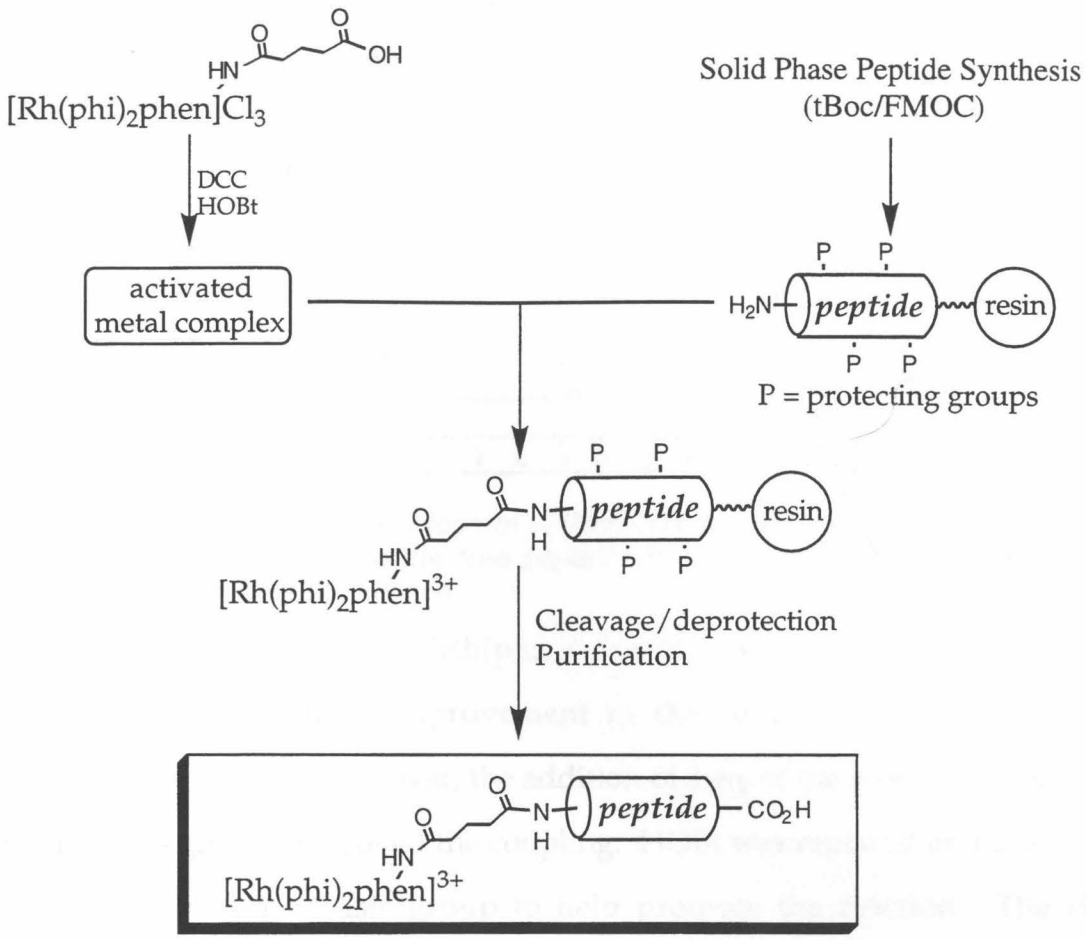

Scheme 2.3. *The direct coupling method for the synthesis of rhodium(III) - peptide chimeras.*

Previously, it was reported that DCC/HOBt or DSC/DMAP were found to be the most efficient reagents for direct coupling of $[Rh(phi)_2(bpy')]^{3+}$ and $[Rh(phi)_2(phen')]^{3+}$ to the peptide resin.[25] More recently, it has been determined that the HOBt can be replaced with an excess of OPfp. In the presence of OPfp, the coupling is achieved in three days and similar coupling efficiencies as with the DCC/HOBt method are obtained. Figure 2.5 shows the HPLC chromatogram of the $[Rh(phi)_2(bpy')]^{3+}$-ADR1b made via the OPfp method after cleavage and deprotection. The peaks corresponding to the free peptide and metal-peptide chimera (oxidized and reduced) are marked. The coupling exceeds a 90% yield.

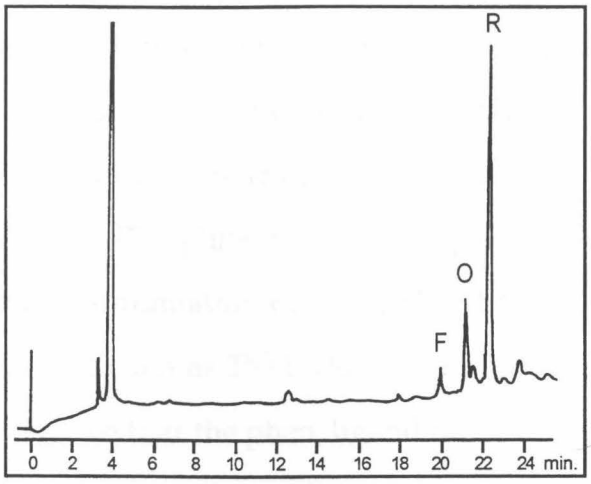

Figure 2.5. *The HPLC chromatogram of [Rh(phi)$_2$(bpy')]$^{3+}$ - ADR1b. λ_{obs} = 220 nm. The peaks corresponding to the free peptide (F) and coupled metal - peptide (O = oxidized, R = reduced) are marked.*

For the synthesis of [Rh(phi)$_2$(phen')]$^{3+}$-peptide conjugates, the OPfp method gave very little improvement in the coupling efficiency over the DCC/HOBt reaction. However, the addition of 4 eq. of the base 2,4,6-collidine to the reaction greatly improved the coupling. HOBt was replaced by HOAt which contains an internal basic group to help promote the reaction. The HPLC chromatogram of [Rh(phi)$_2$(phen')]$^{3+}$-ADR1b made via the collidine method shows ~50% coupling of the metal complex (Figure 2.6).

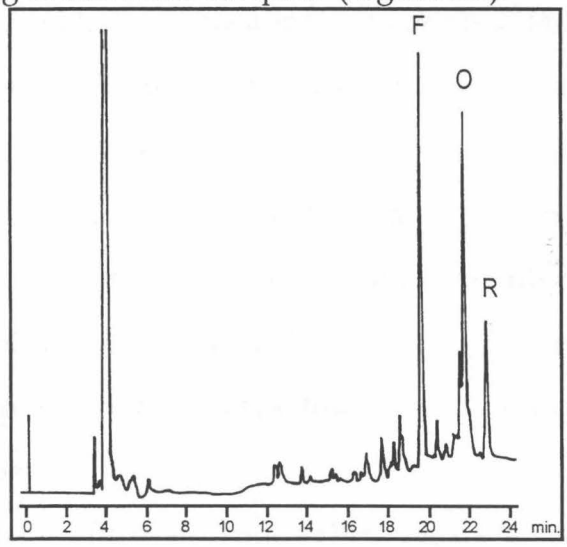

Figure 2.6. *The HPLC chromatogram of [Rh(phi)$_2$(phen')]$^{3+}$ - ADR1b. λ_{obs} = 220 nm. The peaks corresponding to the free peptide (F) and coupled metal - peptide (O = oxidized, R = reduced) are marked.*

While synthesis of $[Rh(phi)_2(bpy')]^{3+}$-peptide conjugates can be performed with a wide variety of reagents and with nearly quantitative yields, the synthesis of $[Rh(phi)_2(phen')]^{3+}$-peptide conjugates has proven to be more difficult. The most efficient coupling of $[Rh(phi)_2(phen')]^{3+}$ to peptides still attached to the resin is obtained from a combination of DCC, HOAt and 2,4,6-collidine. More reactive coupling reagents such as TSTU do not produce any coupled peptides. One reason for this could be that the phen' ligand can undergo an intramolecular cyclization which can compete with coupling in the presence of potent activating agents. However, not all the rhodium recovered after coupling is cyclized as observed by NMR. Thus some other effects such as the steric accessibility of the resin may also play a role in the reduced yields of the $[Rh(phi)_2(phen')]^{3+}$-peptides.

Both $[Rh(phi)_2(bpy')]^{3+}$ and $[Rh(phi)_2(phen')]^{3+}$ are stable to the conditions of cleavage and deprotection of the peptides off the resin. However, the metal-peptide chimeras are more difficult to cleave off the resin than the peptide alone. Longer reaction times are needed for the chimera (8-12 hrs) versus the free peptide (2 hrs). There appears to be no difference in the efficiency of the cleavage of the rhodium - peptide from the resin for $[Rh(phi)_2(bpy')]^{3+}$-peptides versus $[Rh(phi)_2(phen')]^{3+}$-peptides. Since the metal center is stable, pure diastereomers of rhodium(III) - peptide chimeras can then be obtained by direct coupling of the enantiomers of the rhodium complex to the peptide. The metal-peptide complexes were purified by HPLC. The retention time of the metal-peptide complexes was always found to be longer than that of the corresponding free peptide.

Theoretical yields of metal-peptide chimeras have been determined based upon the amount of peptide on the resin assuming 100% yield for the peptide synthesis. For the long zinc finger peptides discussed in this chapter, the final

yields of the metal - peptide conjugates range from 0.5 - 5%. However, the efficiency of the peptide synthesis limits the yields of the chimeras. Therefore, these numbers do not reflect the efficiency of the coupling. The HPLC chromatograms show the ratio of free to coupled peptide presenting a more accurate picture of the yield of the coupling reaction. $[Rh(phi)_2(bpy')]^{3+}$ can be coupled nearly quantitatively while $[Rh(phi)_2(phen')]^{3+}$ is approaching 50%. This is reflected in the fact that from the same peptide resin (ADR1b), almost ten times the amount of $[Rh(phi)_2(bpy')]^{3+}$ chimera (120 nmol) is produced as compared to the $[Rh(phi)_2(phen')]^{3+}$ chimera (15 nmol).

2.4. DISCUSSION

Several rhodium complex - zinc finger peptide chimeras have been successfully synthesized using solid phase coupling methodology. The advantage of the solid phase strategy is that it allows for selective deprotection of one functional group on the peptide which can be used to react with the functionalized metal complex leading to a metal - peptide chimera. Allowing the synthesis to proceed on a solid support also allows for multiple coupling reactions and ensures the removal of unreacted reagents by filtration which makes chromatographic purification easier. The direct coupling method also preserves the integrity of the metal center, allowing facile synthesis of diastereomerically pure chimeras since the conditions for synthesis and deprotection do not lead to racemization about the metal center.

Two variations of coupling reagents have been shown to reliably create chimeras. The use of pentafluorophenol (OPfp) as a coupling reagent instead of HOBt shows almost quantitative coupling of $[Rh(phi)_2(bpy')]^{3+}$ to peptides on the resin. With $[Rh(phi)_2(phen')]^{3+}$, the yields are similar to the original DCC/HOBt protocol. The use of the base 2,4,6-collidine in combination with

DCC and HOAt increases the yield of $[Rh(phi)_2(phen')]^{3+}$-peptide chimeras, but the coupling is still only approximately 50%. However, sufficient chimera is produced to permit characterization and DNA recognition experiments. The results of these experiments are presented in the following chapters.

2.5. REFERENCES

(1) Ghadiri, M. R.; Fernholz, A. K. *J. Am. Chem. Soc.* **1990**, *112*, 9633-9635.

(2) Ghadiri, M. R.; Soares, C.; Choi, C. *J. Am. Chem. Soc.* **1992**, *114*, 4000-4002.

(3) Ghadiri, M. R.; Choi, C. *J. Am. Chem. Soc.* **1990**, *112*, 1630-1632.

(4) Ghadiri, M. R.; Soares, C.; Choi, C. *J. Am. Chem. Soc.* **1992**, *114*, 825-831.

(5) Lieberman, M.; Sasaki, T. *J. Am. Chem. Soc.* **1991**, *113*, 1470-1471.

(6) Lieberman, M.; Tabet, M.; Sasaki, T. *J. Am. Chem. Soc.* **1994**, *116*, 5035-5044.

(7) Ruan, F. Q.; Chen, Y. Q.; Hopkins, P. B. *J. Am. Chem. Soc.* **1990**, *112*, 9403-9404.

(8) Ruan, F. Q.; Chen, Y. Q.; Itoh, K.; Sasaki, T.; Hopkins, P. B. *J. Org. Chem.* **1991**, *56*, 4347-4354.

(9) Imperiali, B.; Kapoor, T. M. *Tetrahedron* **1993**, *49*, 3501-3510.

(10) Robertson, D. E.; Farid, R. S.; Moser, C. C.; Urbauer, J. L.; Mulholland, S. E.; Pidikiti, R.; Lear, J. D.; Wand, A. J.; DeGrado, W. F.; Dutton, P. L. *Nature* **1994**, *368*, 425-431.

(11) Choma, C. T.; Lear, J. D.; Nelson, M. J.; Dutton, P. L.; Robertson, D. E.; DeGrado, W. F. *J. Am. Chem. Soc.* **1994**, *116*, 856-865.

(12) Handel, T. M.; Williams, S. A.; DeGrado, W. F. *Science* **1993**, *261*, 879-885.

(13) Handel, T.; DeGrado, W. F. *J. Am. Chem. Soc.* **1990**, *112*, 6710-6711.

(14) Peek, B. M.; Ross, G. T.; Edwards, S. W.; Meyer, G. J.; Meyer, T. J.;

Erickson, B. W. *Int. J. Pept. Prot. Res.* **1991**, 114-123.

(15) Mecklenburg, S. L.; Peek, B. M.; Schoonover, J. R.; McCafferty, D. G.; Wall, C. G.; Erickson, B. W.; Meyer, T. J. *J. Am. Chem. Soc.* **1993**, *115*, 5479-5495.

(16) Imperiali, B.; Fisher, S. L. *J. Am. Chem. Soc.* **1991**, *113*, 8527-8528.

(17) Wuttke, D. S.; Gray, H. B.; Fisher, S. L.; Imperiali, B. *J. Am. Chem. Soc.* **1993**, *115*, 8455-8456.

(18) Pessi, A.; Bianchi, E.; Crameri, A.; Venturini, S.; Tramontano, A.; Sollazzo, M. *Nature* **1993**, *362*, 367-369.

(19) Merkle, D. L.; Schmidt, M. H.; Berg, J. M. *J. Am. Chem. Soc.* **1991**, *113*, 5450-5451.

(20) Krizek, B. A.; Merkle, D. L.; Berg, J. M. *Inorg. Chem.* **1993**, *32*, 937-940.

(21) Wade, W. S.; Koh, J. S.; Han, N.; Hoekstra, D. M.; Lerner, R. A. *J. Am. Chem. Soc.* **1993**, *115*, 4449-4456.

(22) Barbas III, C. F.; Rosenblum, J. S.; Lerner, R. A. *Proc. Natl. Acad. Sci. USA* **1993**, *90*, 6385-6389.

(23) Wade, W. S.; Ashley, J. A.; Jahangiri, G. K.; McElhaney, G.; Janda, K. D.; Lerner, R. A. *J. Am. Chem. Soc.* **1993**, *115*, 4906-4907.

(24) Shullenberger, D. F.; Eason, P. D.; Long, E. C. *J. Am. Chem. Soc.* **1993**, *115*, 11038-11039.

(25) Sardesai, N. Y.; Lin, S. C.; Zimmermann, K.; Barton, J. K. *Bioconj. Chem.* **1995**, *6*, 302-312.

(26) Stewart, J. M.; Young, J. D. *Solid Phase Peptide Synthesis*; 2nd ed.; Pierce Chemical Company: Rockford, Illinois, 1984.

(27) Edmondson, J. M.; Klebe, R. J.; Zardeneta, G.; Weintraub, S. T.; Kanda, P. *BioTech.* **1988**, *6*, 866-876.

(28) Atherton, E.; Sheppard, R. C. *Solid Phase Peptide Synthesis: A Practical*

Approach; IRL Press: Oxford, 1989.

(29) Ciana, L. D.; Hamachi, I.; J., M. T. *J. Org. Chem.* **1989**, *54*, 1731-1735.

(30) Pyle, A. M.; Chiang, M. Y.; Barton, J. K. *Inorg. Chem.* **1990**, *29*, 4487-4495.

(31) Cartwright, P. S.; Gillard, R. D.; Sillanpää, E. R. J. *Polyhedron* **1987**, *6*, 105-110.

(32) Dollimore, L. S.; Gillard, R. D. *J.C.S Dalton Trans.* **1973**, 933-940.

(33) Wade, J. D.; Bedford, J.; Sheppard, R. C.; Tregear, G. W. *Pept. Res.* **1991**, *4*, 194-199.

(34) Sarin, V. K.; Kent, S. B. H.; Tam, J. P.; Merrifield, R. B. *Anal. Biochem.* **1981**, *117*, 147-157.

(35) King, D. S.; Fields, C. G.; Fields, G. B. *Int. J. Pep. Prot. Res.* **1990**, *36*, 255-266.

(36) David, S. S.; Barton, J. K. *J. Am. Chem. Soc.* **1993**, *115*, 2984-2985.

(37) Krotz, A. H.; Kuo, L. Y.; Shields, T. P.; Barton, J. K. *J. Am. Chem. Soc.* **1993**, *115*, 3877-3882.

(38) Klevit, R. E.; Herriott, J. R.; Horvath, S. J. *Prot. Struct. Funct. Gen.* **1990**, *7*, 215-226.

(39) Thukral, S. K.; Morrison, M. L.; Young, E. T. *Mol. Cell. Biol.* **1992**, *12*, 2784-2792.

(40) Thukral, S. K.; Morrison, M. L.; Young, E. T. *Proc. Natl. Acad. Sci., USA* **1991**, *88*, 9188-9192.

(41) Pavletich, N. P.; Pabo, C. O. *Science* **1991**, *252*, 809-817.

(42) Crosby, S. D.; Puetz, J. J.; Simburger, K. S.; Fahrner, T. J.; Milbrandt, J. *J. Mol. Cell. Bio.* **1991**, *11*, 3841-3841.

(43) Berg, J. M. *Proc. Natl. Acad. Sci., USA* **1992**, *89*, 11109-11110.

(44) Giodoni, D.; Dynan, S. W.; Tjian, R. *Nature* **1984**, *312*, 409-413.

(45) Kadonaga, J. T.; Jones, K. A.; Tijan, R. *TIBS* **1986**, *11*, 20-23.

(46) Kadonaga, J. T.; Courey, A. J.; Ladika, J.; Tjian, R. *Science* **1988**, *242*, 1566-1570.

(47) Posewitz, M. C.; Wilcox, D. E. *Chem. Res. Toxicol.* **1995**, *8*, 1020-1028.

(48) Thiesen, H.-J.; Schroder, B. *Biochem. Biophys. Res. Comm.* **1991**, *175*, 333-338.

(49) Thukral, S. K.; Eisen, A.; Young, E. T. *Mol. Cell. Biol.* **1991**, *11*, 1566-1577.

Chapter 3. Characterization of Rhodium(III) - Zinc Finger Peptide Chimeras*

3.1. INTRODUCTION

A general method for the synthesis of rhodium(III) - peptide chimeras has been developed and successfully applied to create zinc finger conjugates.[1] The next step is to spectroscopically characterize these molecules. For the DNA recognition studies, the rhodium complex functions as the DNA binding moiety, and the zinc finger functions as the DNA recognition moiety. For this purpose, the rhodium complex and peptide should maintain their separate characteristics when they are covalently attached.

The chimeras were characterized by electronic spectroscopy to investigate whether there was any coupling between the metal complex and the peptide. Mass spectrometry was used to confirm that the rhodium complex and the zinc finger peptide were covalently tethered. It should be noted that several types of mass spectroscopy were used: ^{252}Cf plasma desorption mass spectrometry (PD MS†), matrix assisted laser desorption/ionization time of flight mass spectrometry (MALDI MS), and electrospray ionization mass spectrometry (ESI MS).

The zinc finger moiety was chosen for these studies because it forms a distinct, compact structure. The addition of a rhodium(III) complex to the amino terminus of the zinc finger could possibly interfere with the folding of the peptide. Therefore, the structure of the zinc finger portion of the chimera was

---

*Part of this chapter was adapted from Sardesai, N. Y.; Lin, S. C.; Zimmermann, K.; Barton, J. K. *Bioconj. Chem.* **1995**, *6*, 302-312.

†The abbreviations used in this chapter are as follows: bpy': 4-(4-carboxybutyl),4'-methyl-2,2'-bipyridine; DIEA: *N,N*-diisopropylethylamine; DTT: dithiothreitol; ESI: electrospray ionization; MALDI: matrix assisted laser desorption/ionization; MS: mass spectrometry; PD: plasma desorption; phen': (5-amidoglutaryl)-1,10-phenanthroline; phi: 9,10-phenanthrenequinone diimine.

investigated. Multidimensional NMR spectroscopy and x-ray crystallographic studies have been used to determine the complete structure of zinc finger peptides and proteins.[2-18] However, simpler spectroscopic techniques such as circular dichroism, UV-visible and one-dimensional NMR spectroscopy have been used to monitor the folding of the zinc finger peptides.[16,19-23]

Circular dichroism spectroscopy shows an increase in α-helicity when the peptide folds.[19,20] However, the strong absorbance of the rhodium complex in the 200 nm region would make acquiring data difficult. Alternatively, cobalt(II) has been shown to induce peptide folding, producing a distinctive UV-visible spectrum.[19-21] Once folded, cobalt can be displaced by zinc to form the native structure.[22] However, the intensity of the Co^{2+} d-d band is fairly weak ($\varepsilon = 400\ M^{-1}cm^{-1}$ at 635 nm),[21] and the strong absorbance of the rhodium complex compared to the weak cobalt(III) absorption may obscure the band. In contrast, one-dimensional ^1H NMR spectra of the peptides show distinct shifts in specific residues (especially histidine, methyl) in the presence of zinc.[16,21,23] In fact, a complete NMR structure of the ADR1b peptide including the one-dimensional ^1H NMR spectrum of the zinc folded form has been published.[7] In the case of the Sp1 zinc fingers, there are conserved residues whose resonances are distinctive for the folded form of the peptide.[16] Thus, a direct comparison of the one-dimensional ^1H NMR spectrum of the free peptide with that of the peptide in the presence of zinc will reveal whether the addition of zinc is inducing the peptide to fold. As a result, one-dimensional ^1H NMR spectroscopy is the most suitable method for determining the structure of our rhodium(III) - zinc finger chimeras, and was used to confirm that the zinc induced folding of the peptide portion of the rhodium(III) chimeras.

3.2. EXPERIMENTAL

3.2.1. Instrumentation. ^{1}H-NMR spectra were recorded on either a 500 MHz Bruker AM spectrometer using water presaturation or a 500 MHz Bruker AMX spectrometer using WATERGATE water suppression. The peaks were referenced to D_2O = 4.65 ppm. An Orion Model SA720 pH meter was used to determine the pH of solutions. Ultraviolet-visible (UV-visible) spectra were recorded on a Hewlett-Packard 8452A diode array or Cary 219 UV-visible spectrophotometer. The concentrations of metal-peptide conjugates were determined by UV-visible spectroscopy using ε_{350} (isosbestic) = 23,600 $M^{-1}cm^{-1}$. High performance liquid chromatography (HPLC) was carried out on a Waters 600E system equipped with a Waters 484 UV-visible tunable detector. Analytical HPLC was done on a Hewlett-Packard 1090 system. ^{252}Cf plasma desorption mass spectrometry (PD MS) was recorded on the Bio-Ion/Applied Biosystems 20 K time-of-flight spectrometer by the Biopolymer Synthesis and Analysis Resource Center at Caltech. The mass scale was calibrated on the hydrogen and nitrate ions and the experimental error is <1 m/z per 2000 m/z. Matrix assisted laser desorption/ionization time of flight mass spectrometry (MALDI MS) was done on a Voyager-Rp mass spectrometer containing a PerSeptive Biosystem/Vestec Lasertech II reflector at the Protein and Peptide Micro Analytical Facility in the Beckman Institute at Caltech. Electrospray ionization mass spectrometry (ESI MS) was done on a Hewlett-Packard 59987A Electrospray Interface and an HP 5989B MS Engine quadrapole mass spectrometer by the Caltech Division of Chemistry and Chemical Engineering Mass Spectrometry Laboratory which was part of the Bank of America Environmental Analysis Center. Under the low resolution conditions used, the molecular weights determined will fall between the 'monoisotopic mass' and the

average molecular weight. The experimental error was ± 0.1 m/z.

3.2.2. Mass Spectrometric Characterization. ^{252}Cf PDMS was carried out at an accelerating voltage of 15 kV. The samples were adsorbed on nitrocellulose surfaces by applying solutions of the chimera (200 pmol) in 25% acetonitrile(0.1% TFA) / 75% water and allowed to dry. Excess salt, if present, was removed from the adsorbed samples by rinsing with 1:1 EtOH/water prior to data accumulation. For MALDI MS analysis, the sample was used directly from the HPLC. For ESI MS, the HPLC samples were lyophilized and dissolved to 10 μM in 19.5% H_2O/79.5% CH_3CN/1% HOAc. The sample (10 μL) was introduced into the spray via loop injection with a sample flow rate of 10 μL/min. Nitrogen gas was passed over the sample at a flow rate of 6 - 13 L/min. and 175°C. Nebulizing gas was supplied at 80 psi. Peak widths were set to 1 m/z at half height.

3.2.3. Chemical Stability.

Stability of [Rh(phi)$_2$(phen')]Cl$_3$ to Aqueous Base. The pH of a 13 μM solution of [Rh(phi)$_2$(phen')]Cl_3 was adjusted from 5.2 to 12.8 using aliquots of 0.1 M, 1 M and 50% w/w NaOH, and the UV-visible spectrum was taken at different pH points. The solution was then acidified to pH 5.8 with 12 M HCl. The final solution was brought to pH 12.8 with 300 μl of 50% NaOH and was allowed to sit at room temperature for several days. During this time, the UV-visible spectrum was checked periodically. During this time, precipitation occurred. After 15 days, the solution was acidified to pH 5.7 with 12.0 M and 1.0 M HCl. The final UV-visible spectrum was taken of this solution. There was considerable degradation with a substantial loss of the absorbance above 300 nm.

Stability of [Rh(phi)$_2$(phen')]Cl$_3$ to 2-Mercaptoethanol. [Rh(phi)$_2$(phen')]Cl_3 (3.0 mg, 3.2 μmol) was reacted with 200 μl of 20% (v/v) 2-

mercaptoethanol/10% DIEA.[24] The solution was stirred for 1.5 hrs at room temperature. After a few minutes, the solution turned yellow-brown. Diethyl ether (5 mL) was added and a brown precipitate formed. The precipitate was isolated and washed with cold ether. The ^{1}H NMR spectrum of the complex indicated that significant degradation had occurred. FPLC chromatography of the brown solid confirmed that ~50% of the rhodium complex had degraded.

Stability of [Rh(phi)$_2$(phen')]Cl$_3$ to Dithiothreitol. [Rh(phi)$_2$(phen')]Cl$_3$ (0.2 mM) was treated with 50 mM DTT in 100 mM Tris•HCl (pH 7.7) at 90°C for 1 hr.[19] The solution was washed three times with diethyl ether in a separatory funnel. The first wash was yellow, and the rest were clear. The aqueous layer was stripped of solvent. The ^{1}H NMR spectrum indicated that the rhodium complex had degraded considerably.

Reaction of [Rh(phi)$_2$(phen')]$^{3+}$-Sp1-2d Zinc Finger with DTT. A partially oxidized sample of [Rh(phi)$_2$(phen')]$^{3+}$-Sp1-2d (7 μM) was subjected to different amounts of DTT (1 eq, 6.5 eq, 10 eq, 1 mM) in 100 mM Tris, pH 8.0 buffer. Analytical HPLC spectra were taken at 5 min. and then at 30 min. intervals after addition of thiol. A C_{18} reverse phase column was used with a water (0.1% TFA)/acetonitrile (0.1% TFA) gradient (20-40% acetonitrile. for 12 min., then 40-45% acetonitrile for 3 min.).

3.2.4. The Folding of Zinc Finger Peptides.

The Folding of Zinc Finger Peptides. Purified zinc finger peptides were reduced using 200 mM DTT in 100 mM Tris, pH 8.0 at 90°C for 30 minutes.[19] The reduced peak was isolated by HPLC chromatography and lyophilized to dryness. The peptide was dissolved in buffered D_2O containing one equivalent $ZnCl_2$ or EDTA.

The Folding of Rhodium(III) - Zinc Finger Peptide Chimeras. The cleavage, deprotection and HPLC purification protocols for the rhodium(III) - zinc finger chimeras are provided in Chapter 2. Immediately after HPLC purification, the UV-visible spectrum of the rhodium - zinc finger conjugate was taken and at least a 120% molar excess of 1 mM $ZnSO_4$ was added. Next, 25 μL of 1 M d^{11}-Tris (Cambridge Isotope Laboratories) was added. The pH was adjusted to 7 (uncorrected for isotope effect) using 0.1 M NaOH. The sample was sealed and left at room temperature for 1 hr. Then, it was frozen and lyophilized. Once dry, 500 μL D_2O was added. After brief stirring, the metal-peptide was filtered through a 0.45 μm cellulose acetate microcentrifuge filter and the supernatant was placed in an NMR tube under argon.

3.3. RESULTS

3.3.1. Electronic Spectroscopy. Figure 3.1 shows the UV-visible spectra of $[Rh(phi)_2(phen')]Cl_3$, the Sp1-2d zinc finger and their covalent chimera. The spectrum of the rhodium - zinc finger conjugate is the composite of the spectra of the two independent parts. The concentration of chimera can be quantitated based upon the extinction coefficient of the rhodium complex at 350 nm (ε = 23,600 $M^{-1}cm^{-1}$) since the peptides do not absorb significant light at wavelengths $\geq$ 300 nm. As with the parent metal complexes, there are pH dependent changes observed in the spectrum which depend upon the protonation state of the coordinated phi ligands.[25,26] At $\leq$ 300 nm, some reduction in the absorption intensity for the metal-peptide chimera compared to the metal complex is observed. Thus, the rhodium complex and peptide are slightly coupled, but are essentially two independent units.

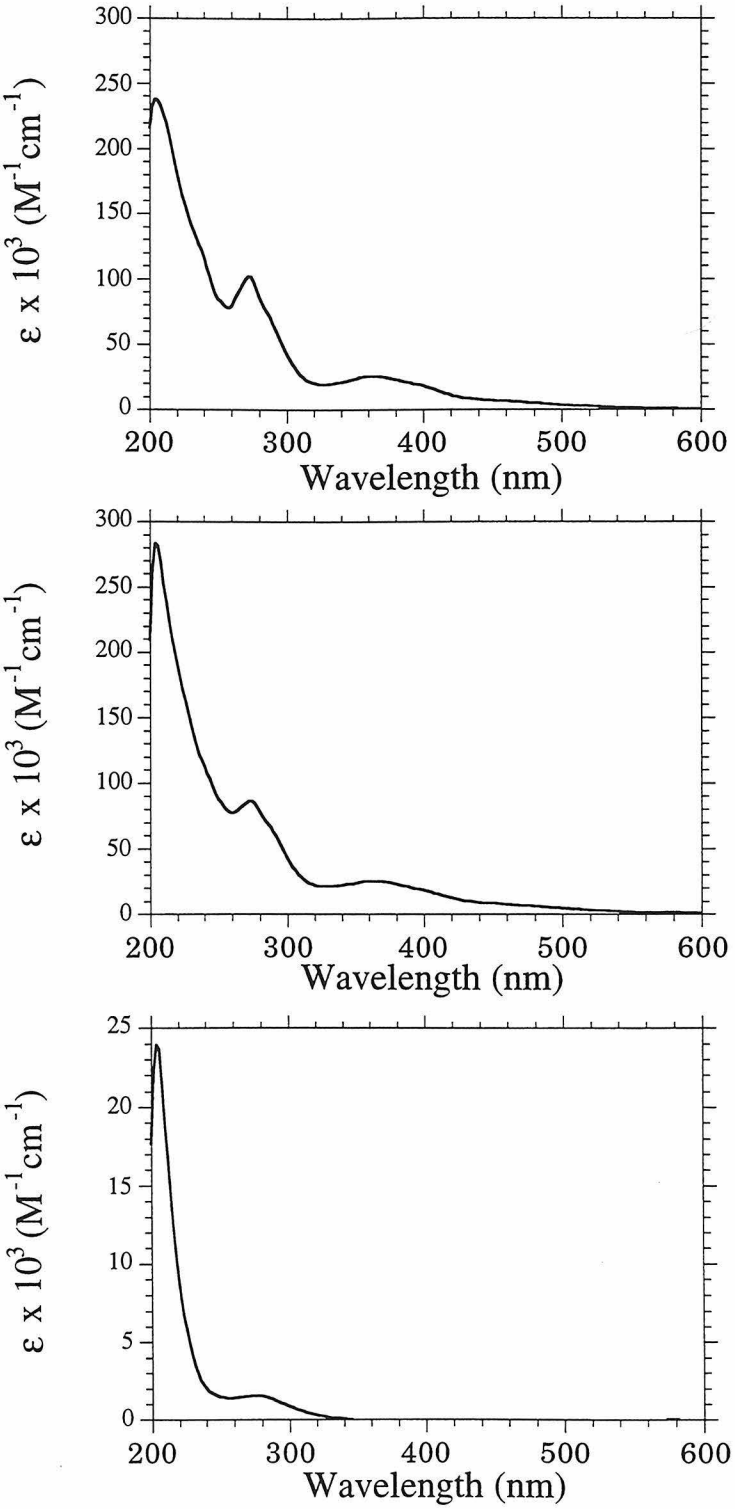

Figure 3.1. *UV-Visible spectra in 10 mM Tris•HCl, pH 7.0 of [Rh(phi)$_2$(phen')]Cl$_3$ (top), [Rh(phi)$_2$–(phen')]$^{3+}$-Sp1-2d (middle) and H_2N-Sp1-2d (bottom).*

3.3.2. Mass Spectrometry. The MS of the chimera establishes that the metal complex and peptide are covalently bound. The rhodium(III) - zinc finger conjugates have been analyzed using three different types of mass spectrometry: PD, MALDI and ESI.

Plasma desorption mass spectrometry (PD MS) was the first method to successfully obtain spectra containing peaks corresponding to intact rhodium(III) - peptide chimeras. As is evident in Figure 3.2, the PD mass spectrum of $[Rh(phi)_2(phen')]^{3+}$-Sp1-2d shows the expected molecular ion peak $[M^{3+}\text{-}2H^+]^+$ at (obs.) *m/z* 4233.4, (calc.) *m/z* 4233.5 and doubly charged peak $[M^{3+}\text{-}H^+]^{2+}$ at (obs.) *m/z* 2116.9, (calc.) *m/z* 2117.3. In addition, the presence of the covalently attached metal complex promotes fragmentation of the attached peptide. As shown in Figure 3.2, we observe a series of A_n fragments which reflect cleavage of the C_α-CO bond in the metal-peptide chimera. In contrast, no fragmentation is evident for the peptide lacking the metal complex. In addition, for each A_n fragment we observe a corresponding fragment of 206 m/z lower which corresponds to the loss of one phi ligand. For metal- zinc finger peptide chimeras, only the first few N-terminal fragments are found. Presumably folding of the longer peptide inhibits fragmentation. For metal-peptide chimeras containing $\leq$ 14 residues, the complete series of A_n fragments is observed. Figure 3.3 shows the complete fragmentation pattern for the five amino acid conjugate, $[Rh(phi)_2(phen')]^{3+}$-GGFAE-CO_2H.

All the peaks observed for the metal-peptide complexes correspond to the singly charged species. It is unlikely that these fragments correspond to Rh(I) complexes, but rather to $[Rh(III)\text{-}2H^+]^+$. This feature is observed even with highly positive charged metal-peptide complexes. The doubly or triply charged ion peaks are small or not observable for the fragments. Therefore, the molecular ion and fragment peaks are calculated as $[M^{3+}\text{-}2H^+]^+$.

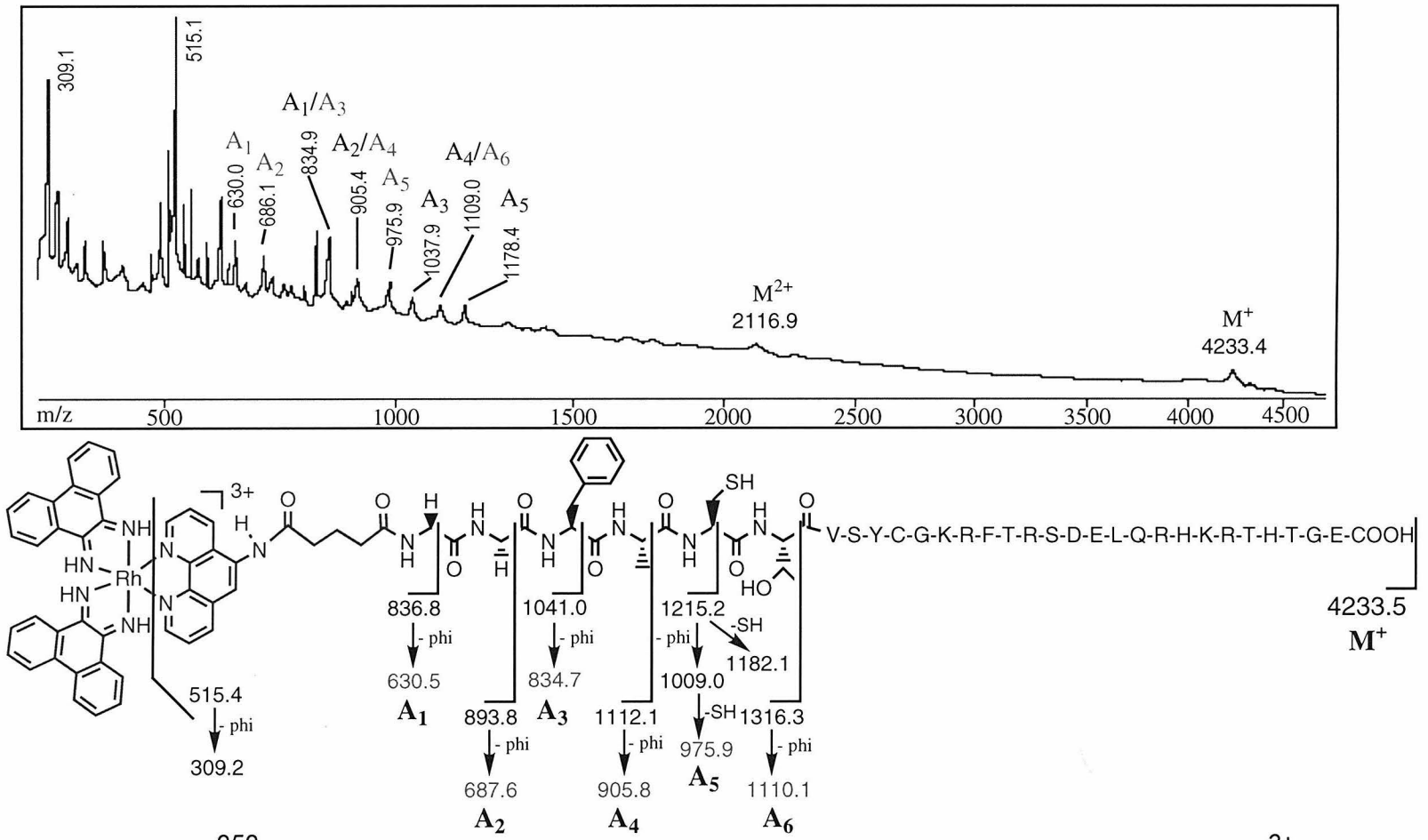

Figure 3.2. *The ^{252}Cf PD mass spectrum and fragmentation pattern of $[Rh(phi)_2(phen')]^{3+}$-Sp1-2d. The PDMS Spectrum fo the metal-peptide complex (top) showing the molecular ion (M^+) peak, fragments. The schematic representation of the fragments for the metal-peptide complex (bottom) and their calculated mass.*

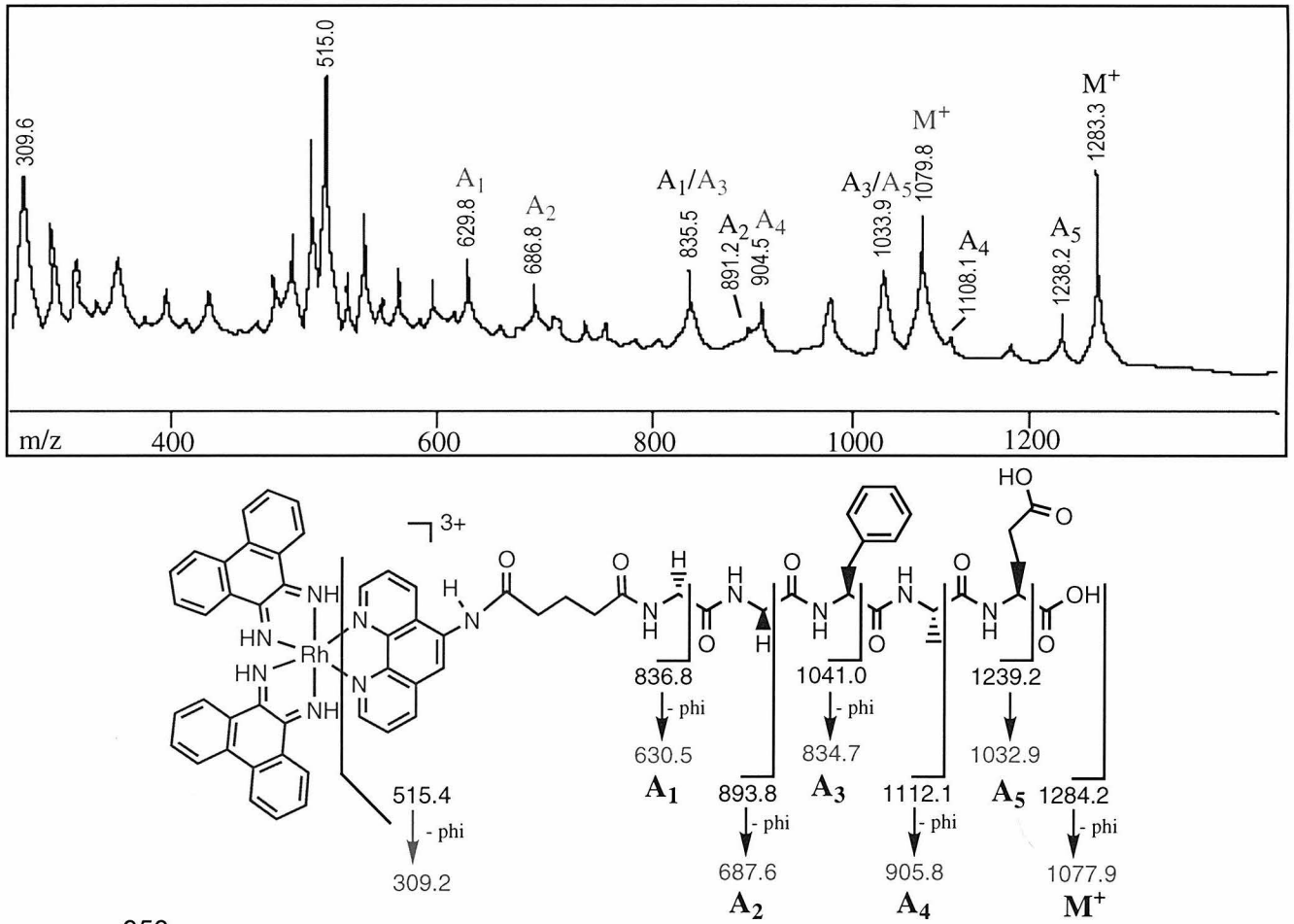

Figure 3.3. *The ^{252}Cf PD mass spectrum and fragmentation pattern of $[Rh(phi)_2(phen')]^{3+}$-GGFAE-CO_2H. The PDMS Spectrum fo the metal-peptide complex (top) showing the molecular ion (M^+) peak, fragments. The schematic representation of the fragments for the metal-peptide complex (bottom) and their calculated mass.*

In addition to PDMS, the rhodium - zinc finger conjugates were analyzed using electrospray ionization (ESI) mass spectrometry. Figure 3.4 shows the mass spectrum for $[Rh(phi)_2(bpy')]^{3+}$-Sp1-3. The peaks correspond to differently charged species of the rhodium - peptide conjugate. Since the rhodium complex itself has a +3 charge, the +4, +5, +6 and +7 peaks would correspond to the addition of 1, 2, 3 and 4 protons respectively. The observed and calculated masses agree: M^{4+} (obs.) *m/z* 954.70, (calc.) *m/z* 954.55; M^{5+} (obs.) *m/z* 763.90, (calc.) *m/z* 763.44; M^{6+} (obs.) *m/z* 636.80, (calc.) *m/z* 636.03; M^{7+} (obs.) *m/z* 545.95, (calc.) *m/z* 545.02. No fragmentation is seen and the spectrum is clean indicating that the sample is pure. All the chimeras synthesized have been successfully analyzed by ESI mass spectrometry.

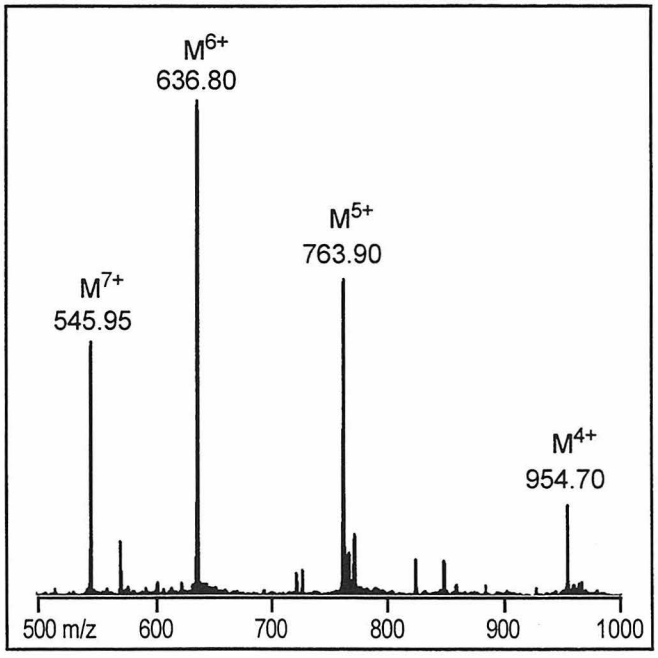

Figure 3.4. *The ESI mass spectrum of $[Rh(phi)_2(phen')]^{3+}$-Sp1-3. The peaks correspond to differently charged states of the whole chimera.*

In contrast, MALDI mass spectrometry has not been very successful for these large rhodium(III) - peptide conjugates. Figure 3.5 shows a MALDI spectrum for $[Rh(phi)_2(phen')]^{3+}$-ADR1b. It shows peaks corresponding to the

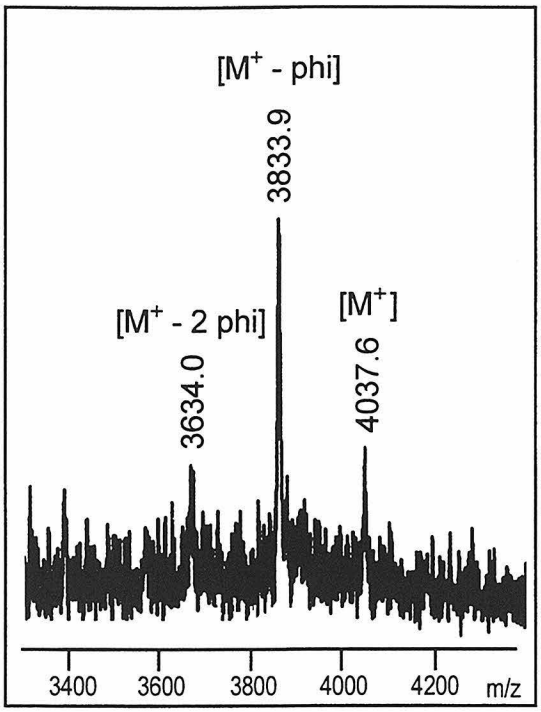

Figure 3.5. *The MALDI mass spectrum of [Rh(phi)$_2$(phen')]$^{3+}$-ADR1b. The calculated molecular weights are: [M^{3+}-2H$^+$]$^+$ m/z 4038.4, [M^{3+}-2H$^+$ - phi]$^+$ m/z 3832.1, or [M^{3+}-2H$^+$ - 2 phi]$^+$ m/z 3625.9.*

mass of the chimera, [M^{3+}-2H$^+$]$^+$: (obs.) *m/z* 4037.6, (calc.) *m/z* 4038.4, in addition to loss of one phi, (obs.) *m/z* 3833.9, (calc.) *m/z* 3832.1, and loss of two phi ligands, (obs.) *m/z* 3634.0, (calc.) *m/z* 3625.9. For rhodium chimeras of smaller peptides (<14 a. a..), the spectra typically contain these three peaks. However, for the rhodium - zinc finger chimeras, spectra of this quality were only obtained twice. Numerous other samples gave either no peaks or several smaller fragments. For comparison, identical samples were run on MALDI and ESI mass spectrometers. As shown in Figure 3.6A, the MALDI spectrum of another sample of [Rh(phi)$_2$(phen')]$^{3+}$-ADR1b contains numerous peaks. None of the peaks correspond to the expected [M^{3+}-2H$^+$]$^+$ *m/z* 4038.4, loss of one phi, *m/z* 3832.1, or loss of two phi ligands, *m/z* 3625.9. This may lead to the conclusion that the sample was heterogeneous. However, the ESI mass spectrum (Figure 3.6B) is very clean showing that the chimera is intact and quite pure: M^{4+} (obs.) *m/z*

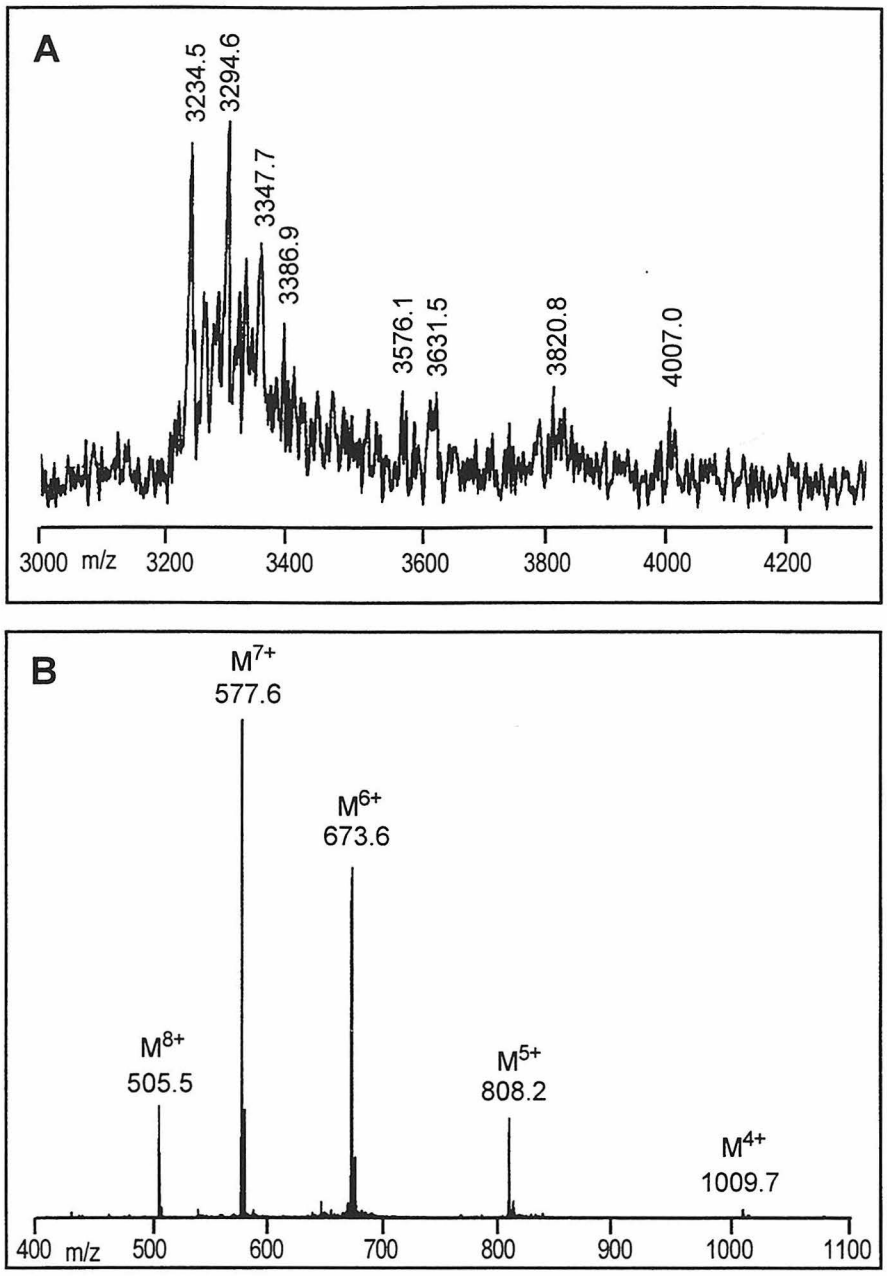

Figure 3.6. *The MALDI (**A**) and ESI (**B**) mass spectra of [Rh(phi)$_2$(phen')]$^{3+}$-ADR1b.*

1009.7, (calc.) *m/z* 1009.8; M^{5+} (obs.) *m/z* 808.2, (calc.) *m/z* 807.7; M^{6+} (obs.) *m/z* 673.6, (calc.) *m/z* 672.9; M^{7+} (obs.) *m/z* 577.6, (calc.) *m/z* 576.6; M^{8+} (obs.) *m/z* 505.5, (calc.) *m/z* 504.4. Since MALDI uses a laser (at ~ 330 nm) to desorb the sample, it is not surprising that the chimera is fragmenting since the rhodium complex absorbs strongly in that region of the spectrum and photolysis in this band

promotes ligand loss.[27]

3.3.3. Zinc Finger Folding and NMR Spectroscopy. Zinc finger peptides use two histidine and two cysteine ligands to coordinate to the zinc and form its tertiary structure.[28] Since the cysteines are in close proximity in the absence of zinc, they can easily oxidize to form a disulfide bond resulting in a peptide that cannot coordinate zinc. In the case of the free peptide, this disulfide can easily be reduced to the free thiols using dithiothreitol (DTT). Furthermore, the reduced and oxidized peptides can easily be separated by HPLC, with the disulfide peptide eluting first.[19,20]

Once reduced, the peptide folds upon the addition of zinc providing the solution is between pH 5.5 and 7.8.[21] Figure 3.7 shows the NMR spectra of the ADR1b peptide in the presence of EDTA or $ZnCl_2$. Several distinct changes are apparent. First, the imidazole C^{ε} proton resonances (~ 8 ppm) shift downfield upon zinc coordination. Second, several C^{α} resonances (~ 5-4.6 ppm) shift downfield and a methyl resonance (0.5 ppm) shifts upfield. The folded spectrum agrees with the published spectrum for ADR1b in the presence of zinc.[7] Similarly, the Sp1 finger 2 and finger 3 have been folded with zinc and the corresponding NMR spectra are shown in Figures 3.8 and 3.9. They both show the characteristic changes in the imidazole and C^{α} proton resonances. The Sp1-2 zinc finger also has two methyl resonances that shift into the region of 0 - 0.5 ppm. Therefore, all three peptides have easily identifiable resonances that indicate that the zinc finger has folded properly.

Unfortunately, the reduction of the disulfide bond of the rhodium(III) - zinc finger chimeras is not feasible since $[Rh(phi)_2(phen')]^{3+}$ is not stable to nucleophilic bases. Thus, when $[Rh(phi)_2(phen')]^{3+}$ was subject to a highly basic aqueous solution (pH 12), the electronic spectrum changed. Most notably, the phi transition (360 nm) decreases significantly in intensity (Figure 3.10).

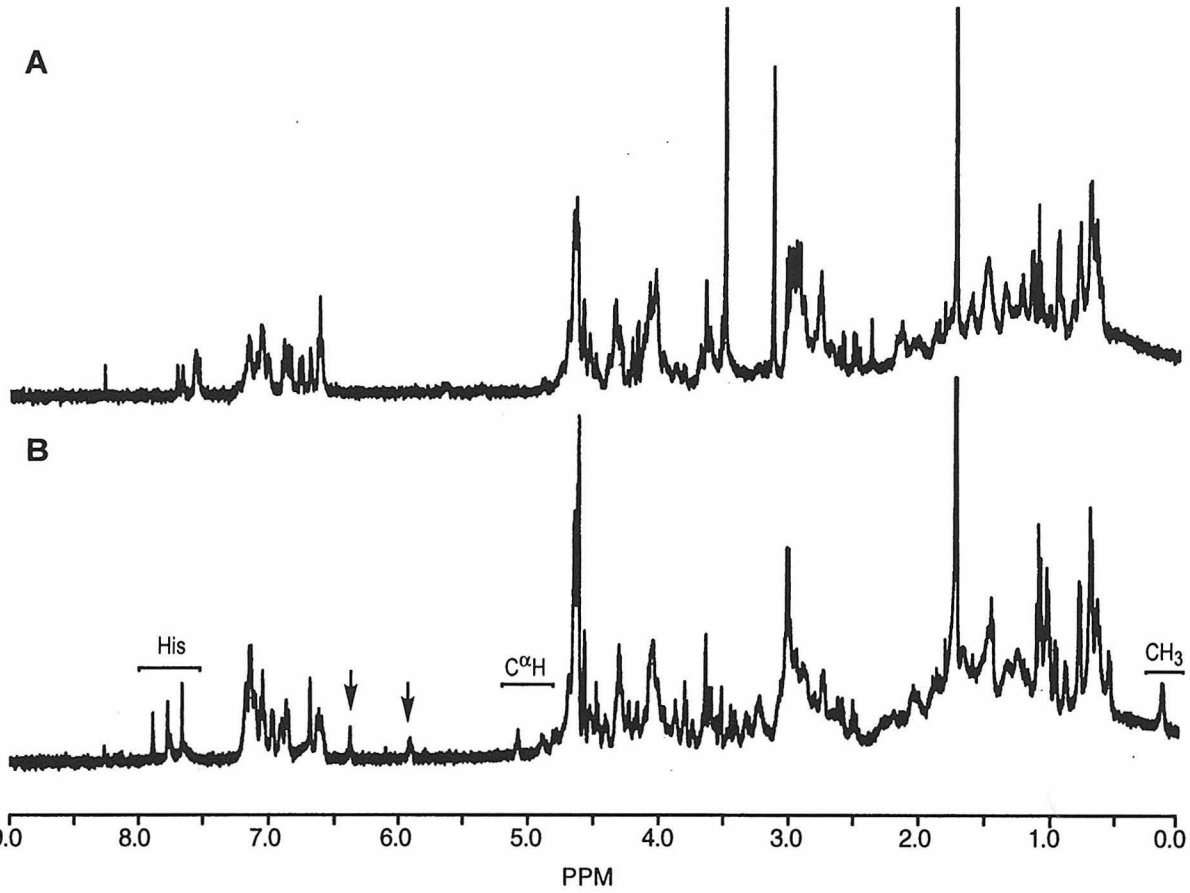

Figure 3.7. *The 500 mHz ^1H NMR spectra of 1 mM ADR1b in 50 mM d^{11}-Tris, d^3-acetate, pH 7.5, in the presence of:* ***A****) 1 mM EDTA* ***B****) 1 mM $ZnCl_2$. The resonances that are distinctive for the folded structure are indicated.*

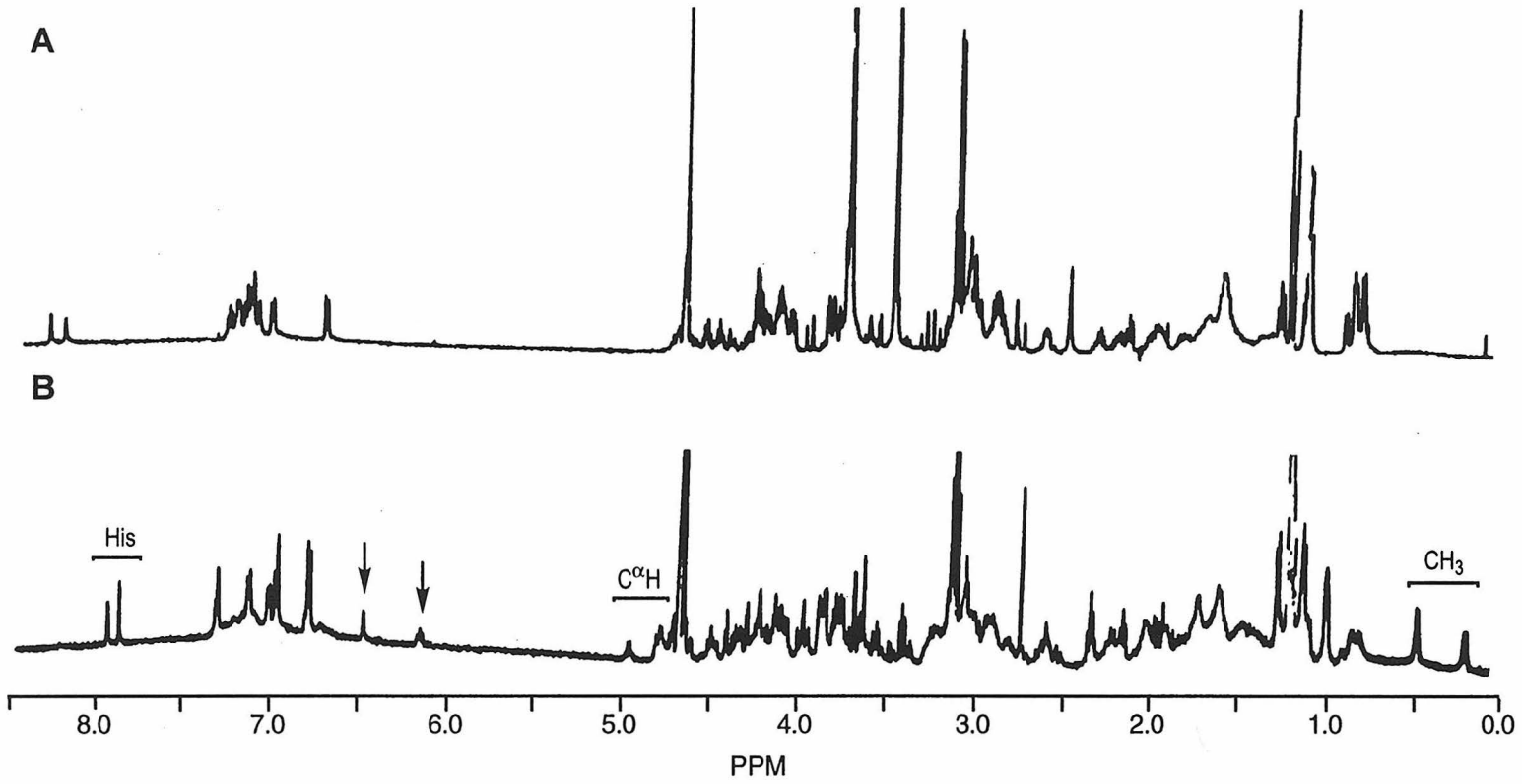

Figure 3.8. *The 500 mHz ^1H NMR spectra of 0.5 mM Sp1-2d in 50 mM d^3- acetate, pH 5.5, in the presence of:* ***A****) 2.5 mM EDTA* ***B****) 2.5 mM $ZnCl_2$. The resonances that are distinctive for the folded structure are marked.*

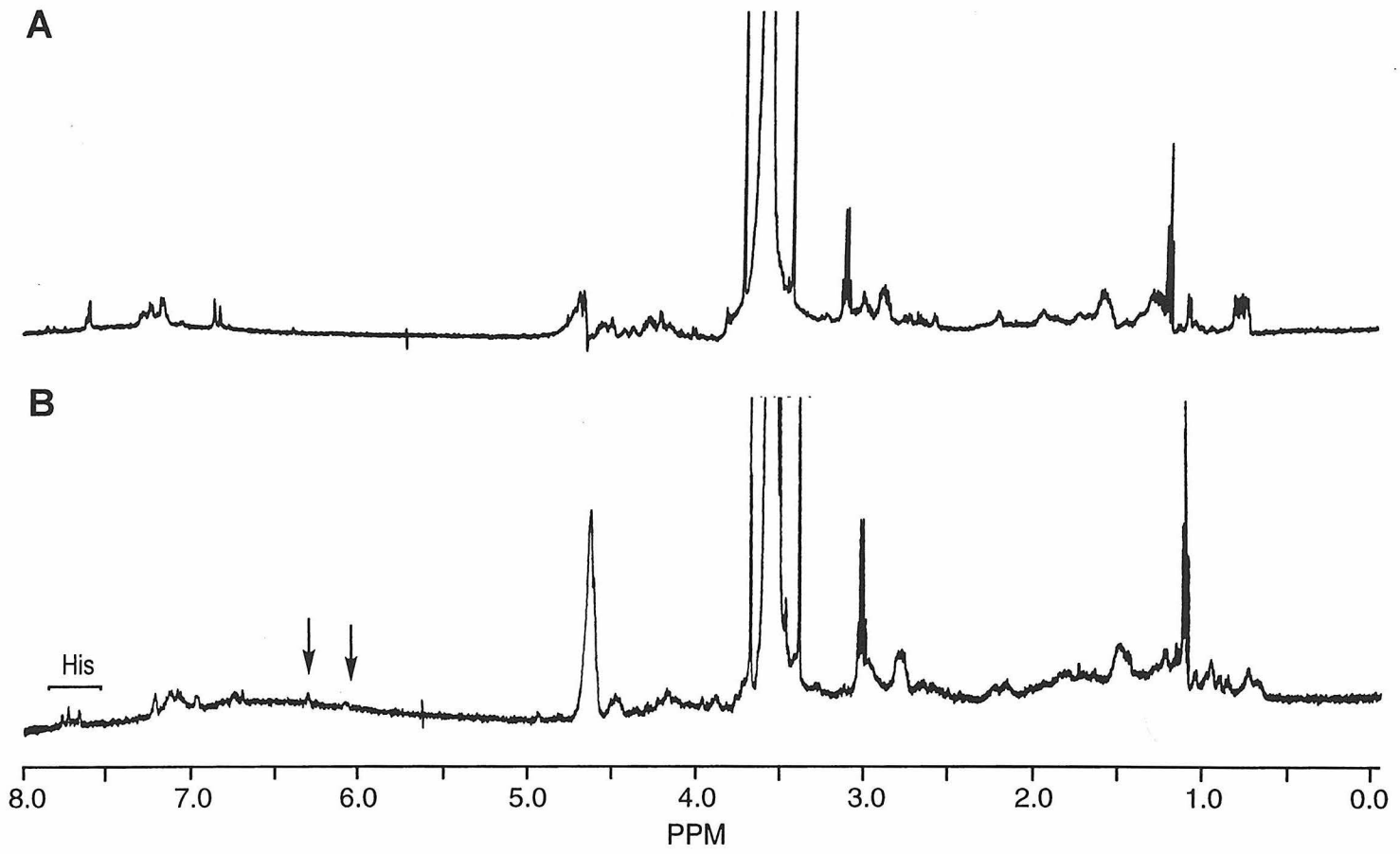

Figure 3.9. *The 500 mHz ^{1}H NMR spectra of 1.3 mM Sp1-3 in 50 mM d^{5}- tris, pH 7.8, in the presence of:* ***A****) no zinc* ***B****) 1.4 mM $ZnCl_2$. The resonances that are distinctive for the folded structure are marked.*

However, it should be noted that $[Rh(phi)_2(phen')]^{3+}$ is stable to non-nucleophilic bases such as 2,4,6-collidine. Reduction of the disulfide bond with thiols is also not possible since $[Rh(phi)_2(phen')]^{3+}$ is not stable under DTT reduction conditions used to reduce the free peptide (100 fold excess at 90°C for 1 hour).[19] In addition, the rhodium complex is also unstable to treatment with 2-mercaptoethanol which has also been shown to reduce disulfide bonds.[24]

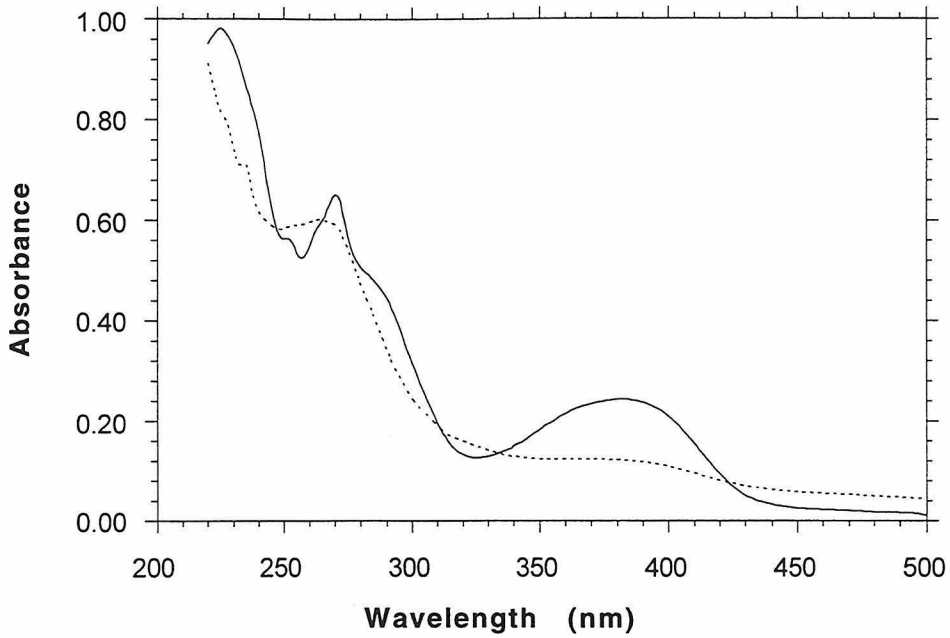

Figure 3.10. *UV-Visible spectra of $[Rh(phi)_2(phen')]Cl_3$ before (-----) and after (·····) exposure to NaOH. Both spectra are at pH 5.*

Studies designed to investigate the feasibility of the DTT reduction of partially oxidized $Rh(phi)_2(phen')]^{3+}$ - Sp1-2d were performed (Figure 3.11A). When the chimera was treated with 10 eq. of DTT in 10 mM Tris•HCl, pH 8, some reduction occurred, but with a great loss of material after 30 minutes (Figure 3.11B). When the concentration of DTT was lowered to one equivalent per chimera, most of the chimera was reduced after 30 minutes (Figure 3.11C). After 3 hrs, the same sample showed only a 10% degradation of the rhodium

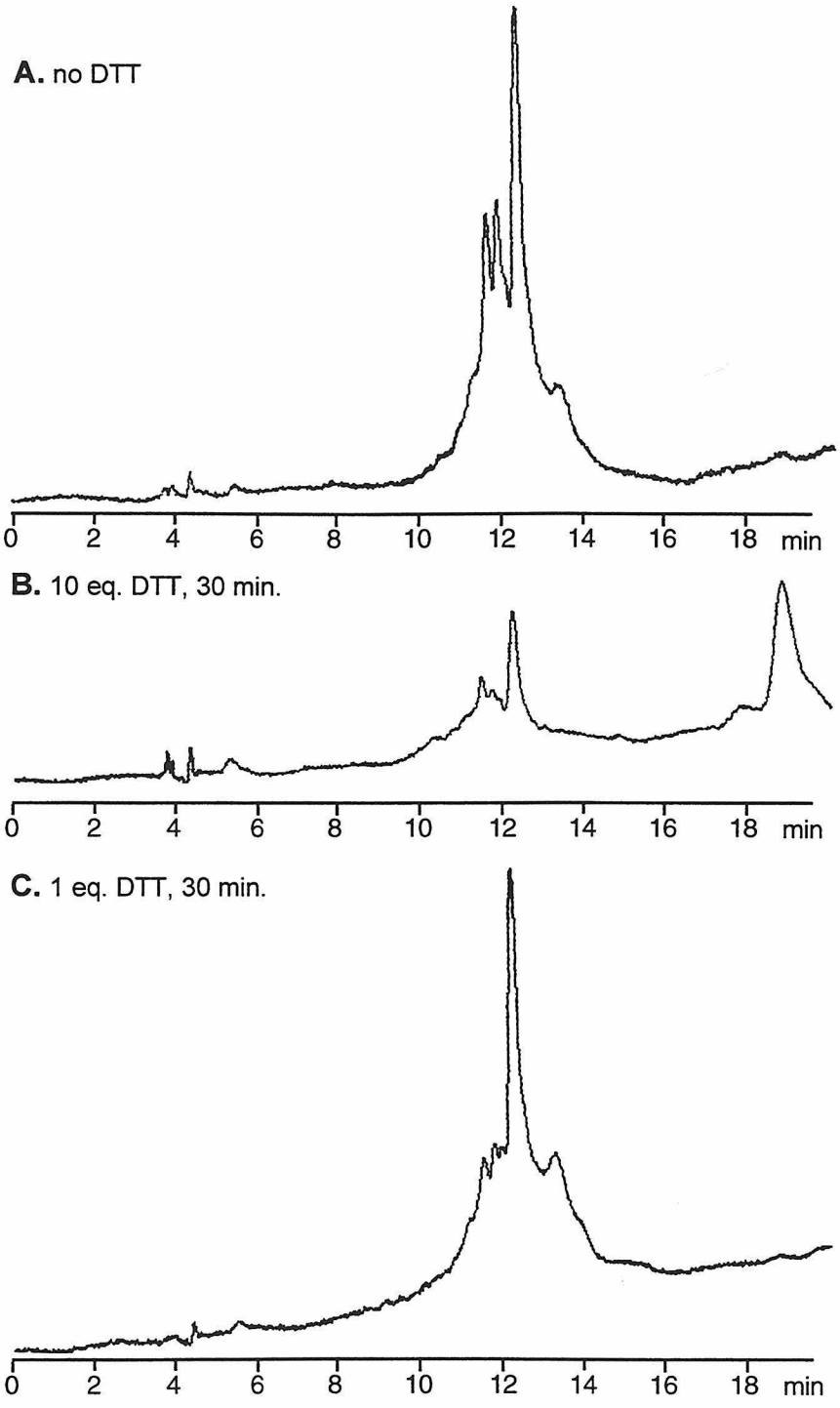

Figure 3.11. *The HPLC chromatogram of the reduction of* $[Rh(phi)_2(phen')]^{3+}$ *- Sp1-2f with DTT.* λ_{obs} *= 360 nm.* ***A****) The chimera with no DTT.* ***B****) The chimera after treatment with 10 eq. DTT for 30 min.* ***C****) The chimera after treatment with 1 eq. DTT for 30 min.*

complex. This indicates that the reduction occurs slightly faster than the degradation of the rhodium complex. However, when a completely oxidized sample of $Rh(phi)_2(phen')]^{3+}$ - ADR1b was treated with 1 eq. of DTT on a large scale, the reduction was not clean (Figure 3.12). The isolation of reduced rhodium(III) - zinc finger from an oxidized sample was therefore not feasible.

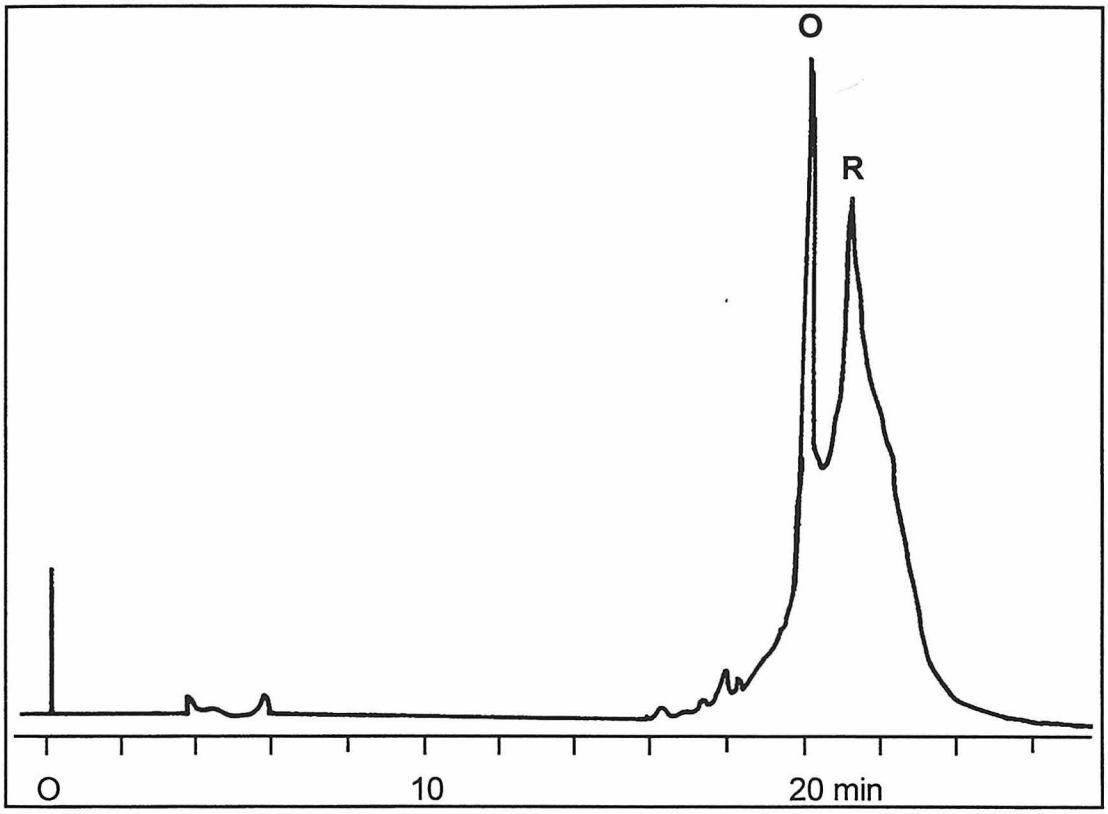

Figure 3.12. *The HPLC chromatogram of $[Rh(phi)_2(phen')]^{3+}$-ADR1b. λ_{obs} = 360 nm. The peaks corresponding to the oxidized (**O**) and reduced (**R**) metal - peptide chimeras are marked.*

Due to the inability to reduce already oxidized chimeras, it is necessary to fold the peptide with zinc before oxidation occurs. If the rhodium(III) - zinc finger conjugate is dried after cleavage and deprotection but before purification, the sample shows HPLC retention times corresponding to oxidized peptide and does not coordinate zinc. If the chimera is purified immediately after deprotection, the size of the oxidized peak increases and the reduced peak

decreases with time. Thus, the purification should be done as quickly as possible after cleavage and deprotection to minimize the disulfide bond formation. Once the reduced metal - peptide is isolated, lyophilization and storage under vacuum leads to oxidation. Addition of zinc after purification, but before lyophilization, does not prevent disulfides from forming since the solution is very acidic, and thus zinc cannot coordinate. Figure 3.13 shows the 1D NMR of $[Rh(phi)_2(bpy')]^{3+}$-ADR1b that was prepared in the manner described above. Based on the spectroscopy, it is evident that the rhodium(III) - peptide did not fold in the presence of zinc. However, since lyophilization of the chimera causes oxidation, the zinc finger must be folded with zinc prior to drying.

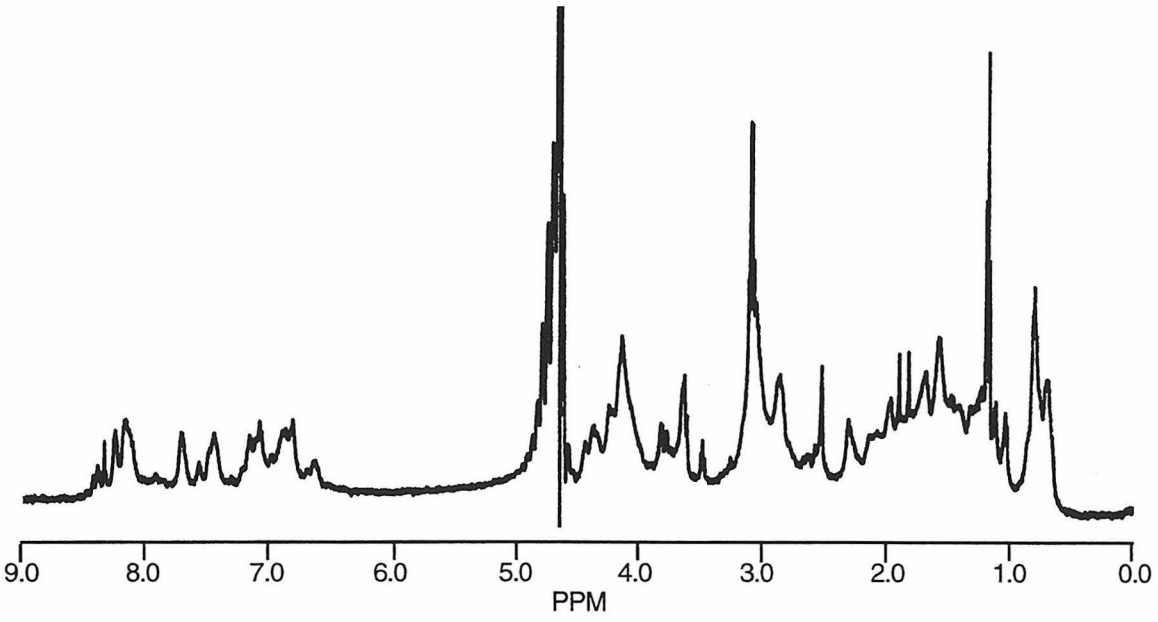

Figure 3.13. *The 500 mHz 1H NMR spectrum of oxidized $[Rh(phi)_2(bpy')]^{3+}$-ADR1b in the presence of $ZnCl_2$ in d^{11}-Tris-d^3-acetate, pH 5.5.*

In order to overcome these difficulties, a protocol to minimize the oxidation of the rhodium(III) - zinc finger conjugates was developed. After cleavage and deprotection, the chimera was immediately HPLC purified in one injection. The concentration of the major peaks was determined by UV-Visible

spectroscopy and at least 1.2 equivalents of $ZnSO_4$ was added. Then, the sample was adjusted to pH 7 with deuterated Tris buffer and sodium hydroxide. The color of the solution changed from light to dark orange when the pH reached 5.5. The chimera was lyophilized and dissolved in D_2O, and the residual precipitate was removed by filtration. The ^1H NMR of the solution showed a completely folded zinc finger (Figure 3.14A). The precipitate was found to contain unfolded chimera (Figure 3.14B). This procedure reproducibly produces folded rhodium(III) - zinc finger chimeras.

Figures 3.15-3.21 show the NMR spectra of folded rhodium(III) - zinc finger chimeras. While the NMR spectrum of non-covalently bound $[Rh(phi)_2(phen')]^{3+}$ and Sp1-2f is the sum of the spectra of the individual entities, NMR spectrum of the covalent chimera is not (Figure 3.20). The peaks corresponding to the peptide portion of the chimera appear to be virtually identical to free peptide. The aromatic resonances for the rhodium complexes are small and difficult to identify. Some of the resonances appear to be shifted upfield (~7.0 ppm) compared to those of free $[Rh(phi)_2(phen')]^{3+}$ (>7.5 ppm). Furthermore, since the chimera was synthesized with racemic rhodium complex, two diastereomers of the chimera are present. Also, the protons that are equivalent in the metal complex may be rendered inequivalent in the chimera. Thus, multiple peaks or multiple splitting of the peaks would make the resonances difficult to detect. However, the presence of the rhodium complex does not interfere with the formation of the zinc finger structure, and therefore the components of the chimera are essentially independent of each other.

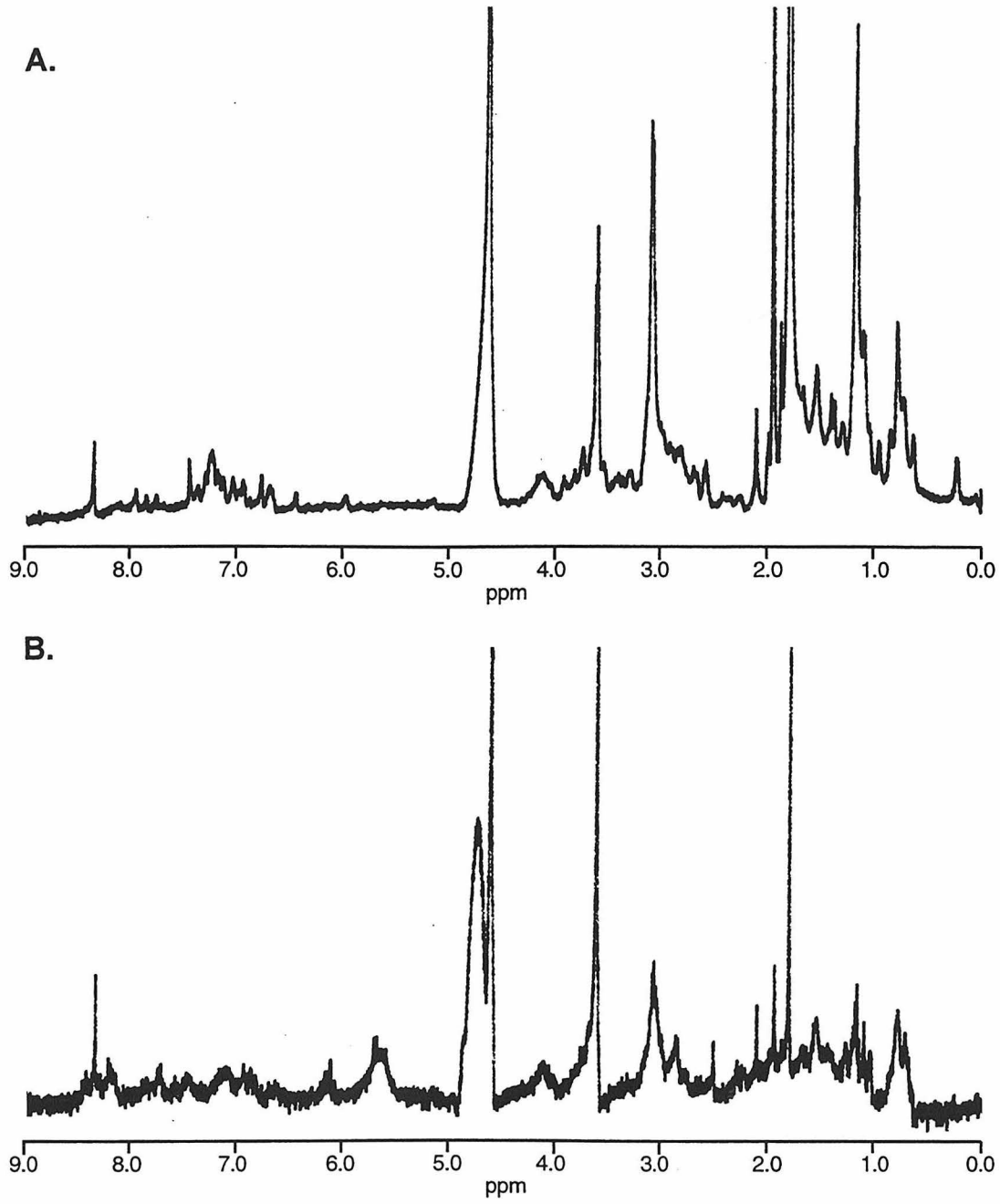

Figure 3.14. *The 500 mHz ^{1}H NMR spectra of $[Rh(phi)_2(bpy')]^{3+}$ - ADR1b.* ***A****) Folded chimera in d^{11}-Tris, pH 7.1.* ***B****) The precipitate which was redissolved in D_2O, pH 5.75.*

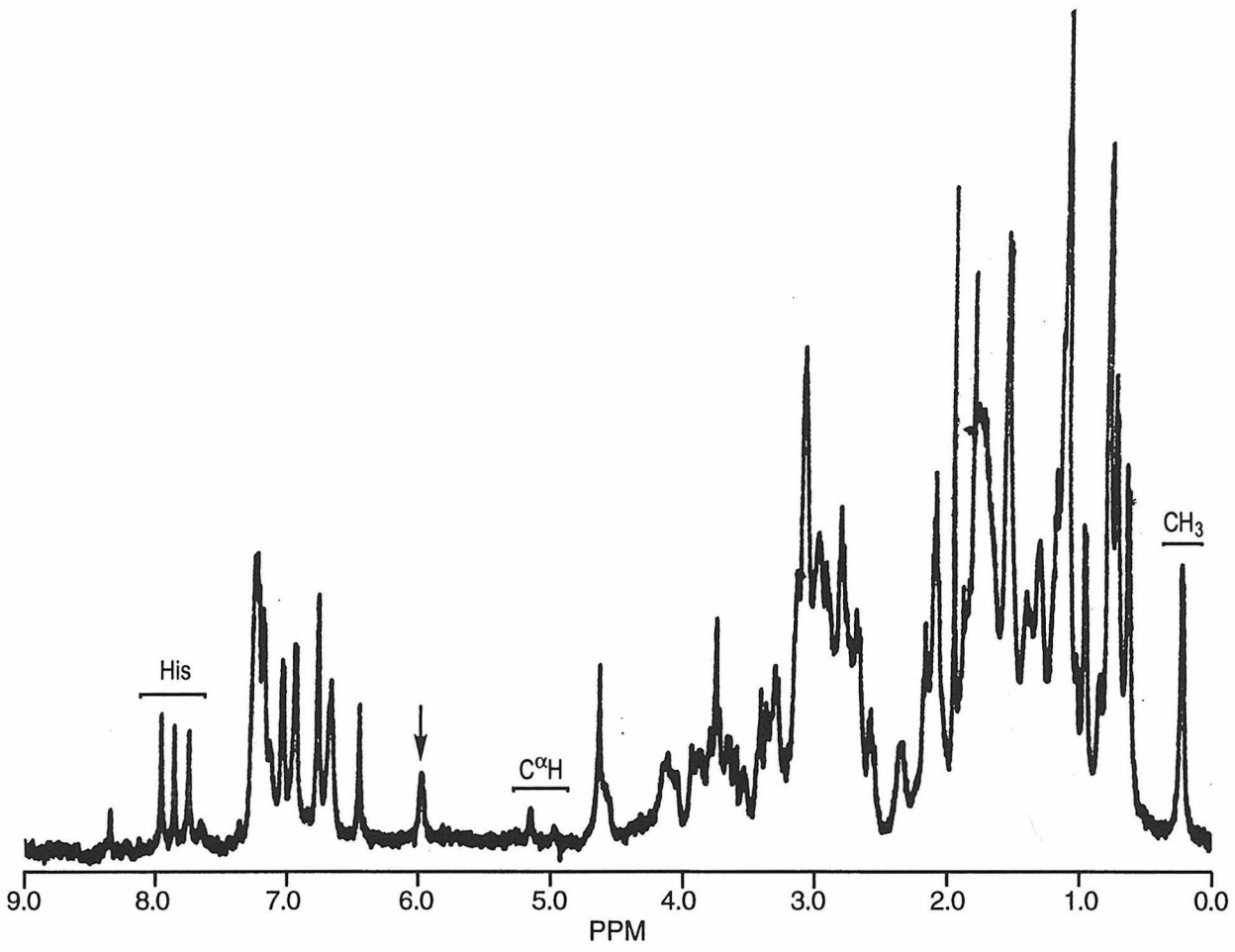

Figure 3.15. *The 500 mHz ^{1}H NMR spectrum of 2.5 μM $[Rh(phi)_2(phen')]^{3+}$ - ADR1b in the presence of $ZnSO_4$ in 50 mM d^{11}-Tris, pH 7.0. The resonances that are distinctive for folded structure are marked.*

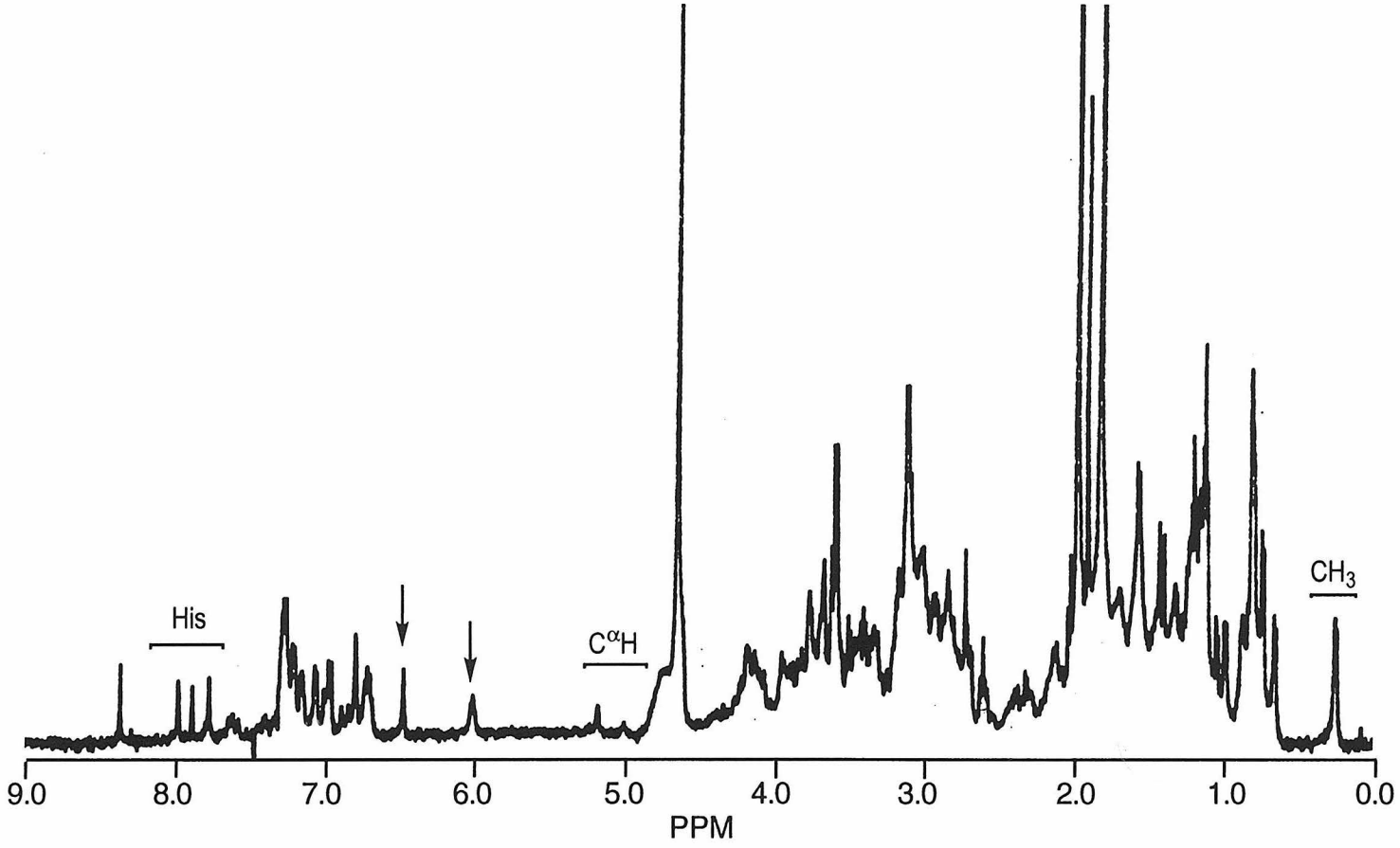

Figure 3.16. *The 500 mHz ^{1}H NMR spectrum of 1.5 μM $[Rh(phi)_2(bpy')]^{3+}$ - ADR1b in the presence of $ZnSO_4$ in 50 mM d^{11}-Tris, pH 7.7. The resonances that are distinctive for folded structure are marked.*

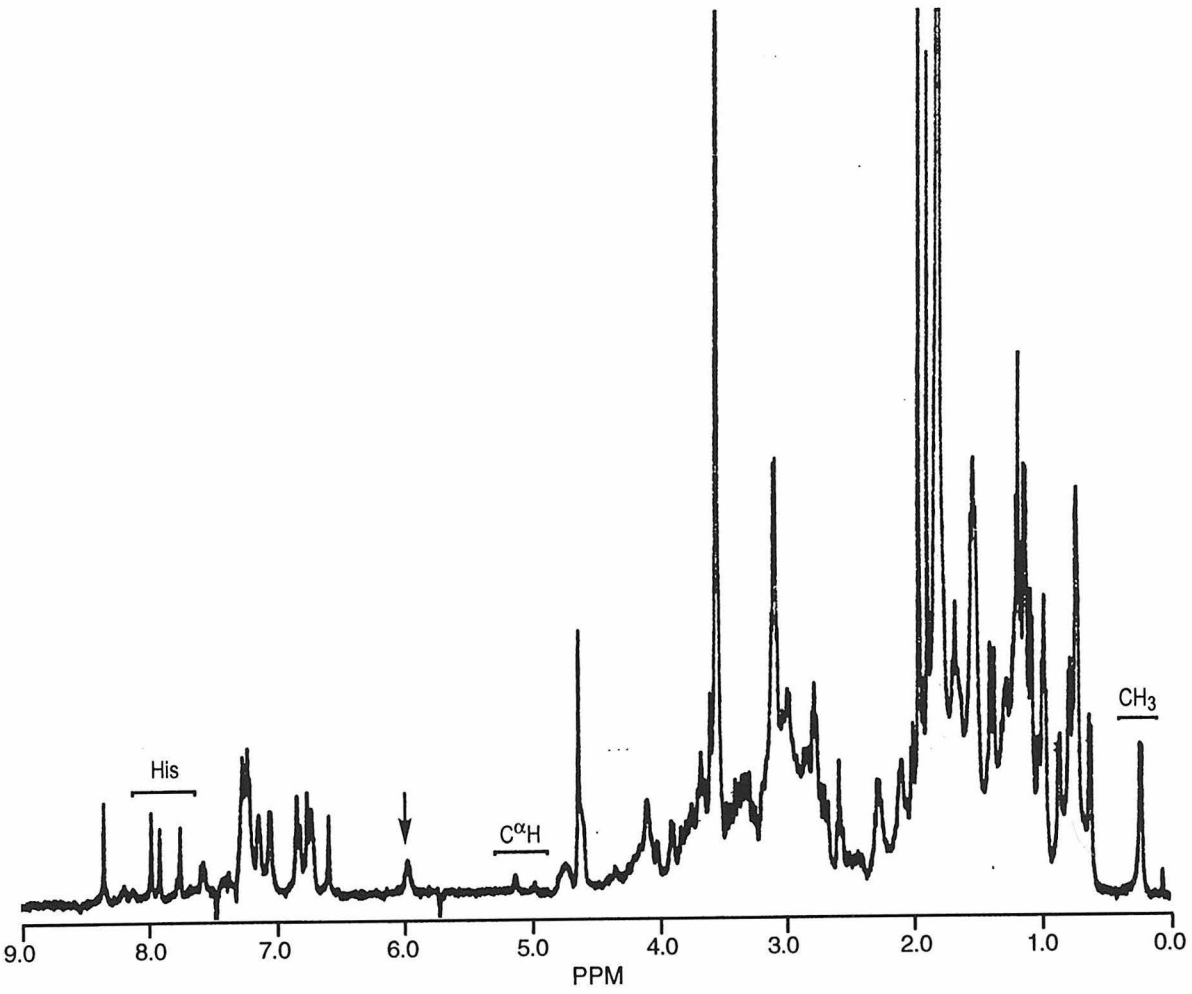

Figure 3.17. *The 500 mHz ^{1}H NMR spectra of 56 μM $[Rh(phi)_2(bpy')]^{3+}$ - ADR1b-Ala in the presence of $ZnSO_4$ in 20 mM d^{11}-Tris, pH 7.0. The resonances that are distinctive for folded structure are marked.*

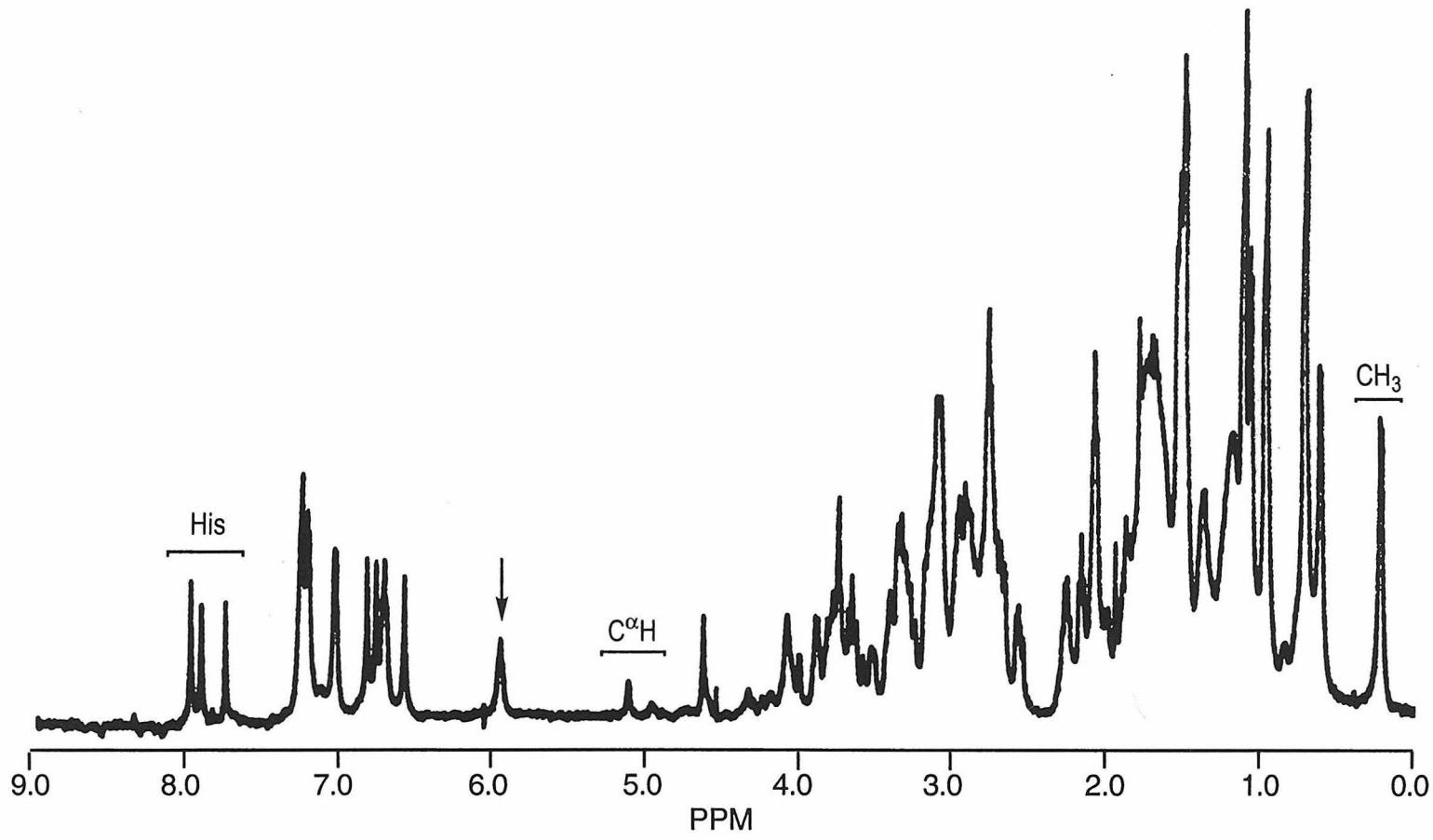

Figure 3.18. *The 500 mHz ^{1}H NMR spectrum of 2.7 μM $[Rh(phi)_2(phen')]^{3+}$ - ADR1b-Ala in the presence of $ZnSO_4$ in 50 mM d^{11}-Tris, pH 7.4. The resonances that are distinctive for folded structure are marked.*

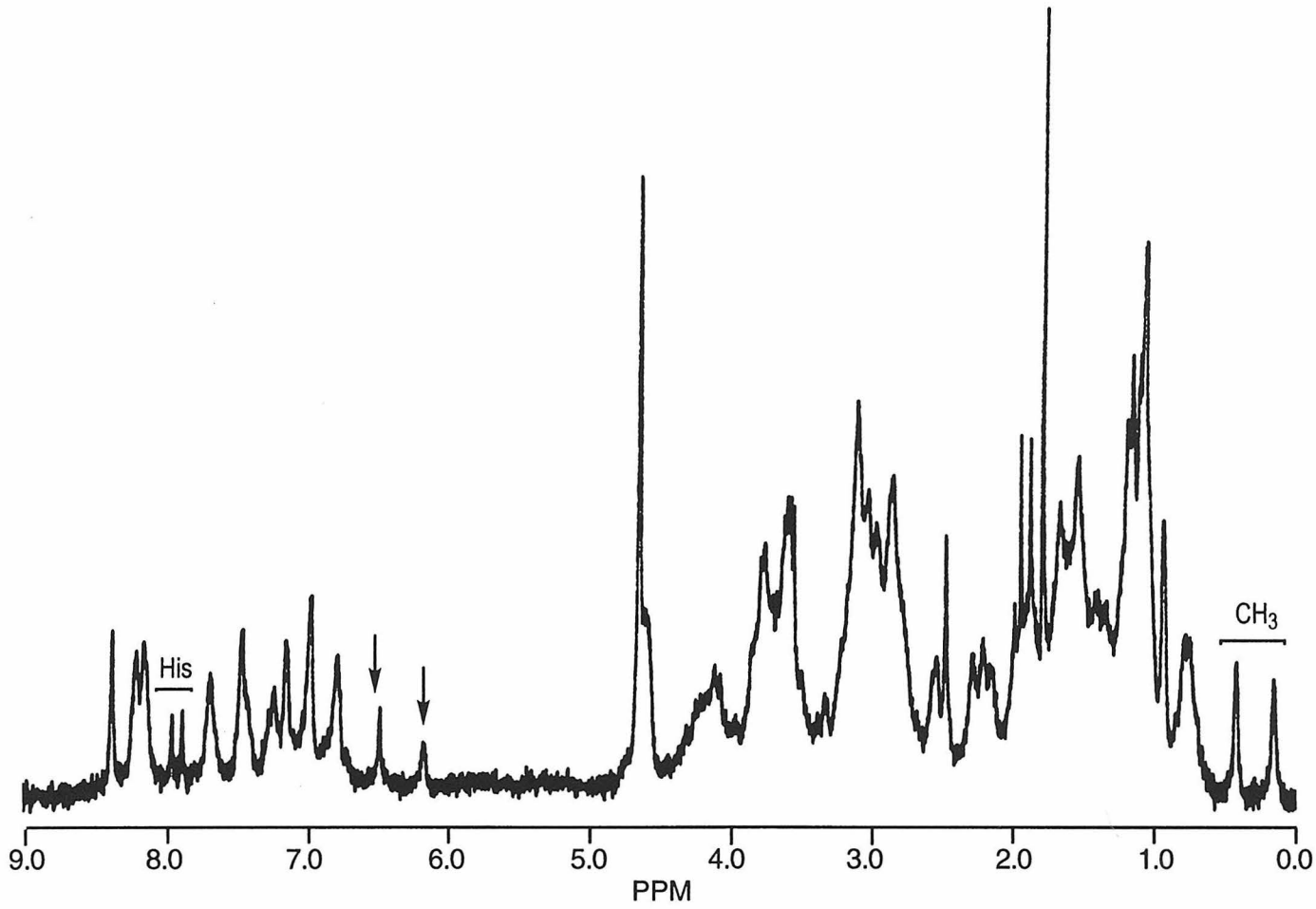

Figure 3.19. *The 500 mHz ^{1}H NMR spectrum of 56 μM $[Rh(phi)_2(bpy')]^{3+}$ - Sp1-2f in the presence of $ZnSO_4$ in 50 mM d^{11}-Tris, pH 7.9. The resonances that are distinctive for folded structure are marked.*

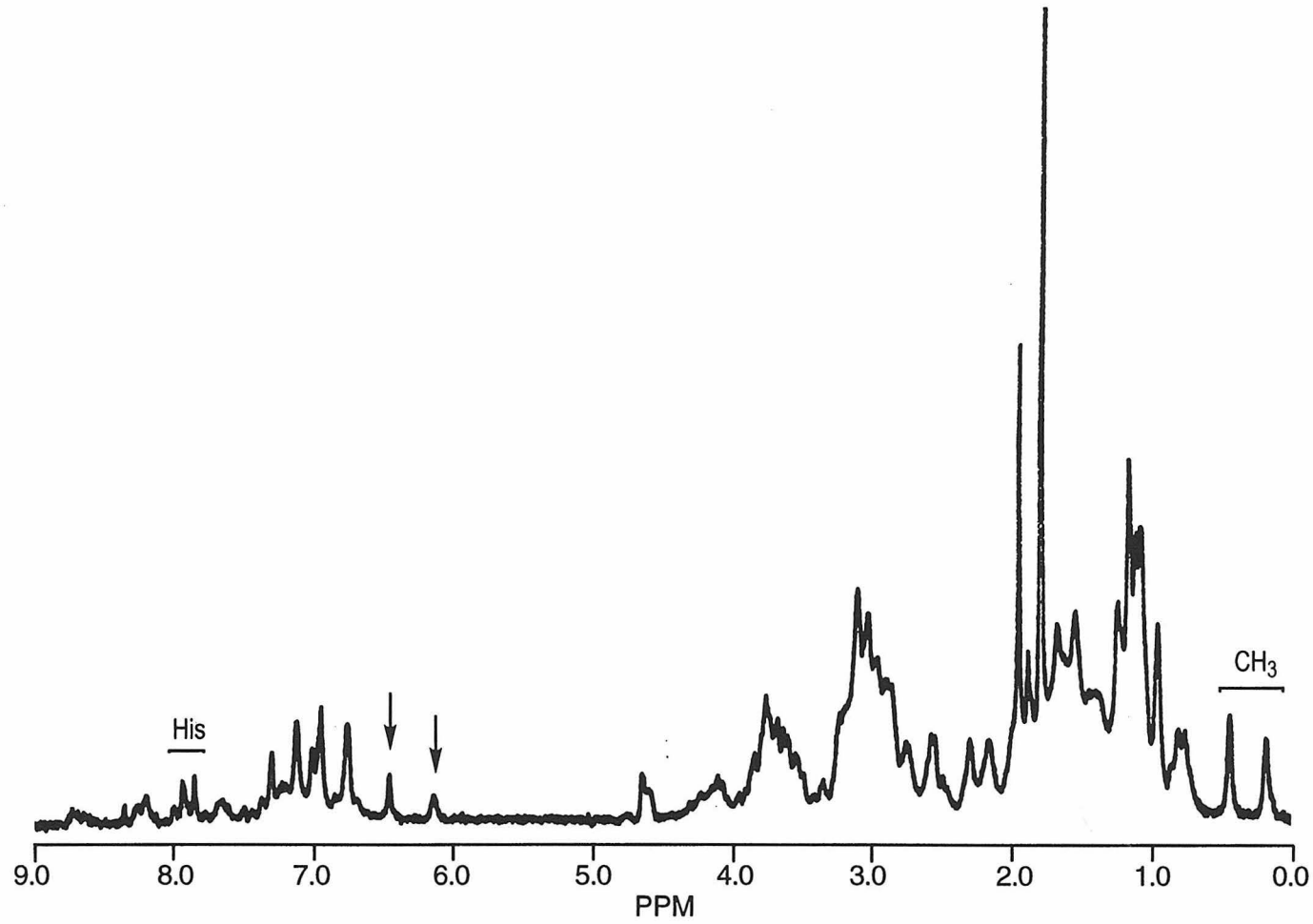

Figure 3.20. *The 500 mHz ^{1}H NMR spectrum of 35 μM $[Rh(phi)_2(phen')]^{3+}$ - Sp1-2f in the presence of $ZnSO_4$ in 20 mM d^{11}-Tris, pH 7.0. The resonances that are distinctive for folded structure are marked.*

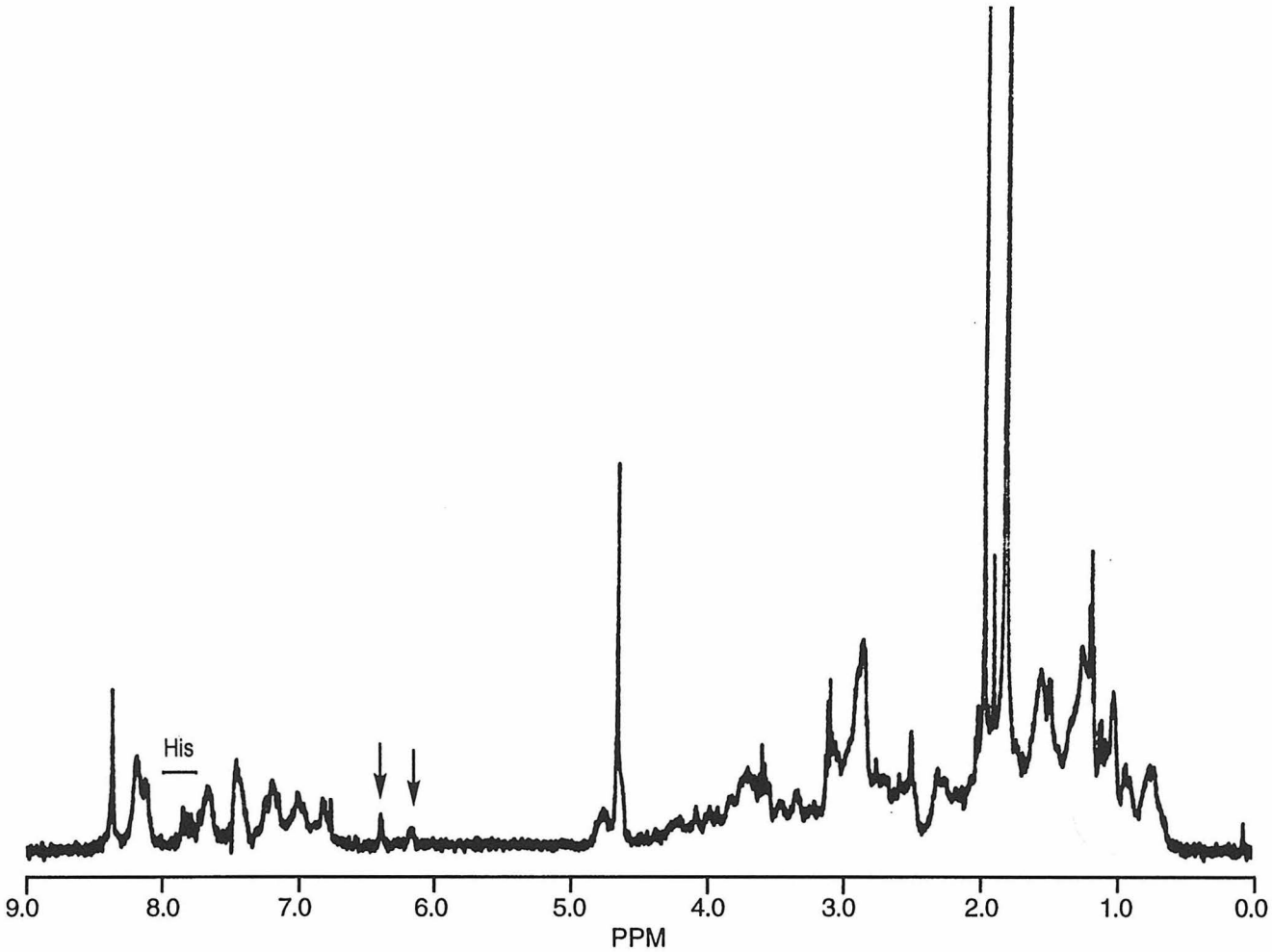

Figure 3.21. *The 500 mHz ^{1}H NMR spectrum of 36 μM $[Rh(phi)_2(bpy')]^{3+}$ - Sp1-3 in the presence of $ZnSO_4$ in 20 mM d^{11}-Tris, pH 7.0. The resonances that are distinctive for folded structure are marked.*

3.4. DISCUSSION

The spectroscopic characteristics of the metal-peptide conjugates are found to be similar to those of the isolated metal complex and those of the appended peptide. The electronic spectra for the chimeras are very similar to those of the parent $[Rh(phi)_2L]^{3+}$ (L = phen' or bpy') complexes. The coordination sphere of the rhodium is not perturbed by coupling to the peptide since any change in ligands would be evident in the spectra. In addition to providing a measure of concentration, the electronic spectrum is also diagnostic of the integrity of the metal-peptide complex. Thus, the rhodium complex and the peptide are essentially electronically independent.

Rhodium(III) - zinc finger chimeras have also been characterized by mass spectrometry. The PDMS spectra of the metal-peptide complexes show, in addition to the parent molecular ion peaks, two families of fragments that reflect the sequential analysis of the metal-peptides. Under conditions used in our experiments, no fragmentation of the peptide is evident without the metal being attached. Thus the covalently bound metal complex enhances the intensity of the A_n fragments substantially, probably because the nascent positive charge on the rhodium center causes charge remote fragmentation of the peptide. In other studies, derivatization of both the N- and C-terminus by organic molecule that place a fixed positive[29] or negative[30] charge on the peptide has caused an increase in fragmentation as seen by FAB-MS-MS or FAB/CID respectively. With these methods, many different series of fragments are seen which makes complete sequence analysis possible but difficult. With PDMS, derivatization of the N-terminus of ribonuclease A via a (ethyl)triphenylphosphonium produced only a weak incomplete series of A_n fragments. It was postulated that the labile nature of the phosphonium group inhibited the fragmentation. Guanidination of the amino terminal lysine residue produced better fragmentation.[31] However,

the attachment of the rhodium complex is not dependent on the presence of any amino acid, and derivatization of other positions is precluded while it produces a clean and complete series of sequence-specific fragments.

Electrospray ionization mass spectrometry has been used to successfully analyze rhodium(III) - zinc finger chimeras. In contrast to PDMS, the presence of the covalently attached metal complex does not promote any fragmentation of the peptide. The only peaks obtained are different charged states of the whole chimera. Thus, ESI is useful for verifying the integrity, effective deprotection and purity of the rhodium(III) - zinc finger conjugates.

In contrast, matrix assisted laser desorption ionization mass spectroscopy has given mixed results. A good spectrum contains the whole MW fragment with loss of one and two phi ligands. With these larger zinc finger peptides (~30 a. a.), smaller fragments are often obtained for chimeras that were shown to be intact by ESI mass spectrometry. MALDI is useful only if the spectra shows the characteristic triad of MW and loss of phi ligands.

The structure of the zinc finger portion of the chimera was verified by NMR spectroscopy. A procedure to reliably fold the zinc finger chimera was developed. Since $[Rh(phi)_2L]^{3+}$ complexes are unstable to thiols, the reduction of the disulfide bond that often forms in the absence of the zinc is not feasible. Thus, the rhodium(III) - zinc finger chimeras must be folded immediately after purification before oxidation can occur. Fortunately, the unfolded/oxidized chimeras precipitate out of the NMR buffer solution. The NMR spectra of the solution show resonances characteristic of the zinc folded form. Therefore, the presence of a rhodium complex covalently attached to the amino terminus of the zinc finger does not interfere with the binding of zinc.

The chemical shifts of the zinc finger peptide in the chimera are not significantly perturbed by attaching a rhodium complex to the amino terminus.

The peaks corresponding to the phi and phen ligand protons are smaller than expected and difficult to detect. In addition, once the peptide is attached, the two isomers of the rhodium center are now inequivalent. Thus, the resonances of the protons associated with the ligands may be further split into multiplets and may be broadened. In contrast, the resonances of the zinc finger are very distinct. Thus, the two parts of the chimeras are virtually structurally independent.

The spectroscopy of these rhodium(III) - zinc fingers has shown that they are nearly independent domains that are covalently linked together. Also, the zinc finger portion is found to form the proper structure upon binding to zinc. Thus, since they are independent domains structurally, the next question is whether they are independent domains functionally. To investigate this, the DNA recognition characteristics of these rhodium(III) - zinc finger peptide chimeras will be described in the following chapter.

3.5. REFERENCES

(1) Sardesai, N. Y.; Lin, S. C.; Zimmermann, K.; Barton, J. K. *Bioconj. Chem.* **1995**, *6*, 302-312.

(2) Pavletich, N. P.; Pabo, C. O. *Science* **1991**, *252*, 809-817.

(3) Pavletich, N. P.; Pabo, C. O. *Science* **1993**, *261*, 1701-1707.

(4) Fairall, L.; Schwabe, J. W. R.; Chapman, L.; Finch, J. T.; Rhodes, D. *Nature* **1993**, *366*, 483-487.

(5) Párraga, G.; Horvath, S. J.; Eisen, A.; Taylor, W. E.; Hood, L.; Young, E. T.; Klevit, R. E. *Science* **1988**, *241*, 1489-1492.

(6) Lee, M. S.; Gippert, G. P.; Soman, K. V.; Case, D. A.; Wright, P. E. *Science* **1989**, *245*, 635-637.

(7) Klevit, R. E.; Herriott, J. R.; Horvath, S. J. *Prot. Struct. Funct. Gen.* **1990**, *7*, 215-226.

(8) Omichinski, J. G.; Clore, G. M.; Appella, E.; Sakaguchi, K.; Gronenborn, A. M. *Biochem.* **1990**, *29*, 9324-9334.

(9) Neuhaus, D.; Nakaseko, Y.; Nagai, K.; Klug, A. *FEBS Lett.* **1990**, *262*, 179-184.

(10) Kochoyan, M.; Keutmann, H. T.; Weiss, M. A. *Biochem.* **1991**, *30*, 7063-7072.

(11) Kochoyan, M.; Havel, T. F.; Nguyen, D. T.; Dahl, C. E.; Keutmann, H. T.; Weiss, M. A. *Biochem.* **1991**, *30*, 3371-3386.

(12) Xu, R. X.; Horvath, S. J.; Klevit, R. E. *Biochem.* **1991**, *30*, 3365-3371.

(13) Palmer III, A. G.; Rance, M.; Wright, P. E. *J. Am. Chem. Soc.* **1991**, *113*, 4371-4380.

(14) Omichinski, J. G.; Clore, G. M.; Robien, M.; Sakaguchi, K.; Appella, E.; Gronenborn, A. *Biochem.* **1992**, *31*, 3907-3917.

(15) Nakaseko, Y.; Neuhaus, D.; Klug, A.; Rhodes, D. *J. Mol. Biol.* **1992**, *228*, 619-636.

(16) Lee, M. S.; Palmer III, A. G.; Wright, P. E. *J. Biomol. NMR* **1992**, *2*, 307-322.

(17) Neuhaus, D.; Nakaseko, Y.; Schwabe, J. W. R.; Klug, A. *J. Mol. Biol.* **1992**, *228*, 637-651.

(18) Bernstein, B. E.; Hoffman, R. C.; Horvath, S.; Heriott, J. R.; Klevit, R. E. *Biochem.* **1994**, *33*, 4460-4470.

(19) Frankel, A. D.; Berg, J. M.; Pabo, C. O. *Proc. Natl. Acad. Sci. USA* **1987**, *84*, 4841-4845.

(20) Weiss, M. A.; Keutmann, H. T. *Biochem.* **1990**, *29*, 9808-9813.

(21) Párraga, G.; Horvath, S. J.; Hood, L.; Young, E. T.; Klevit, R. E. *Proc. Natl. Acad. Sci. USA* **1990**, *87*, 137-141.

(22) Berg, J. M.; Merkle, D. L. *J. Am. Chem. Soc.* **1989**, *111*, 3759-3761.

(23) Lee, M. S.; Mortshire-Smith, R. J.; Wright, P. E. *FEBS Lett.* **1992**, *309*, 29-32.

(24) Sluka, J. P.; Griffin, J. H.; Mack, D. P.; Dervan, P. B. *J. Am. Chem. Soc.* **1990**, *112*, 6369-6374.

(25) Pyle, A. M.; Chiang, M. Y.; Barton, J. K. *Inorg. Chem.* **1990**, *29*, 4487-4495.

(26) Krotz, A. H.; Kuo, L. Y.; Barton, J. K. *Inorg. Chem.* **1993**, *32*, 5963-5974.

(27) Sitlani, A.; Long, E. C.; Pyle, A. M.; Barton, J. K. *J. Am. Chem. Soc.* **1992**, *114*, 2303-2312.

(28) Berg, J. M. *Curr. Op. Struct. Biol.* **1993**, *3*, 11-16.

(29) Watson, J. T.; Wagner, D. S.; Chang, Y.; Strahler, J. R.; Hanash, S. M.; Gage, D. A. *Int. J. Mass Spectrom. Ion Proc.* **1991**, *111*, 191-209.

(30) Lindh, I.; Griffiths, W. J.; Bergman, T.; Sjovall, J. *Rapid Comm. Mass Spectrom.* **1994**, *8*, 797-803.

(31) Bunk, D. M.; Macfarlane, R. D. *Int. J. Mass Spectrom. Ion Proc.* **1993**, *126*, 123-136.

Chapter 4. DNA Recognition by Rhodium(III) - Zinc Finger Peptide Chimeras

4.1. INTRODUCTION

The synthesis and characterization of rhodium(III) - zinc finger peptide chimeras were discussed in detail in Chapters 2 and 3. Spectroscopic evidence indicated that the rhodium complex and the zinc finger peptide are virtually structurally independent. In this chapter, DNA recognition studies are being used to determine if metal complex and peptide function independently as well. Ideally, the rhodium complex should deliver the zinc finger to DNA with a high, but non-specific affinity, while the zinc finger is expected to direct specific binding using its amino acid residues.

Previous work has focused on the DNA recognition properties of $[Rh(phi)_2(phen')]^{3+}$-α-helix chimeras (phi = phenanthrenequinone diimine; phen' = (5-amidoglutaryl)-1,10-phenanthroline).[1,2] These conjugates contained the recognition helices of the P_{22} and 434 repressor helix - turn - helix transcription factor proteins. In these systems, the rhodium complex was bound in the major groove of DNA and the peptide governed the recognition characteristics by interaction with the DNA. In the studies of the P_{22} family of rhodium(III) - α-helix chimeras, a single glutamate was identified to be the DNA recognition 'switch'.[1] The function of this residue is to maintain the helical structure of the peptide and to directly contact the DNA. However, the chimera did not recognize the P_{22} operator site since the helix was not correctly oriented in the major groove, thereby placing the recognition glutamate on the opposite face of the helix from the residues that should contact the P_{22} operator site. In contrast, the 434 family of rhodium(III) - α-helix chimeras did recognize the 5'-ACAA-3' operator site.[2] However, an additional cleavage site within the DNA sequence

were also seen. It was postulated that the peptide was adopting multiple orientations relative to the intercalated rhodium complex. This is a reasonable assumption since the these small α-helical peptides lack defined rigid structures and has a flexible linkage to the rhodium. Therefore, for the P_{22} and 434 metal - helix chimeras systems, the structure of the α-helix is variable which in turn affects the DNA recognition characteristics of the chimeras.

In contrast, zinc finger peptides provide a small well-defined structural domain that can be used for DNA recognition.[3] The crystal structure of Zif268 with DNA reveals that each finger is an independent modular unit recognizing a three base pair sequence.[4] However, a single finger does not exhibit any DNA binding specificity even though it has been proven to fold correctly.[5,6] In order to study the sequence-specific interactions of individual zinc fingers with DNA, rhodium - zinc finger chimeras were constructed by covalently attaching the complex to the amino terminus of a single zinc finger peptide. Phi complexes of rhodium are particularly useful for these studies since they intercalate with high affinity into the major groove of DNA and cleave DNA by photoinduced hydrogen atom abstraction.[7-9] For the experiments discussed in this chapter, $[Rh(phi)_2(bpy')]^{3+}$ or $[Rh(phi)_2(phen')]^{3+}$, both sequence-neutral molecules, were used to deliver zinc finger peptides to the DNA major groove such that the peptide provided the sequence-specific interactions with the DNA bases. For our studies, four different zinc fingers were synthesized. The ADR1b finger was chosen because NMR structural data[10] and change of specificity mutation studies have been published.[11,12] The Sp1 zinc finger protein also has many studies done on changing the DNA binding specificity though amino acid mutations[13-17] and derives from the same family of the zinc fingers as the Zif268 protein whose crystal structure bound to DNA has been published.[4,18,19] It should be noted that the two Sp1 zinc fingers and the ADR1b zinc finger recognizes different DNA

triplets.[12,20] Table 4.1 shows the sequences and the recognition sites of the zinc finger peptides that were prepared.

In addition to binding to the major groove of DNA,[7,21-23] phi complexes of rhodium(III) also induce DNA cleavage upon photoactivation at their site of binding.[9] This property allows the recognition sites for the rhodium(III) - zinc finger chimeras to be determined using polyacrylamide gel electrophoresis.[7] The metal-peptide conjugates are incubated with 5'-^{32}P-end-labeled double-stranded DNA. Upon irradiation with ultra-violet light, there is a ligand to metal charge transfer in the rhodium complex which creates a radical on the phi ligand. This radical abstracts the 3'-hydrogen from the DNA sugar phosphate backbone resulting in strand scission.[9] The DNA is then denatured and electrophoresed on a high resolution polyacrylamide gel which allows determination of the binding site to single base resolution by comparison to standard Maxam-Gilbert sequencing reactions[24] (Scheme 4.1). This scheme has been used successfully to analyze rhodium(III) - α-helix peptide chimeras.[1,2]

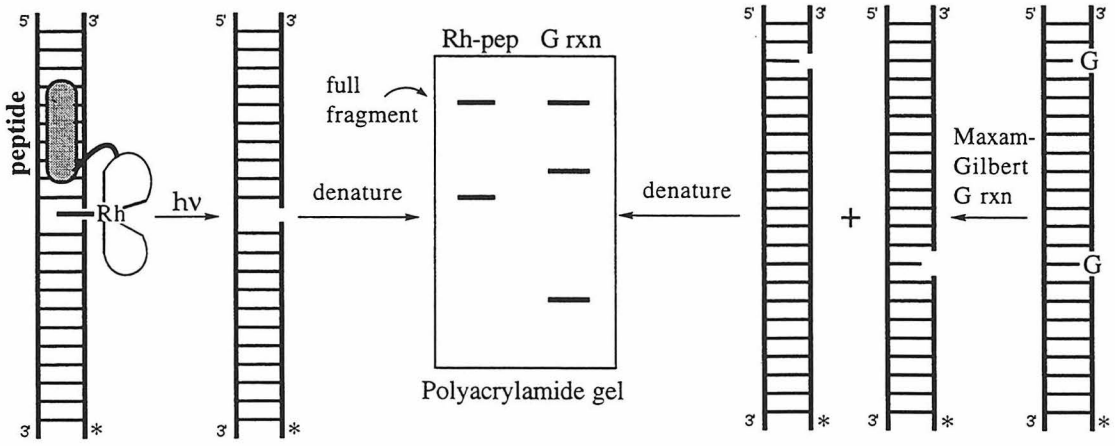

Scheme 4.1. *The method for the analysis DNA binding sites of covalent chimeras of zinc finger peptides and phi complexes of rhodium(III) by polyacrylamide gel electrophoresis of photoactivated cleavage products. The * represents a ^{32}P-label on the terminal phosphate of the DNA.*

Table 4.1: The Sequences of the Zinc Finger Peptides and Their DNA Recognition Sites[a]

Name	Sequence	DNA site
ADR1b	NH_2 - G S **F** V **C** - - E V **C** T R A **F** A R Q E H **L** K R **H** Y R S **H** T N - CO_2H	5'-GAG-3'
ADR1b-Ala[b]	NH_2 - G S **F** V **C** - - E V **C** T R A **F** A R Q E H **L** K R **H** *A* R S **H** T N -CO_2H	5'-GAG-3'
Sp1-2	NH_2 - G G **F** A **C** T V S Y **C** G K R **F** T R S D E **L** Q R **H** K R T **H** T G -CO_2H	5'-GCG-3'
Sp1-3	NH_2 - G G **F** A **C** - - P E **C** P K R **F** A R S D H **L** S K **H** I K T **H** Q N -CO_2H	5'-GGG-3'

[a]The conserved residues are in bold and the DNA recognition residues are underlined. [b]For the ADR1b-Ala peptide, the only tyrosine in ADR1b was changed to an alanine (italics).

Using this photocleavage assay, the DNA recognition characteristics of the rhodium(III) - zinc finger chimeras were investigated. Initial studies were done on a DNA restriction fragment such that a large variety of potential binding site on the DNA could be investigated. Based on those results, an oligonucleotide was designed to further investigate the specificity and affinity of the rhodium(III) - zinc finger chimeras at different DNA sites.

4.2. EXPERIMENTAL

4.2.1. Materials. Denaturing polyacrylamide gels were made from SequaGel reagents (National Diagnostics). Sonicated calf thymus was purchased from Pharmacia, pUC18 from Boehringer-Mannheim and other enzymes from New England Biolabs. [γ-^{32}P]-ATP and [α-^{32}P]-dATP came from NEN-Dupont.

4.2.2. Instrumentation. Photocleavage experiments were carried out using an Oriel Model 6140 1000W Hg/Xe lamp fitted with a monochromator and 300 nm cutoff filter. Ultraviolet-visible spectra were recorded on a Hewlett-Packard 8452A diode array or Cary 219 spectrophotometer. The concentrations of metal-peptide chimeras were determined by UV-visible spectroscopy using ε_{350} (isobestic)=23,600 $M^{-1}cm^{-1}$. High performance liquid chromatography (HPLC) was carried out on a Waters 600E system equipped with a Waters 484 tunable detector using a Dynamax C-18 reverse phase column. All oligonucleotides were synthesized on an ABI391 DNA synthesizer. Gel electrophoresis experiments were scanned using Molecular Dynamics phosphoroimager and then visualized and quantified using ImageQuant software. Modeling was done using InsightII (Biosym) software on a Silicon Graphics Indigo xs/24 system.

4.2.3. Photocleavage of Restriction Fragments. The plasmid pUC18 was digested with the restriction endonuclease NdeI. For 5'-end labeling, the plasmid was treated with calf alkaline phosphatase followed by T4 polynucleotide kinase and [γ-^{32}P]-ATP. After labeling, the DNA was digested with HindIII. The 215 base pair fragment was isolated using 4% nondenaturing polyacrylamide gel electrophoresis, electroelution and a Nensorb column.

Sample irradiations were carried out in 20 μL total volume in 1.7 mL presiliconized eppendorf tubes. The reactions contained ~20,000 counts of end-labeled fragment, 22.5 μM (base pairs) calf thymus DNA and 450 nM rhodium complex in 25 mM Tris•HCl, pH 8.0, 25 mM NaCl, 100 μM $ZnSO_4$ and 10% glycerol. The samples were incubated overnight at room temperature and then irradiated at 313 nm for 15 min. The light control was irradiated in the absence of metal to test for light damage to the DNA. The dark control contained metal - peptide chimera but was not irradiated.

After irradiating, the samples were then ethanol precipitated by adding 1.5 μL 2 mM (base pairs) calf thymus DNA, 10 μL 7.5 M NH_4OAc and 120 μL ethanol, cooling on dry ice for 15 min. and spinning on a microcentrifuge. The resulting DNA pellet was washed twice with 80% ethanol, resuspended in 20 μL water and dried. Next, the DNA was resuspended in loading dye (~2 μL). The samples, along with Maxam-Gilbert A+G and C+T sequencing reactions,[24] were denatured at 90°C for 1.5 minutes and directly loaded on an 8% denaturing polyacrylamide gel. The gel was electrophoresed at 2000 V (85 W maximum) for about 1.5 hrs. The gel was transferred to 3 mm Whatman filter paper, dried and exposed on a Molecular Dynamics phosphoroimager screen.

4.2.4. Photocleavage of Oligonucleotides. The oligonucleotide, O1: (5'-GACTCGCACTGTGACTGCGACTGAGACTGGGACTG-3') and its complement,

O2 were synthesized and purified by HPLC. For 5'-end labeling, each oligonucleotide was treated with T4 polynucleotide kinase and [γ-^{32}P]-ATP. Then, a tenfold fold molar excess of the complementary strand was added to the labeling solution. After heating to 90°C, the solution was allowed to cool for several hours to allow proper annealing. The double stranded, labeled oligonucleotide was resolved on a 20% non-denaturing polyacrylamide gel. The DNA was isolated by crushing the gel pieces and incubating in 10 mM Tris, pH 7.4, 1 mM EDTA at 37°C for 4 hours. The gel pieces were removed using a 0.45 μM cellulose acetate microcentrifuge filter and desalted using a Nensorb column.

The irradiations were carried out in the same manner as in the restriction fragment experiments except that the reactions were dried instead of ethanol precipitated. The DNA was resuspended in ~20 μL dye and 2 μL were denatured and loaded along with Maxam-Gilbert A+G and C+T sequencing reactions[24] on a 20% denaturing polyacrylamide gel. The gel was electrophoresed at 2000V (85 W maximum) for 2 hrs, transferred to a film and exposed on a phosphoroimager screen.

4.2.5. Quantitative Photocleavage Titrations for Binding Constant Determinations. The protocol was based on the quantitative affinity cleavage titration method developed by Singleton and Dervan.[25] A series of solutions were prepared ranging from 15 nM to 15 μM rhodium with a constant 2:1 rhodium to DNA duplex ratio. Since the amount of labeled duplex was kept low (~12,000 cts), the DNA concentration was based on the amount of unlabeled double stranded oligonucleotide present. All samples were prepared as 20 μL reaction volume in the irradiation buffer, incubated overnight at room temperature and irradiated at 313 nm for 15 minutes. The samples were dried and resuspended in loading dye (~6 μL) and 2 μL were denatured and loaded

along with Maxam-Gilbert A+G and C+T sequencing reactions,[24] on a 20% denaturing polyacrylamide gel and electrophoresed at 2000V (85 W maximum) for 2 hrs. The gel was transferred to a film and exposed on a phosphoroimager screen.

The cleavage bands were quantitated and corrected for loading and controls. A theoretical binding curve was fit to the experimental data using K_a as the adjustable parameter:

$$\frac{I_{fit}}{I_{max}} = \frac{K_a[DNA]_{tot}}{1 + K_a[DNA]_{tot}}$$

The difference between I_{fit} and I_{site} for all points was minimized using the non-linear least-squares fitting procedure. All data points were included unless the I_{site} value for a single lane was greater than two standards deviations from the adjacent lanes.

4.3. RESULTS

4.3.1. Modeling Studies. The interaction of rhodium(III) - zinc finger chimeras with DNA was modeled. The zinc finger - DNA structure was taken from the crystal structure of the Zif268 bound to DNA.[4] The first finger of Zif has a 55% homology to the second finger of Sp1 which was used for our experiments. More importantly, the residues implicated in base contacts and the recognition triplet (GCG) are the same for both peptides.

An intercalation site from the structure of dCpG and terpyridine platinum,[26] with addition B-form DNA added on both ends, was attached to the 3'-end of the recognition triplet from the crystal structure of Zif268 and DNA.[4] Two glycines and $[Rh(phi)_2(phen')]^{3+}$ were attached to the amino terminus of the first zinc finger of Zif starting at the conserved tyrosine. This chimera was

docked to the DNA by intercalating the rhodium complex and by placing the zinc finger in its recognition position. The torsion angles in the glutaryl linker and two glycines were varied to allow the docking. It was found that both parts of the chimera could interact with the DNA when the intercalation site was two base pairs to the 3'-side of the GCG recognition triplet (Figure 4.1). The modeling shows that there exists at least one feasible orientation where the rhodium(III) - zinc finger chimera can interact with DNA in the desired manner.

4.3.2. DNA Cleavage by Rhodium(III) -Zinc Finger Chimeras on Restriction Fragments. The DNA recognition properties of rhodium(III) - zinc finger chimeras were investigated using photocleavage assays on the 215 base pair NdeI/HindIII restriction fragment of pUC18. As shown in Figure 4.2, both $[Rh(phi)_2(bpy')]^{3+}$ and $[Rh(phi)_2(phen')]^{3+}$ - chimeras promote DNA strand scission upon photoactivation. More importantly, the pattern of cleavage differs for rhodium - zinc finger peptide chimeras versus the metal complexes alone (e.g., compare lanes 3 and 8 in Fig. 4.2). Also, variations in the zinc fingers produce distinct bands when attached to the same metal complex (e.g., compare lanes 6 and 9 in Fig. 4.2). In turn, $[Rh(phi)_2(bpy')]^{3+}$ and $[Rh(phi)_2(phen')]^{3+}$ chimeras of the same peptide have different specificities (e.g., compare lanes 5 and 6 in Fig. 4.2). Thus, the linker on the rhodium complex and the amino acid sequence of the zinc finger both influence DNA recognition. The cleavage sites are shown in Figure 4.3.

4.3.3. Crosslinking of Restriction Fragments. The photocleavage studies of fragments has produced an interesting aside; namely the prevalence of the band that does not migrate out of the loading wells (Fig. 4.2, lanes 5-7 and 9-11). Since it is not present in the dark control (lane 2), it requires photoactivation. The band also requires the presence of a peptide (lanes 3-4). However, when free

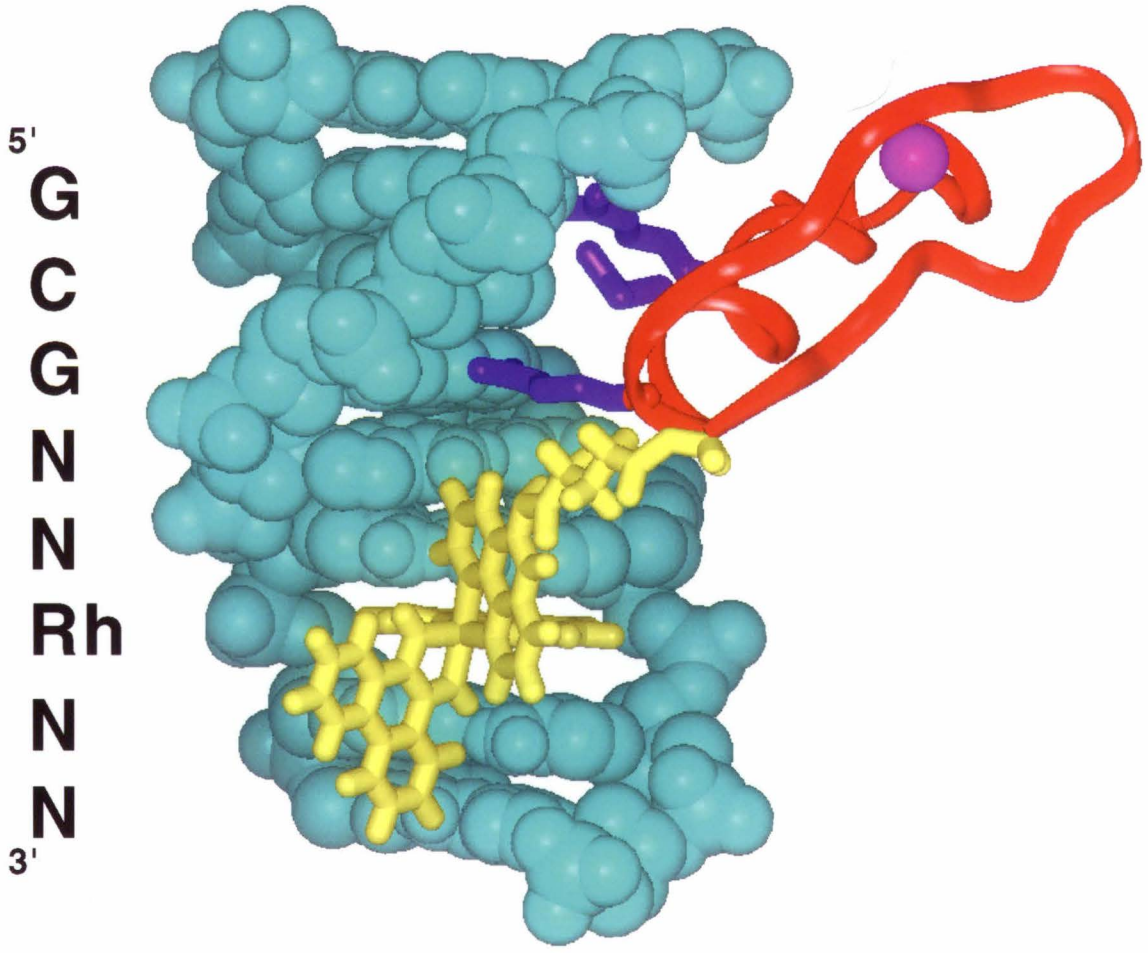

Figure 4.1. *A model of the interaction of a* $[Rh(phi)_2(phen')]^{3+}$*-zinc finger chimera with DNA. The DNA is in aqua, the rhodium in yellow and the zinc finger is in red with the amino acid side chains that contact the DNA base pairs in purple and the zinc in pink. The sequence of the left (top) strand is given on the left.*

Figure 4.2. *An image of a polyacrylamide gel showing the photocleavage of a 5'-^{32}P end labeled 215 base pair NdeI/HindIII restriction fragment of pUC18 by 450 nM rhodium(III) complexes and rhodium (III)-zinc finger chimeras in the presence of 22.5 μM base pairs calf thymus DNA: lane 1, light control (LC); lane 2, dark control with [Rh(phi)$_2$(phen')]$^{3+}$-Sp1–2f (DC); lane 3, [Rh(phi)$_2$(bpy')]$^{3+}$ (B); lane 4, [Rh(phi)$_2$(phen')]$^{3+}$ (P); lane 5, [Rh(phi)$_2$(bpy')]$^{3+}$-Sp1-2f (BS2); lane 6, [Rh(phi)$_2$(phen')]$^{3+}$-Sp1-2f (PS2); lane 7, [Rh(phi)$_2$(bpy')]$^{3+}$-Sp1-3 (BS3); lane 8, [Rh(phi)$_2$(bpy')]$^{3+}$-ADR1b (BA); lane 9, [Rh(phi)$_2$(phen')]$^{3+}$-ADR1b (PA); lane 10, [Rh(phi)$_2$(bpy')]$^{3+}$-ADR1b-Ala (BAla); lane 11, [Rh(phi)$_2$(phen)]$^{3+}$-ADR1b-Ala (PAla); lane 12, Maxam-Gilbert A+G sequencing reaction; lane 13, Maxam-Gilbert C+T sequencing reaction. All samples were incubated overnight in 25 mM Tris•HCl, pH 8.0, 25 mM NaCl, 100 μM ZnS0$_4$, 10% glycerol and irradiated for 15 min at 313 nm. The bracket represents the portion of the fragment (246-330) that is analyzed in Figure 4.3.*

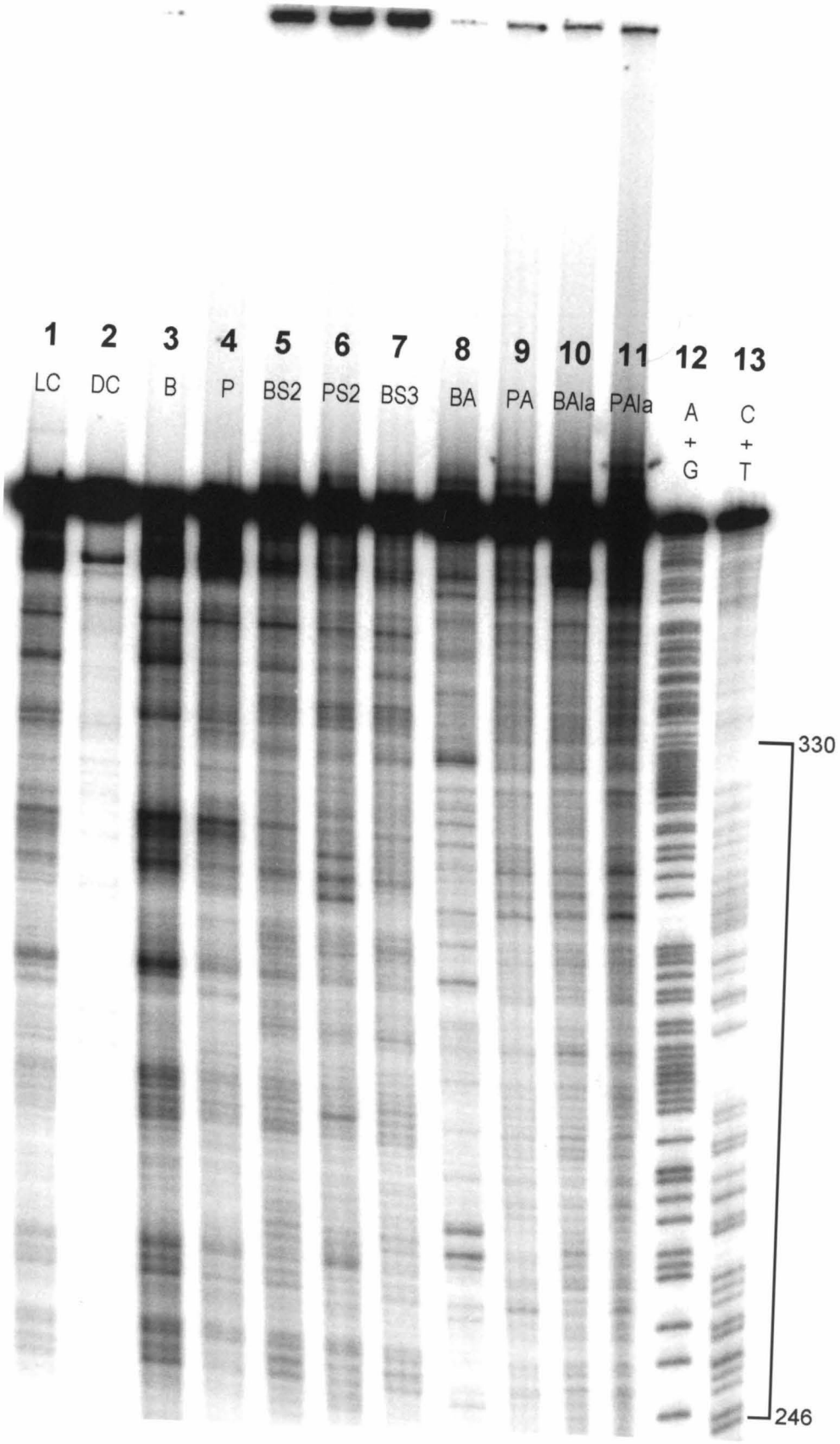
1
LC
2
DC
3
B
4
P
5
BS2
6
PS2
7
BS3
8
BA
9
PA
10
BAla
11
PAla
12
A + G
13
C + T
330
246

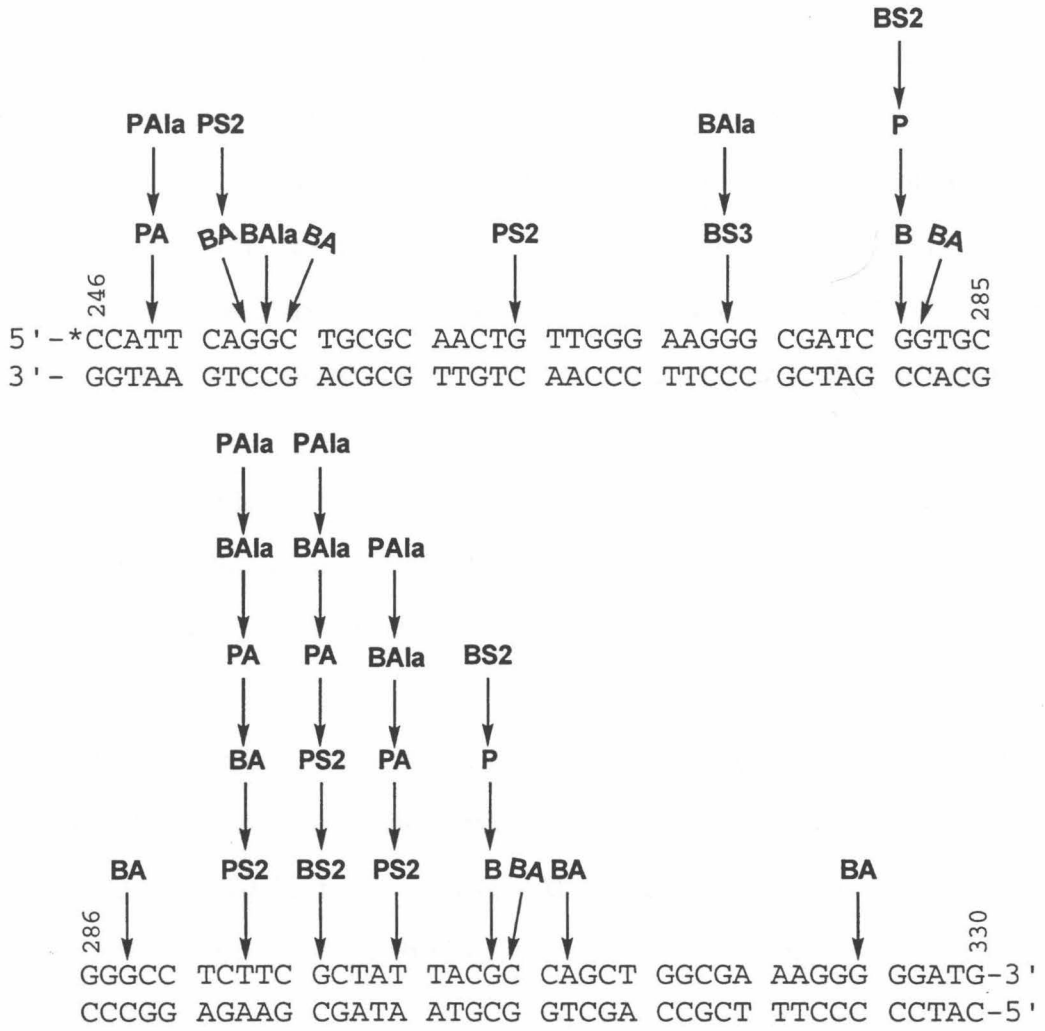

Figure 4.3. *The sequence of the portion of the 5'-^{32}P end labeled 215 base pair NdeI/HindIII restriction fragment of pUC18 denoted between the brackets on the right hand side of the gel in Figure 4.2. The arrows represent the strong photocleavage sites for the various rhodium complexes and zinc finger chimeras: B = [Rh(phi)$_2$(bpy')]$^{3+}$; P = [Rh(phi)$_2$(phen')]$^{3+}$; BS2 = [Rh(phi)$_2$(bpy')]$^{3+}$-Sp1-2f; PS2 = [Rh(phi)$_2$(phen')]$^{3+}$-Sp1-2f; BS3 = [Rh(phi)$_2$(bpy')]$^{3+}$-Sp1-3; BA = [Rh(phi)$_2$(bpy')]$^{3+}$-ADR1b; PA = [Rh(phi)$_2$(phen')]$^{3+}$-ADR1b; BAla = [Rh(phi)$_2$(bpy')]$^{3+}$-ADR1b-Ala; PAla = [Rh(phi)$_2$(phen)]$^{3+}$-ADR1b-Ala. The * represents the site of the P-32 label.*

ADR1b is irradiated in the presence of DNA, no band appears in the wells (data not shown). The band also does not need the correct folded zinc finger since it is also produced with chimeras containing oxidized peptides (data not shown). The top band can be isolated using phenol/chloroform extraction in the same manner that a crosslink between the catabolite gene activator protein (CAP) and its DNA has been isolated.[27] Thus, the top band is most likely a crosslink between the chimera and DNA. For the CAP-DNA system, heat/alkali treatment reveals the site of crosslink. When the top band caused by $[Rh(phi)_2(phen')]^{3+}$-ADR1b was treated with sodium hydroxide and heat, the band was no longer present in the well, but several new bands with greater mobility were observed. The cleavage pattern was identical to the one produced by $[Rh(phi)_2(phen')]^{3+}$-ADR1b, indicating that the crosslinking is not affecting the specificity of the chimera.

The possibility of rhodium complex creating a tyrosine radical on the peptide which in turn could covalently bind to DNA was explored. To investigate this possibility, the ADR1b-Ala peptide, which has the single tyrosine of the ADR1b peptide replaced with an alanine, was synthesized. Studies on the intact ADR1b protein indicate that this T to A mutation decreases the binding affinity, but does not change the specificity of the protein for its DNA site.[12] Upon irradiation, both $[Rh(phi)_2(bpy')]^{3+}$ and $[Rh(phi)_2(phen')]^{3+}$ - ADR1b-Ala chimeras produce slightly more crosslink than the native ADR1b chimeras (Figure 4.2 lanes 8 and 9 versus 10 and 11). This indicates that the tyrosine is not responsible for the crosslinking of this peptide to DNA.

Therefore, the crosslink is probably between the rhodium complex and DNA. When phi complexes of rhodium(III) are irradiated, they undergo decomposition with the preferential loss of a phi ligand.[8] Since it is the phi

ligand that intercalates into DNA, the residual rhodium complex should dissociate from the DNA. For the zinc finger chimeras, the presence of the peptide could increase the binding constant such that the residual rhodium complex is held in the vicinity of the DNA. Then, the open coordination sites on the rhodium could crosslink to the DNA bases. In fact, *cis*-$[Rh(phen)_2Cl_2]^+$ has been found to photochemically produce covalent adducts with calf thymus DNA, nucleotides and nucleosides.[28,29] Irradiation of *cis*-$[Rh(phen)_2Cl_2]^+$ causes dissociation of the chloride ligands, allowing subsequent coordination to the N7 or N3 of guanine.

Since no new sites are revealed by treating the crosslink with base, the presence of the crosslink does not appear to affect the DNA binding specificity of the rhodium(III) - zinc finger chimeras. Further investigations, though interesting, are therefore not relevant to delineating the DNA recognition properties of the chimera.

4.3.4. Recognition of Oligonucleotides. Based on the results of the photocleavage studies on the DNA restriction fragment, an oligonucleotide was designed to further investigate the recognition of these rhodium(III) - zinc finger chimeras. It contains all four possible GXG DNA triplets and a CGC (GCG on the opposite strand) separated by the identical intervening rhodium binding site (ACT) (Figure 4.4). Photocleavage studies on this oligonucleotide show differences in DNA site preferences for the various rhodium(III) - zinc finger chimeras. $[Rh(phi)_2(bpy')]^{3+}$-Sp1-2f and $[Rh(phi)_2(phen')]^{3+}$-Sp1-2f display the strongest photocleavage (Figure 4.5). Based on the modeling studies, the cleavage site should be in the intervening sequence 3' to the zinc finger recognition triplet.

```
                10          20          30
O1:5'-GACTCGCACTGTGACTGCGACTGAGACTGGGACTG-3'
O2:3'-CTGAGCGTGACACTGACGCTGACTCTGACCCTGAC-5'
```

Figure 4.4. *Sequences of oligonucleotides O1 and O2.*

The photocleavage sites for the rhodium(III)-Sp1-2f chimeras fall into two categories. Firstly, $[Rh(phi)_2(bpy')]^{3+}$-Sp1-2f cleaves at cytosines (C15, C21) on O1 and thymine (T20) on O2 in the intervening sequence between the recognition triplets (Figure 4.5, lanes 5 and 13 respectively). However, the parent rhodium complex also cleaves preferentially at these sites (lanes 3 and 11). Secondly, the bpy' - zinc finger chimera recognizes a site on O2 (C19) that is the 5' base of a recognition triplet (lane 13). In an analogous fashion, the other chimera, $[Rh(phi)_2(phen')]^{3+}$-Sp1-2f cleaves strongly at additional sites on O1 (C5, G11) and O2 (C25) which are also the 5' base of a recognition triplet (lanes 6 and 14, respectively).

4.3.5. Binding Constant Determinations. A more accurate picture of the specificity was obtained using quantitative photocleavage titrations. The binding constants for $[Rh(phi)_2(bpy')]^{3+}$, $[Rh(phi)_2(phen')]^{3+}$ and their respective Sp1-2f chimeras were obtained for sites on the O1 strand of the duplex by determining the fraction cleaved at each site as a function of concentration at a constant rhodium to DNA ratio (2:1 duplex). A gel of a quantitative photocleavage titration for $[Rh(phi)_2(phen')]^{3+}$-Sp1-2f is shown in Figure 4.6. The cleavage at the rhodium binding sites (C3, C9, C15, C21 and C27) and the other strong binding sites (C5, G11 and G17) were quantitated. Similar studies were also carried out for $[Rh(phi)_2(phen')]^{3+}$, $[Rh(phi)_2(bpy')]^{3+}$ and $[Rh(phi)_2(phen')]^{3+}$-Sp1-2f (data not shown). The binding constants at these sites for $[Rh(phi)_2(bpy')]^{3+}$, $[Rh(phi)_2(phen')]^{3+}$ and their respective Sp1-2f chimeras are presented in Table 4.2.

Figure 4.5. *An image of a polyacrylamide gel showing the photocleavage of a 5'-^{32}P end labeled O1 (lanes 1-8) and O2 (lanes 9-16) oligonucleotides by 1 μM rhodium(III) complexes and their zinc finger peptide chimeras in the presence of 50 μM (base pairs) calf thymus DNA: lanes 1 and 9, light control (LC); lanes 2 and 10, dark control with $[Rh(phi)_2(phen')]^{3+}$-Sp1–2f (DC); lanes 3 and 11, $[Rh(phi)_2(bpy')]^{3+}$ (B); lanes 4 and 12, $[Rh(phi)_2(phen')]^{3+}$ (P); lanes 5 and 13, $[Rh(phi)_2(bpy')]^{3+}$-Sp1-2f (BS2); lanes 6 and 14, $[Rh(phi)_2(phen')]^{3+}$-Sp1-2f (PS2); lanes 7 and 15, Maxam-Gilbert A+G sequencing reaction; lanes 8 and 16, Maxam-Gilbert C+T sequencing reaction. All samples were incubated overnight in 25 mM Tris•HCl, pH 8.0, 25 mM NaCl, 100 μM $ZnSO_4$, 10% glycerol and irradiated for 15 min at 313 nm.*

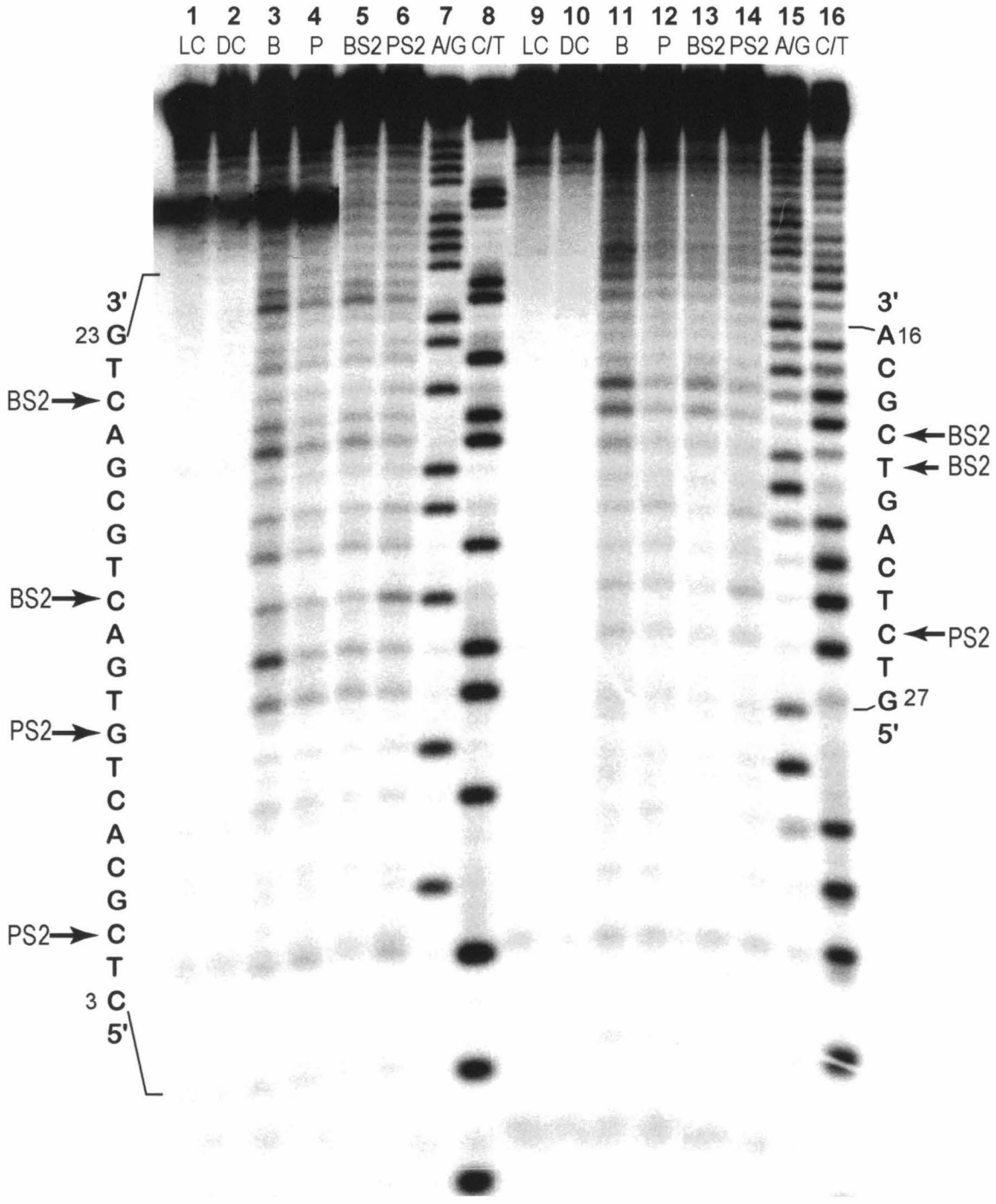
1 2 3 4 5 6 7 8 9 10 11 12 13 14 15 16
LC DC B P BS2 PS2 A/G C/T LC DC B P BS2 PS2 A/G C/T
3'
23 G
T
BS2 C
A
G
C
G
T
BS2 C
A
G
T
PS2 G
T
C
A
C
G
PS2 C
T
3 C
5'
3'
A 16
C
G
C BS2
T BS2
G
A
C
T
C PS2
T
G 27
5'

Figure 4.6. *An image of a polyacrylamide gel showing the quantitative affinity photocleavage titration of a 5'-^{32}P end labeled O1 oligonucleotide and [Rh(phi)$_2$(bpy')]$^{3+}$-Sp1–2f. The ratio of rhodium to DNA duplex was kept at a constant 2:1 ratio. The concentration of DNA is as follows: lane 1, light control (LC); lane 2, dark control 7.5 μM DNA (DC); lane 3, 0.0075 μM; lane 4, 0.025 μM; lane 5, 0.075 μM; lane 6, 0.25 μM; lane 7, 0.75 μM; lane 8, 2.5 μM; lane 9, 5.0 μM; lane 10, 7.5 μM; lane 11, Maxam-Gilbert A+G sequencing reaction; lane 12, Maxam-Gilbert C+T sequencing reaction. All samples were incubated overnight in 25 mM Tris•HCl, pH 8.0, 25 mM NaCl, 100 μM ZnS0$_4$, 10% glycerol and irradiated for 15 min at 313 nm.*

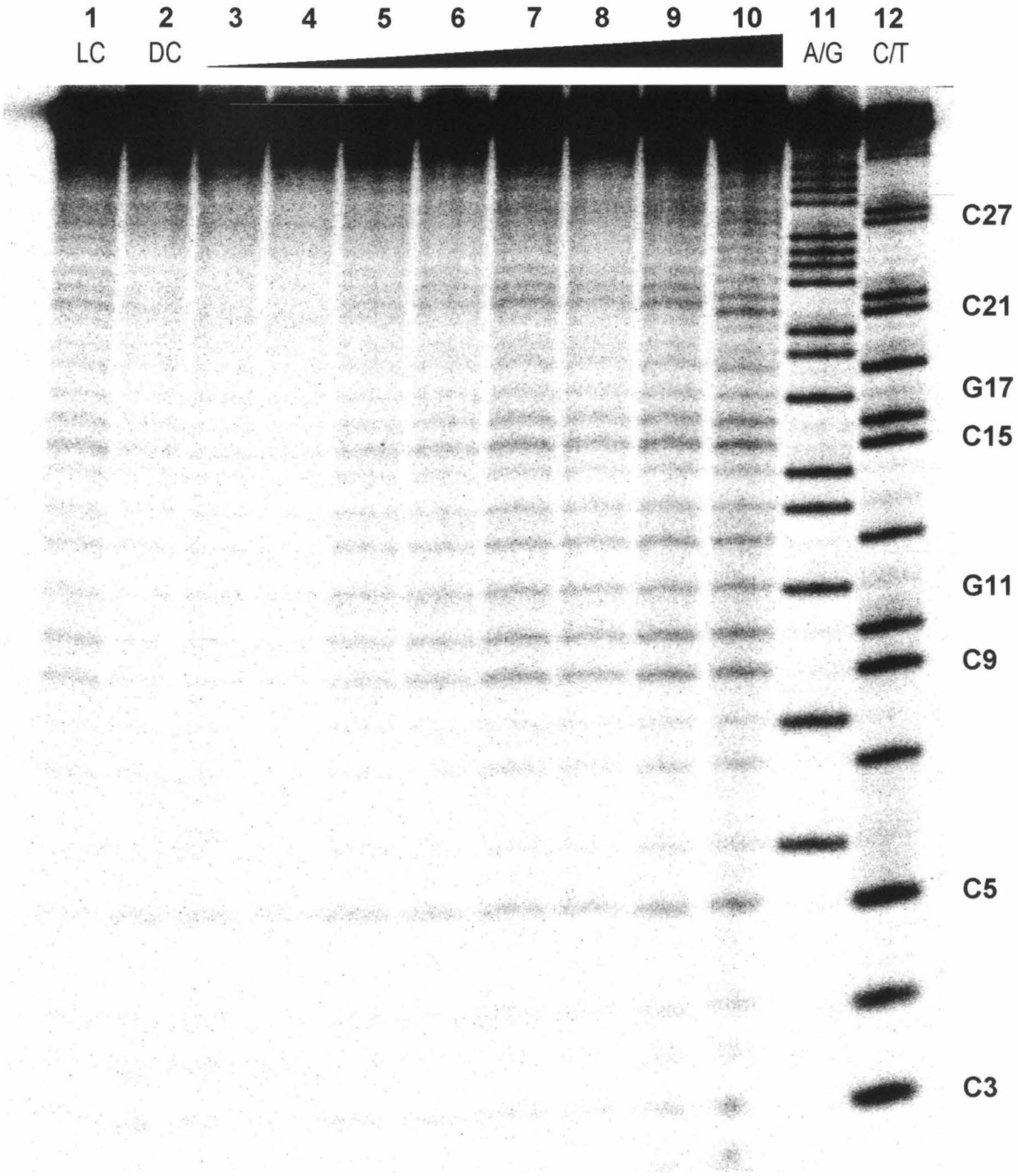
1
LC
2
DC
3
4
5
6
7
8
9
10
11
A/G
12
C/T
C27
C21
G17
C15
G11
C9
C5
C3

Table 4.2: The Binding Constants For Rhodium(III) Complexes and their Zinc Finger Chimeras[a]

	K_a (x 10^6 M^{-1}) at specific bases on O1							
	C3	C9	C15	C21	C27	C5	G11	G17
$[Rh(phi)_2(bpy')]^{3+}$	nb[b]	3.2 (± 0.9)	4 (± 1)	5 (± 1)	nb	nb	3.2 (± 0.8)	2.1 (± 0.7)
$[Rh(phi)_2(bpy')]^{3+}$-Sp1-2f	nb	11 (± 2)	8 (± 1)	9 (± 2)	nb	10 [c]	30 (± 10)[d]	20 (± 10)[d]
$[Rh(phi)_2(phen')]^{3+}$	nb	3.1 (± 0.6)	6 (± 1)	6 (± 1)	nb	nb	3.0 (± 0.5)	3.7 (± 0.6)
$[Rh(phi)_2(phen')]^{3+}$-Sp1-2f	nb	>100 (± 20)[de]	10 [c]	nb	nb	>180 (± 40)[e]	>90 (± 40)[e]	40 (± 10)

[a]Values reported in the table are measured from quantitative photocleavage experiments performed in 25 mM Tris, pH 8.0, 25 mM NaCl, 100 μM $ZnSO_4$, 10% glycerol. [b]nb = no binding seen at these sites. [c]These numbers are questionable since the fit to the data was poor ($R^2 = 0.6$). [d]These numbers are less accurate since the fit to the data was $R^2 \sim 0.8$. [e]Since the bottom of the titration curves were not obtained, these numbers should be considered lower limits.

The data and the binding curves fits for $[Rh(phi)_2(bpy')]^{3+}$ and $[Rh(phi)_2(bpy')]^{3+}$-Sp1-2f are shown in Figure 4.7. In general, the presence of the peptide leads to higher binding affinities. The curves are shifted to a 2-10 fold higher binding constant for the chimera compared to the rhodium complex. The relative order of affinities for $[Rh(phi)_2(bpy')]^{3+}$ is C21 ≥ C15 ≥ C9 = G11 ≥ G17 while the order for $[Rh(phi)_2(bpy')]^{3+}$-Sp1-2f is G11 ≈ C5 > G17 > C9 ≥ C21 ≥ C15 (Figure 4.8). For the rhodium binding sites (C9, C15, C21), the rhodium complex and the chimera have quite similar recognition. The binding affinities for these sites are close, but there is a difference in the site preference between the rhodium intercalator and the chimera. $[Rh(phi)_2(bpy')]^{3+}$-Sp1-2f prefers the C9 site which is the least preferred for $[Rh(phi)_2(bpy')]^{3+}$ alone. The difference in affinities between the rhodium intercalator and the chimera is almost 4 fold at this site but only 2 fold for the other two sites. Thus, the peptide is effecting the site recognition of the parent metal complex an effect on the specificity of the metal complex. For the other sites (G11 and G17), the increase in the binding affinity is 10 fold, but the order of specificity is identical. The C5 site, however, goes from no recognition to ~10^7 M^{-1} binding affinity. Again, the presence of the peptide is affecting not only the binding affinity, but the sequence-specific DNA recognition of the $[Rh(phi)_2(bpy')]^{3+}$-Sp1-2f chimera.

The titration data and binding curve fits for $[Rh(phi)_2(phen')]^{3+}$ and $[Rh(phi)_2(phen')]^{3+}$-Sp1-2f are shown in Figure 4.9. The $[Rh(phi)_2(phen')]^{3+}$ has almost identical binding constants and specificities as its bpy' analog. The peptide has increased the binding affinity of the rhodium complex in the range of 10 to 100 fold with one site (C5) going from no binding to a > 10^8 M^{-1} association constant. Since only the top half of the curves were obtained for sites C9, C5 and G11, the 10^8 M^{-1} binding constant numbers are a lower limit. The relative order of affinities for $[Rh(phi)_2(phen')]^{3+}$ is C15 = C21 > G17 > C9 = G11 while the

Figure 4.7. *Data for quantitative affinity photocleavage experiments for different sites on oligonucleotide O1 for* $[Rh(phi)_2(bpy')]^{3+}$ *(top) and* $[Rh(phi)_2(bpy')]^{3+}$*-Sp1-2f (bottom) in 25 mM Tris•HCl, pH 8.0, 25 mM NaCl, 100* μ*M* $ZnSO_4$*, 10% glycerol after incubation overnight and irradiation for 15 min at 313 nm. The sigmoidal curves show the titration binding isotherms. The data for the different sites are represented by red circles for C9, dark blue diamonds for C15, black upright triangles for C21, pink crosses for C5, light blue squares for G11 and green triangles for G17.*

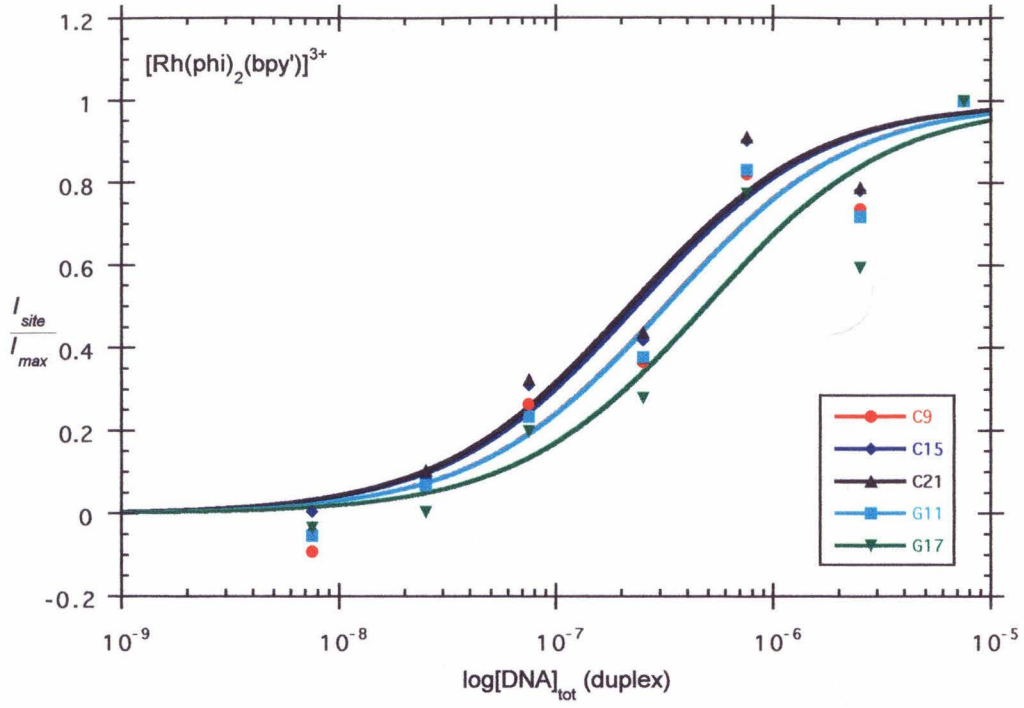
[Rh(phi)2(bpy')]3+
1.2
1
0.8
0.6
0.4
0.2
0
-0.2
I site / I max
10-9
10-8
10-7
10-6
10-5
log[DNA]tot (duplex)
C9
C15
C21
G11
G17

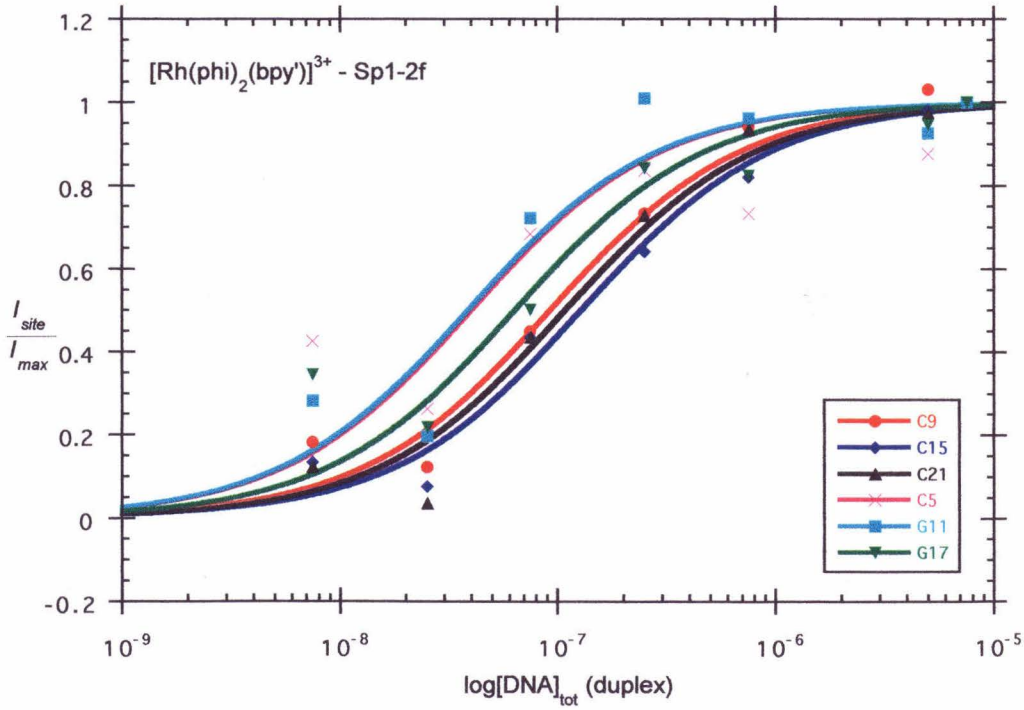
[Rh(phi)2(bpy')]3+ - Sp1-2f
1.2
1
0.8
0.6
0.4
0.2
0
-0.2
I site / I max
10-9
10-8
10-7
10-6
10-5
log[DNA]tot (duplex)
C9
C15
C21
C5
G11
G17

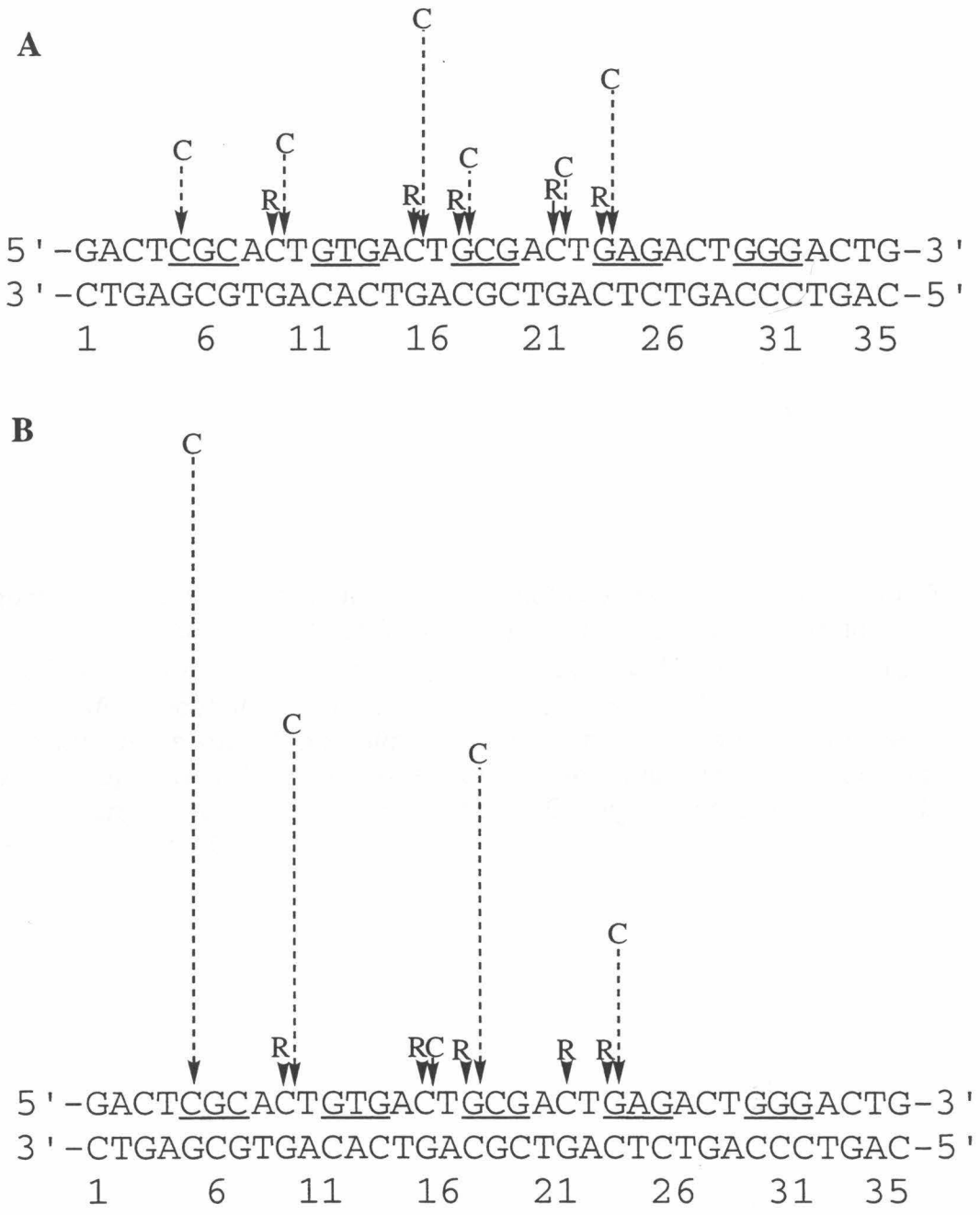

Figure 4.8. *Depiction of the relative binding constants obtained for [Rh(phi)$_2$(bpy')]$^{3+}$ (R) and [Rh(phi)$_2$(bpy')]$^{3+}$-Sp1-2f (C) (**A**) and [Rh(phi)$_2$(phen')]$^{3+}$ (R) and [Rh(phi)$_2$(phen')]$^{3+}$-Sp1-2f (C) (**B**). The size of the arrows is proportional to the calculated binding affinites. Due to the large binding constants obtained, the arrows in B are 50% the size of the arrows in A.*

Figure 4.9. *Data for quantitative affinity photocleavage experiments for different sites on oligonucleotide O1 for* $[Rh(phi)_2(phen')]^{3+}$ *(top) and* $[Rh(phi)_2(phen')]^{3+}$*-Sp1-2f (bottom) in 25 mM Tris•HCl, pH 8.0, 25 mM NaCl, 100* μ*M* $ZnSO_4$*, 10% glycerol after incubation overnight and irradiation for 15 min at 313 nm. The sigmoidal curves show the titration binding isotherms. The data for the different sites are represented by red circles for C9, dark blue diamonds for C15, black upright triangles for C21, pink crosses for C5, light blue squares for G11 and green triangles for G17.*

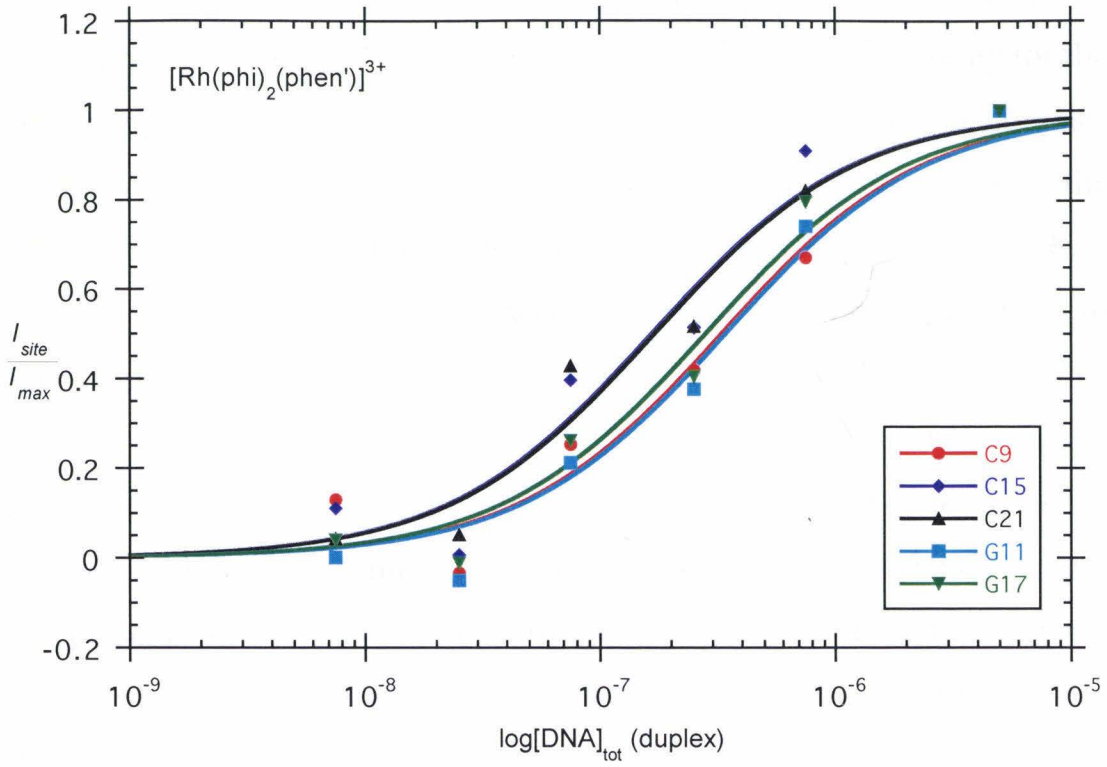
[Rh(phi)2(phen')]3+
1.2
1
0.8
0.6
0.4
0.2
0
-0.2
I site / I max
10-9
10-8
10-7
10-6
10-5
log[DNA]tot (duplex)
C9
C15
C21
G11
G17

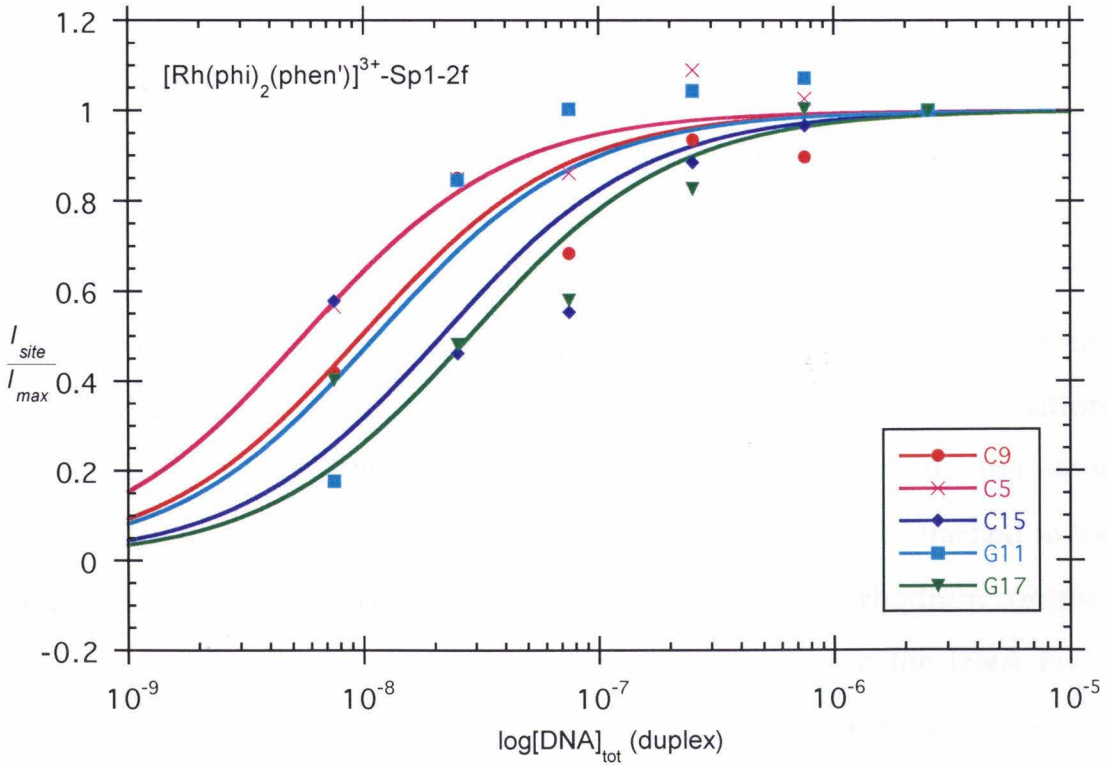
[Rh(phi)2(phen')]3+-Sp1-2f
1.2
1
0.8
0.6
0.4
0.2
0
-0.2
I site / I max
10-9
10-8
10-7
10-6
10-5
log[DNA]tot (duplex)
C9
C5
C15
G11
G17

order for $[Rh(phi)_2(bpy')]^{3+}$-Sp1-2f is C5 > C9 ≈ G11 > C15 > G17 (Figure 4.8). In contrast to the bpy' chimera, the changes seen for the rhodium sites for the phen' chimera vary widely. The C9 site has at least a 33 fold increase in affinity for the chimera over the metal complex while the C15 site has only a 2 fold increase. The effect on C15 is the same as in the bpy' chimeras. Interestingly, the $[Rh(phi)_2(phen')]^{3+}$-Sp1-2f chimera loses its affinity for C21 altogether. Thus, there is a definite change in specificity from $[Rh(phi)_2(bpy')]^{3+}$ to $[Rh(phi)_2(bpy')]^{3+}$-Sp1-2f. The other three sites (C5, G11 and G17) also show differential increases in binding affinity. One site shows a great increase in affinity (C5), one is modest (G11) an one is small (G17). The G17 site shows the same effect as in the bpy' chimera. Thus, in the case of $[Rh(phi)_2(phen')]^{3+}$- Sp1-2f, the presence of the peptide not only greatly increases the affinity of the rhodium intercalator, but also drastically changes the specificity over the rhodium intercalator.

4.4. DISCUSSION

Rhodium(III) - zinc finger chimeras are able to bind and recognize DNA. Since DNA is cleaved upon irradiation, the peptide does not interfere with intercalation of the phi ligand of the rhodium complex into DNA. The photocleavage experiments on restriction fragments demonstrate that the presence of the peptide affects the specificity of the cleavage. In addition, $[Rh(phi)_2(bpy')]^{3+}$ and $[Rh(phi)_2(phen')]^{3+}$, which have virtually the same sequence specificity show very different cleavage patterns when attached to the same zinc finger peptide. Thus, the different linkages on the rhodium complex are placing the zinc finger at distinct orientations relative to the DNA helix. However, the rhodium complex delivers the peptide to the major groove of DNA, and the peptide is responsible for direct recognition.

The oligonucleotide experiments described above allow closer investigation into the factors involved in recognition of the chimera. The oligonucleotide contains variations on the GCG recognition triplet which are separated by identical rhodium binding sites (ACT). Some of the chimeras show only weak cleavage on this oligonucleotide. This is not surprising since the studies on the restriction fragment indicate that the recognition sites can vary highly between the different chimeras. It is likely that other chimeras may need different spacing between the recognition triplet and the rhodium intercalation site in order to bind tightly to DNA. The Sp1- finger 2 chimeras have strong cleavage sites on the oligonucleotide allowing calculation of binding constants for these chimeras and their respective rhodium complexes. In general, the presence of the peptide increases the binding affinity for the sites as compared to the rhodium complex. This increase could result from simply the electrostatic attraction of the highly positively charged peptide for the negatively charged DNA. This is unlikely since all the zinc finger peptides have the same net charge, but different specificities. In fact, ADR1b and Sp1-3 zinc finger chimeras weakly cleave at these sites. For $[Rh(phi)_2(phen')]^{3+}$- Sp1-2f, there is a more dramatic change in binding affinity and specificity at this site when compared to $[Rh(phi)_2(phen')]^{3+}$. Thus for this chimera, the zinc finger peptide has more interactions with the DNA than in the bpy' system. The photocleavage at these sites for both $[Rh(phi)_2(bpy')]^{3+}$- and $[Rh(phi)_2(phen')]^{3+}$- Sp1-2f chimeras is probably due the rhodium complex and zinc finger binding to adjacent DNA sites as modeled in Figure 4.1.

In contrast, the sites with the highest binding affinities for both chimeras are at the 5' base of the recognition triplet. Again, the changes in affinity and specificity are more dramatic for the $[Rh(phi)_2(phen')]^{3+}$ chimera versus the $[Rh(phi)_2(bpy')]^{3+}$ chimera. $[Rh(phi)_2(phen')]^{3+}$ does not recognize the C5 site

while its Sp1-2f chimera has a $>10^8$ M^{-1} binding affinity for the site. In order for this to occur, the rhodium complex and the peptide must be interacting in a cooperative fashion. This high affinity C5 base is the complementary base of the 5'-G of a GCG recognition triplet for the Sp1-2 zinc finger. According to the crystal structure of Zif268 zinc finger protein with DNA, the zinc fingers make direct contacts to only the G rich strand of the DNA. Thus, it is possible for both the zinc finger and the rhodium complex to bind in the major groove at the GCG site. The zinc finger would be contacting the GCG strand and the rhodium intercalator would be canted towards the CGC strand. A model of this interaction is shown in Figure 4.9. The hydrophobic ancillary ligands of the rhodium complexes could be forming a conformation with the zinc finger which could be adding to cooperativity of the binding interaction. This combination of conformation and direct DNA recognition could be responsible for the high binding affinity and specificity for this site.

Thus, there are two models for the interaction of rhodium(III) - zinc finger chimeras with DNA. At the lower affinity sites, the zinc finger and rhodium complex are binding independently to a separate but adjacent site. At the high affinity sites, the peptide and metal complex are binding cooperatively to the same site. This can be correlated with the spectroscopic and structural studies which indicated that the zinc finger and rhodium are virtually independent, but some indication of interaction between the two moieties was evident as discussed in Chapter 3.

In conclusion, a rhodium(III) - zinc finger chimera that exhibits a high affinity ($>10^8$ M^{-1}) for a specific DNA sequence has been successfully created. This chimera is the first example of the molecular recognition of DNA by a single zinc finger peptide.

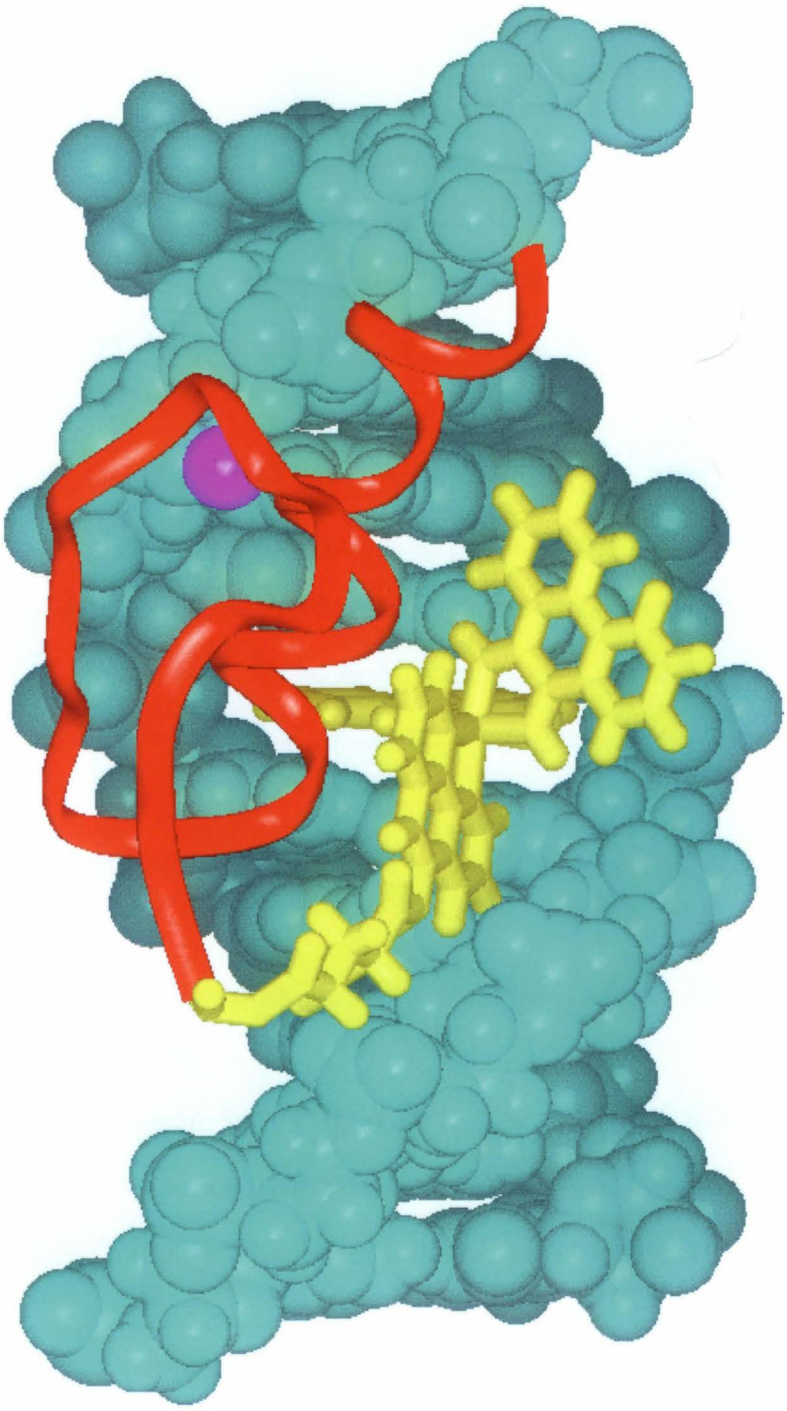

Figure 4.10. *A model of the interaction of the $[Rh(phi)_2(phen')]^{3+}$-Sp1-2f zinc finger chimera with DNA. The DNA is in aqua, the rhodium in yellow and the zinc finger peptide is in red with the zinc in pink.*

4.5. REFERENCES

(1) Sardesai, N. Y.; Zimmermann, K.; Barton, J. K. *J. Am. Chem. Soc.* **1994**, *116*, 7502-7508.

(2) Sardesai, N. Y. Ph.D. Thesis, California Institute of Technology 1995.

(3) Berg, J. M. *Acc. Chem. Res.* **1995**, *28*, 14-19.

(4) Pavletich, N. P.; Pabo, C. O. *Science* **1991**, *252*, 809-817.

(5) Frankel, A. D.; Berg, J. M.; Pabo, C. O. *Proc. Natl. Acad. Sci. USA* **1987**, *84*, 4841-4845.

(6) Lee, M. S.; Gottsfeld, J. M.; Wright, P. E. *FEBS Lett.* **1991**, *279*, 289-294.

(7) Pyle, A. M.; Long, E. C.; Barton, J. K. *J. Am. Chem. Soc.* **1989**, *111*, 4520-4522.

(8) Pyle, A. M.; Chiang, M. Y.; Barton, J. K. *Inorg. Chem.* **1990**, *29*, 4487-4495.

(9) Sitlani, A.; Long, E. C.; Pyle, A. M.; Barton, J. K. **1992**.

(10) Klevit, R. E.; Herriott, J. R.; Horvath, S. J. *Prot. Struct. Funct. Gen.* **1990**, *7*, 215-226.

(11) Thukral, S. K.; Morrison, M. L.; Young, E. T. *Mol. Cell. Biol.* **1992**, *12*, 2784-2792.

(12) Thukral, S. K.; Morrison, M. L.; Young, E. T. *Proc. Natl. Acad. Sci., USA* **1991**, *88*, 9188-9192.

(13) Giodoni, D.; Dynan, S. W.; Tjian, R. *Nature* **1984**, *312*, 409-413.

(14) Kadonaga, J. T.; Jones, K. A.; Tijan, R. *TIBS* **1986**, *11*, 20-23.

(15) Kadonaga, J. T.; Courey, A. J.; Ladika, J.; Tjian, R. *Science* **1988**, *242*, 1566-1570.

(16) Posewitz, M. C.; Wilcox, D. E. *Chem. Res. Toxicol.* **1995**, *8*, 1020-1028.

(17) Thiesen, H.-J.; Schroder, B. *Biochem. Biophys. Res. Comm.* **1991**, *175*, 333-338.

(18) Crosby, S. D.; Puetz, J. J.; Simburger, K. S.; Fahrner, T. J.; Milbrandt, J. *J. Mol. Cell. Bio.* **1991**, *11*, 3841-3841.

(19) Berg, J. M. *Proc. Natl. Acad. Sci., USA* **1992**, *89*, 11109-11110.

(20) Thukral, S. K.; Eisen, A.; Young, E. T. *Mol. Cell. Biol.* **1991**, *11*, 1566-1577.

(21) David, S. S.; Barton, J. K. *J. Am. Chem. Soc.* **1993**, *115*, 2984-2985.

(22) Krotz, A. H.; Kuo, L. Y.; Shields, T. P.; Barton, J. K. *J. Am. Chem. Soc.* **1993**, *115*, 3877-3882.

(23) Hudson, B. P.; Dupureur, C. M.; Barton, J. K. *J. Am. Chem. Soc.* **1995**, *117*, 9379-9380.

(24) Maniatis, T.; Fristch, E. F. *Molecular Cloning*; Cold Spring Harbor Laboratory: Plainview, New York, 1982.

(25) Singleton, S. F.; Dervan, P. B. *Biochem.* **1992**, *31*, 10995.

(26) Wang, A. H.-J.; Nathans, J.; van der Marel, G.; van Boom, J. H.; Rich, A. *Nature* **1978**, *276*, 471.

(27) Pendergrast, P. S.; Chen, Y.; Ebright, Y. W.; Ebright, R. H. *Proc. Natl. Acad. Sci. USA* **1992**, *89*, 10287-10291.

(28) Mahnken, R. E.; Billadeau, M. A.; Nikonowicz, E. P.; Morrison, H. *J. Am. Chem. Soc.* **1992**, *114*, 9253-9265.

(29) Harmon, H. L.; Morrison, H. *Inorg. Chem.* **1995**, *34*, 4937-4938.

Chapter 5. Conclusions and Perspectives

5.1. CONCLUSIONS

In an effort to understand the molecular recognition of DNA, we have developed a small molecule that can interact with DNA in a predictable manner. With a small, well-defined system, the details of the interaction can be elucidated. Thus, covalent chimeras of zinc finger peptide domains with phenanthrenequinone diimine (phi) complexes of rhodium(III) have been designed. The zinc finger motif is a small, structurally rigid peptide that is used by transcription factors to recognize DNA sequence-specifically. In the protein systems, the fingers appear in sets of 2-27 consecutively. Though a single finger has been proven to adopt the correct structure, it does not interact with DNA in a sequence-specific manner. Therefore, in order to study an isolated zinc finger, it needs to be delivered to the DNA. The phi complexes of rhodium(III) complex bind non-specifically in the major groove of DNA by intercalation and, thus, can allow an attached zinc finger peptide to interact with the base pairs of DNA in a sequence-specific manner.

Chimeras of $[Rh(phi)_2(bpy')]^{3+}$ (bpy' = 4-(4-carboxybutyl), 4'-methyl-2,2'-bipyridine) and $[Rh(phi)_2(phen')]^{3+}$ (phen' = (5-amidoglutaryl)-1,10-phenanthroline) and four different zinc finger peptides (Sp1 finger 2 and 3, ADR1b and ADR1b-Ala) have been successfully synthesized using solid phase coupling methodology. In this method, the activated metal complex is directly coupled to the peptide chain, which is still attached to the resin, using standard coupling techniques. Two new combinations of coupling reagents have improved the yields of chimeras. Pentafluorophenol (OPfp) in combination with *N,N*-dissuccinimidyl carbonate (DCC) shows almost quantitative coupling of $[Rh(phi)_2(bpy')]^{3+}$ while $[Rh(phi)_2(phen')]^{3+}$ needs a combination of 2,4,6-

collidine, 1-hydroxy-7-azabenzotriazole (HOAt) and DCC to bring coupling yields up to 50%.

All of the chimeras have been spectroscopically characterized. Electronic spectroscopy showed the rhodium complex and peptide to be essentially independent units. Both plasma desorption (PD) and electrospray ionization (ESI) mass spectroscopy have been used to successfully analyze the chimeras. PD MS shows a sequential fragmentation of the peptide that is dependent on the covalent attachment of the rhodium complex. In contrast, the ESI mass spectra are clean and are useful for verifying the integrity and purity of the rhodium(III) - zinc finger chimeras.

A method to fold successfully the peptide portion of the chimera with zinc has been developed. Due the presence of two cysteines, the zinc finger can oxidize easily which prevent coordination of the zinc(II) ion. In order to prevent this, the chimera must be folded with zinc immediately after purification. One-dimensional ^1H NMR spectroscopy has been used to confirm proper folding of the peptide. The spectrum contained distinct resonances (histidine, methyl, α-carbon) that shift upon coordination of zinc and indicate that the proper structure has been formed. All of the chimeras that were synthesized were proven to fold correctly upon the addition of zinc. Therefore, the presence of rhodium complex does not interfere with the zinc finger structure.

The rhodium(III) - zinc finger chimeras were found to bind tightly to DNA, and to promote DNA cleavage with photoactivation in the same fashion as the rhodium intercalator. Analysis of the DNA sites targeted by the chimeras on DNA restriction fragments have demonstrated that the peptide can direct new recognition. Variations in the rhodium complexes and peptides resulted in differences in specificity as observed by photocleavage. Studies on smaller oligonucleotides containing all four possible zinc finger recognition triplets

(GXG) have shown that $[Rh(phi)_2(bpy')]^{3+}$- and $[Rh(phi)_2(phen')]^{3+}$- Sp1-2 chimeras show different strong cleavage sites. A quantitative affinity photocleavage titration method was used to obtain the binding constants for these chimeras and there analogous rhodium complexes. The chimeras were found to bind with affinities of 10^7-10^8 M^{-1} for their target site. This is an increase of 10-100 fold over the rhodium complexes alone. At the lower affinity sites, the rhodium complex and zinc finger appeared to bind independently to adjacent segments. For the $[Rh(phi)_2(phen')]^{3+}$-Sp1-2f chimera, a strong high affinity site ($K_a \geq 10^8$ M^{-1}) was observed, where it was postulated that the rhodium complex and zinc finger bind to the opposite strands of the GCG binding site in a cooperative fashion. Hence, formation of rhodium(III) - zinc finger chimeras provide a route to establish high affinity DNA binding by a single zinc finger domain.

5.2. PERSPECTIVES

These rhodium(III) - zinc finger chimeras represent a new route to examine the specific interactions of a single zinc finger with DNA in chemical detail and provide the basis to build a family of sequence-specific DNA binding molecules.

To confirm the models of DNA interaction, more studies are necessary. The binding constants for the other chimeras should be determined. This will require the design of new oligonucleotides with various spacing between the recognition triplets and the rhodium binding sites. In addition, many studies have been done where mutations in the recognition amino acids of the zinc finger have caused analogous mutations in the DNA sequence that is recognized. Studies of chimeras containing one of these mutants would confirm the direct interaction of the zinc finger with the DNA base pairs.

In addition, rhodium(III) - peptide chimeras are a good starting point for building a library of sequence-specific DNA binding molecules since the zinc finger peptide has been used to recognize various DNA sequences. Alteration of the recognition only requires the synthesis of a new peptide which can easily be coupled to the rhodium metallointercalator. Thus, the recognition of any desired DNA sequence may be possible using these rhodium(III) - zinc finger peptide chimeras.